A LOAD/COST/MASS COMPARISON OF ALUMINIUM, GLASS, CARBON AND ASBESTOS FIBRE COMPOSITES FOR IMMEDIATE APPLICATION TO AIRCRAFT PRIMARY STRUCTURES

João Manuel Correia SALVA

A Dissertation Submitted to the Faculty of Engineering, University of the Witwatersrand, Johannesburg in fulfilment of the requirements for the degree of Master of Science in Engineering.

Johannesburg 1979.

DECLARATION

I, João Manuel Correia Salva, hereby declare that this dissertation is my own work and has not been submitted by me for a degree at any other University.

João Manuel Correia Salva

ABSTRACT

A comparison of 4 different materials for immediate application to aircraft primary structures was made on the basis of load-to-buckle/cost/mass. The materials tested were: Al-2024 T3 (Alclad), glass fibre cloth, carbon fibre and asbestos fibre (Noramite) composites. A mathematical formulation of the problem was used which was found to give very satisfactory results. This method made use of beam vibration modes and the Rayleigh-Ritz energy formulation and it was found that even with only 4 modes of vibration, the results agreed very well with the computer analysis. A working equation for the design of composite panels in shear is also given.

ACKNOWLEDGEMENTS

Special thanks are due to the following people:

Mr R J Fritz (Mechanical Engineering Department, University of the Witwatersrand) for his continuous support and technical advice.

Dr T L F Müller (Applications Research Manager - Cape Asbestos, South Africa (Pty) Ltd) for supplying the asbestos fibre (Noramite) and the Araldite epoxy resin used.

Dr C G van Niekerk and Mr Speth (Council for Scientific and Industrial Research - CSIR) for supplying all the glass and carbon fibre used.

Mrs F Roxton Wiggill (Mechanical Engineering Department, University of the Witwatersrand) for the excellent work done in typing this report.

TABLE OF CONTENTS

LIST OF SYMBOLS

A	-	Direct force matrix
a	-	Unknown coefficients of the deflection of the plate in the buckled state; plate width; stiffness matrix
B	-	Coupling matrix between direct forces and bending distortions
C	-	Bending stiffness matrix
d	-	Potential energy due to bending of a thin rectangular plate
e	-	Potential energy of the inplane loads
h	-	Plate or laminar thickness
i,j,k,m,n	-	Subscripts denoting matrix element position
M	-	Laminate bending moments
N	-	Laminate direct forces
S_{cr}	-	Buckling load in shear
U	-	Potential energy of the inplane loads
V	-	Potential energy due to bending
x,y	-	Directions
W	-	Deflected shape of the plate
λ	-	Eigenvalue
ξ	-	Percentage coordinate in x or y directions

INTRODUCTION

Composite materials, their testing and analysis is a very broad and specialised field.

Broad in the sense that one can virtually consider an unlimited number of combinations of matrix and reinforcing material. An example is the fact that in the chapter of fiber reinforced plastics, the following synthetic fibres could be tested: glass, carbon, boron, asbestos, all the various polyamides, polyesters, etc, to mention but a few.

Out of these only a very limited number offer mechanical properties which can be considered to be of interest for immediate application to aircraft primary structures.

Glass, carbon, boron and asbestos fall in this category.

Specialised due to the fact that composite materials constitute one subsection in the field of engineering materials and their application to the vast subject of structures.

The object of this report is to establish a comparison between aluminium, carbon, glass and asbestos fibre composites on the basis of load-to-buckle/cost/mass. The possibility of immediate application of the above materials (especially the last three) to aircraft primary structures was also to be investigated and a quick reference design equation for the buckling load to be established.

It should be noted, however, that since the variables

introduced in such a research program are quite different in nature the results will be repeatable only if the same manufacturing techniques are used.

LITERATURE SURVEY

Access to most information published on the subject was extremely difficult since only in recent years have composite materials been developed and not yet to their full potential.

Of the publications reviewed the following were found to be relevant to the type of work that was undertaken by the author.

US Department of Defense, Military Handbook No 17A, 'Plastics for aerospace vehicles

A good description is given of the methods of analysis of composite structures with emphasis on plates and the reduced form of the stiffness matrices for the various types of orthotropy. Equations are also given for the rotation of the loading axes to any required position but no account is given of the values of the terms of the stiffness matrix for a generally orthotropic plate (thus implying plane stresses). A method of approach to design problems is also given. In Chapter 3 values of the various engineering constants are given for a large variety of materials.

Petit, P H and Waddoups, M E. 'A Method of predicting the non-linear behaviour of laminated composites'. Journal of composite materials, 3; 2-20; 1969.

An analytical technique for determining the stress-strain response up to ultimate laminate failure of a composite panel is presented. The technique is restricted to the prediction of ultimate strength for plane anisotropic laminates with mid plane symmetry subject to biaxial membrane loads.

Equations for the calculations of equivalent moduli and Poisson's ratios of a laminate in terms of the elements of the compliance matrix of the laminate are also given (see also theory section). The paper also suggests that 'the lamina stress-strain curves can be obtained empirically by assuming that the stress-strain response of a single lamina of a uni-directional laminate is the same as the response of the total test laminate'.

Ashton, J E and Waddoups, M E, 'Analysis of anisotropic plates'. Journal of composite materials, 3; 148-165; 1969.

An energy formulation and solutions are presented for the analysis of plane anisotropic rectangular plates with various boundary conditions. The formulation includes linear theory stability analysis, the calculation of natural frequencies and mode shapes, and analysis of displacement due to lateral loads. In plane loadings are included in all of th se formulations. The Ritz technique is used to find the minimum of energy expressions using a series expansicn of beam mode shape functions. Graphs are given on pp 158, 159 for the buckling coefficient of plates with free edges in terms of the ratio of two of the elements of the flexural rigidity matrix (D_{16}/D_{11}). It can be seen that this ratio is inversely proportional to the buckling coefficient.

Ashton, J E and Love, T S. 'Shear stability of laminated anisotropic plates', A S T M Conference on composite materials: Testing and design, 352-361, February 10-13, 1969.

An analytical and experimental study of the shear stability of laminated anisotropic plates is presented. The plates considered are rectangular, have clamped edges, and are fabricated with laminated construction of boron-epoxy composite material. The analytical solutions are obtained by means of the principle of stationary potential energy using the Ritz

method. The deflected shape is approximated with beam characteristic functions. Experimental results are presented for 14 boron-epoxy plates and for 2 aluminium plates and the results compared with the theory. Good agreement is shown.

Viswanathan, A V, Tamekuni M and Baker, L L. 'Elastic stability of laminated, flat and curved, long rectangular plates subjected to combined inplane loads', NASA CR-2330, NASA, Washington D C, 1974.

A method is described to predict theoretical buckling loads of long, rectangular flat and curved laminated plates with arbitrary orientation of orthotropic axes in each lamina. The analysis is applicable to (i) finite length plates of special orthotropy when the combined inplane loads do not include shear, (ii) infinitely long plates, for all other cases. The method of analysis can be extended to longitudinally stiffened structures subjected to combined inplane normal and shear loads, in a manner analogous to that of NASA CR-2216.

Arbitrary boundary conditions may be stipulated along the longitudinal sides of the plate. In the absence of inplane shear loads and 'extensional-shear' coupling, the analysis is also applicable to finite length plates. Numerical results are presented for curved laminated composite plates with various boundary conditions and subjected to various loadings. These results indicate some of the complexities involved in the numerical solution of the analysis for general laminates.

The method of analysis makes use of small deflection theory and assumes that the material is linearly elastic. A computer program was written for the CDC 6600 computer thus making the calculations involved considerably easier.

Tsai, S W. 'Strength characteristics of composite materials', NASA CR-224, NASA, Washington D C, 1965.

The strength characteristics of quasi-homogeneous, nonisotropic materials are derived from a generalized distortional work criterion. The strength of a laminated composite consisting of layers of unidirectional composites depends on the strength, thickness, and orientation of each constituent layer and the temperature at which the laminate is cured. In the process of lamination, thermal and mechanical interactions are induced which affect the residual stress and the subsequent stress distribution under external load. A method of strength analysis of laminated composites is delineated using glass-epoxy composites as examples. The validity of the method is demonstrated by appropriate experiments.

Commonly encountered material constants and coefficients for stress and strength analysis for glass-epoxy composites are listed in the Appendix.

Tsai, S W. 'Structural behaviour of composite materials', NASA CR-71, NASA, Washington D C, 1964.

This study is concerned with the analysis of the structural behaviour of composite materials. It is shown that composite materials can be designed to produce a wide range of mechanical properties. Two types of composite materials are investigated: the unidirectional fiber-reinforced composite and the laminated anisotropic composite. Analytical relations are derived between the composite material coefficients and the geometric and material parameters of the constituents. The experimental results show that the relations derived in this study are more accurate than existing theories, which include the netting analysis.

Lekhnitski, S G. Anisotropic plates, 2nd Ed. OGIZ, Moscow-Leningrad, 1947, English Edition translated by Tsai, S W and Cheron T, Gordon and Breach, New York, 1968.

A very good description is given of the energy method of analysis of composite plates in shear for the cases of simply supported edges and all other boundary conditions for infinitely long strips. Special solutions are given for certain orientation of the fiber and for plywood plates. The equation of the deflected shape of the plate is given for the case of simply supported edges. No suggestion could be found as to the solution of the equation for the case of a rectangular plate with edges clamped.

Megson, T H G. Aircraft structures for Engineering students, London, Edward Arnold, 1972.

Although the book does not consider composite materials separately, it gives a good explanation of the Rayleigh-Ritz method of energy analysis of thin plates. Solutions for the buckling modes under shear are given for the cases of simply supported edges and clamped edges in the form of graphs but no analytical derivation could be found. The curves and graphs given (which are normally used for the analysis of plates in shear) are directly applicable to anisotropic plates as long as the stacking sequence is such that the panel can be considered to be isotropic.

Davis, John G; Zeuder, G W. 'Compressive behaviour of plates fabricated from glass filaments and epoxy resin', NASA TND - 3918 NASA, Washington D C, 1964.

Young's modulus, buckling stress and maximum strength were

determined experimentally for 15 glass-filament-reinforced plastic plates of laminated isotropic construction containing either 12 or 18 laminae. Experimentally determined values of Young's modulus and buckling stress are shown to be in reasonable agreement with theoretical calculations. The theoretical predictions make use of the well known isotropic buckling equation and assume that the stacking sequence (0^{o}, 60^{o}, 120^{o}) is such that the material can be considered isotropic. On the basis of strength and modulus data obtained in this study, it is shown that the glass-epoxy composite is competitive as a lightweight material with aluminium in applications where plate buckling strength or crushing strength is the design criterion.

Dow, N F; Rosen, B W. 'Evaluation of filament-reinforced composites for aerospace structural applications', NASA - CR 207 NASA, Washington DC, 1965.

The work describes studies of the influence of constituent properties upon the performance of structural composites for aerospace applications. Also presented is an analysis of compressive strength. These analyses are then used in a structural efficiency study of sandwich cylindrical shells subjected to the load conditions appropriate to the launch vehicle problem.

Garg, S K; Svalbonas, V; Gurtman, G A. Analysis of structural composite materials, Marcel Dekker, Inc, New York, 1973.

This book gives a very good introduction to the general subject of composite materials including netting-type analyses, and stacking analyses. Considerable space has been devoted to statistical theories of fibrous composite tensile strength, and to continuum theories for wave propagation in particle -

- and fiber - reinforced composites and in laminated materials. Attention has also been given to nonstatistical theories for strength of fiber-reinforced composites and laminated media. With the exception of the abovementioned netting and stacking analyses the book is of little relevance to the present research project.

Creszezuk, L B. 'Shear-Modulus determination of isotropic and composite materials'. Composite Materials: Testing and design, ASTM STP 460, 1969.

In this report the author refers to and describes a new test technique for measuring the shear modulus as well as other principal elastic constants of filamentary composites, developed by himself and published as a technical report of the U S, Air force in September 1966. The technique employs strain rosette-instrumented tensile coupons that contain oriented filaments. It is claimed that despite its simplicity the technique yields excellent results.

Broutman, L J; Krock, R H. Composite materials, Volumes 1 to 8, Academic Press, New York, San Francisco, London, 1975.

A compilation of various reports is given, each volume concentrating on a particular aspect of composite materials. Only volumes 2, 7 and 8 were found to contain reports which are relevant to the work being undertaken. Volume 2, Chapter 2, gives numerical results for the stiffness and compliance matrices of a certain composite material; Chapter 9 of the same volume describes a method for predicting the failure of anisotropic panels. This method could be used to predict the after-buckling behaviour and find failure of the panels being tested. Yet another failure criterion is given in Volume 7, Chapter 2, where a failure envelope is drawn for each layer of composite, the innermost resulting envelope for the composite representing final failure of the panel. Chapter 3 gives a buckling equation for simply

- and fiber - reinforced composites and in laminated materials. Attention has also been given to nonstatistical theories for strength of fiber-reinforced composites and laminated media. With the exception of the abovementioned netting and stacking analyses the book is of little relevance to the present research project.

Creszezuk, L B. 'Shear-Modulus determination of isotropic and composite materials'. Composite Materials: Testing and design, ASTM STP 460, 1969.

In this report the author refers to and describes a new test technique for measuring the shear modulus as well as other principal elastic constants of filamentary composites, developed by himself and published as a technical report of the U S, Air force in September 1966. The technique employs strain rosette-instrumented tensile coupons that contain oriented filaments. It is claimed that despite its simplicity the technique yields excellent results.

Broutman, L J; Krock, R H. Composite materials, Volumes 1 to 8, Academic Press, New York, San Francisco, London, 1975.

A compilation of various reports is given, each volume concentrating on a particular aspect of composite materials. Only volumes 2, 7 and 8 were found to contain reports which are relevant to the work being undertaken. Volume 2, Chapter 2, gives numerical results for the stiffness and compliance matrices of a certain composite material; Chapter 9 of the same volume describes a method for predicting the failure of anisotropic panels. This method could be used to predict the after-buckling behaviour and find failure of the panels being tested. Yet another failure criterion is given in Volume Chapter 2, where a failure envelope is drawn for each layer of composite, the innermost resulting envelope for the composite representing final failure of the panel. Chapter 3 gives a buckling equation for simply

- and fiber - reinforced composites and in laminated materials. Attention has also been given to nonstatistical theories for strength of fiber-reinforced composites and laminated media. With the exception of the abovementioned netting and stacking analyses the book is of little relevance to the present research project.

Creszezuk, L B. 'Shear-Modulus determination of isotropic and composite materials'. Composite Materials: Testing and design, ASTM STP 460, 1969.

In this report the author refers to and describes a new test technique for measuring the shear modulus as well as other principal elastic constants of unidirectionary composites, developed by himself and published as a technical report of the U S, Air force in September 1966. The technique employs strain rosette-instrumented tensile coupons that contain oriented filaments. It is claimed that despite its simplicity the technique yields excellent results.

Broutman, L J; Krock, R H. Composite materials, Volumes 1 to 8, Academic Press, New York, San Francisco, London, 1975.

A compilation of various reports is given, each volume concentrating on a particular aspect of composite materials. Only volumes 2, 7 and 8 were found to contain reports which are relevant to the work being undertaken. Volume 2, Chapter 2, gives numerical results for the stiffness and compliance matrices of a certain composite material; Chapter 9 of the same volume describes a method for predicting the failure of anisotropic panels. This method could be used to predict the after-buckling behaviour and find failure of the panels being tested. Yet another failure criterion is given in Volume 7, Chapter 2, where a failure envelope is drawn for each layer of composite, the innermost resulting envelope for the composite representing final failure of the panel. Chapter 3 gives a buckling equation for simply

supported plates under uniaxial compressive loads. A graph is presented for the variation of C (buckling constant) VS p_{1y} orientation for simply supported plates.

Finally, volume 8, Chapter 11, gives graphs of buckling coefficient, K, VS. a plate parameter g, for various boundary conditions under uniaxial compression. Also given are various design methods for composite shells, plates and other geometries.

THEORY

Shear Stability Analysis of Anisotropic Plates

The stress-strain response of composite panels is dictated by the generalized Hooke's law for anisotropic materials (Ref 9, pp 3-24).

The stiffness matrix thus defined is a square-symmetric, 6 x 6 matrix, with 21 independent coefficients. 12 of these positions will become unpopulated if the material is orthotropic. Therefore we have,

$$\sigma_i = C_{ij}\, \varepsilon_j$$

where the C_{ij}'s are defined by the matrix

$$C_{ij} = \begin{bmatrix} C_{11} & C_{12} & C_{13} & 0 & 0 & 0 \\ & C_{22} & C_{23} & 0 & 0 & 0 \\ & & C_{33} & 0 & 0 & 0 \\ & & & C_{44} & 0 & 0 \\ & & & & C_{55} & 0 \\ & & & & & C_{66} \end{bmatrix}$$

If, in addition, a state of plane stress exists we can define a reduced stiffness matrix Q_{ij} such that

$$\sigma_i = Q_{ij}\, \varepsilon_j$$

The special case thus described applies to glass fiber cloth as well as carbon undirectional fiber.

The reduced form of the stiffness matrix is,

$$Q_{ij} = \begin{bmatrix} Q_{11} & Q_{12} & Q_{16} \\ & Q_{22} & Q_{26} \\ & & Q_{66} \end{bmatrix}$$

where the coefficients are defined as,

$$Q_{11} = \frac{E_{11}}{1 - \nu_{12}\,\nu_{21}}$$

$$Q_{22} = \frac{E_{22}}{1 - \nu_{12}\,\nu_{21}}$$

$$Q_{12} = \frac{\nu_{12}\,E_{22}}{1 - \nu_{12}\,\nu_{21}} = \frac{\nu_{21}\,E_{11}}{1 - \nu_{12}\,\nu_{21}}$$

$$Q_{66} = G_{12}$$

and if the reference axes coincide with the fiber axes,
$Q_{16} = Q_{26} = 0$

In the notation used above and hereafter, the following applies:

$\nu_{12} = -\frac{\varepsilon_2}{\varepsilon_1}$; Poisson's ratio for the strain in the 2-direction due to uniaxial normal stress in the 1-direction.

$G_{12} = \frac{\sigma_6}{\varepsilon_6}$; the shear modulus determined by the ratio of pure shear stress σ_6, to its correponding shear strain ε_6. The shear stress and shear strain act on the 1-2 plane.

$E_{11} = \frac{\sigma_1}{\varepsilon_1}$; the modulus of elasticity of the material in the 1-direction due to uniaxial stress, σ_1.

The remaining engineering constants are similarly defined. The directions 1 and 2, referred to above, are defined as follows:

It is, therefore assumed that the element is constructed from thin laminae (monolayers) which are processed to form a mechanically continuous laminate. The laminate coordinates are shown in the figure below.

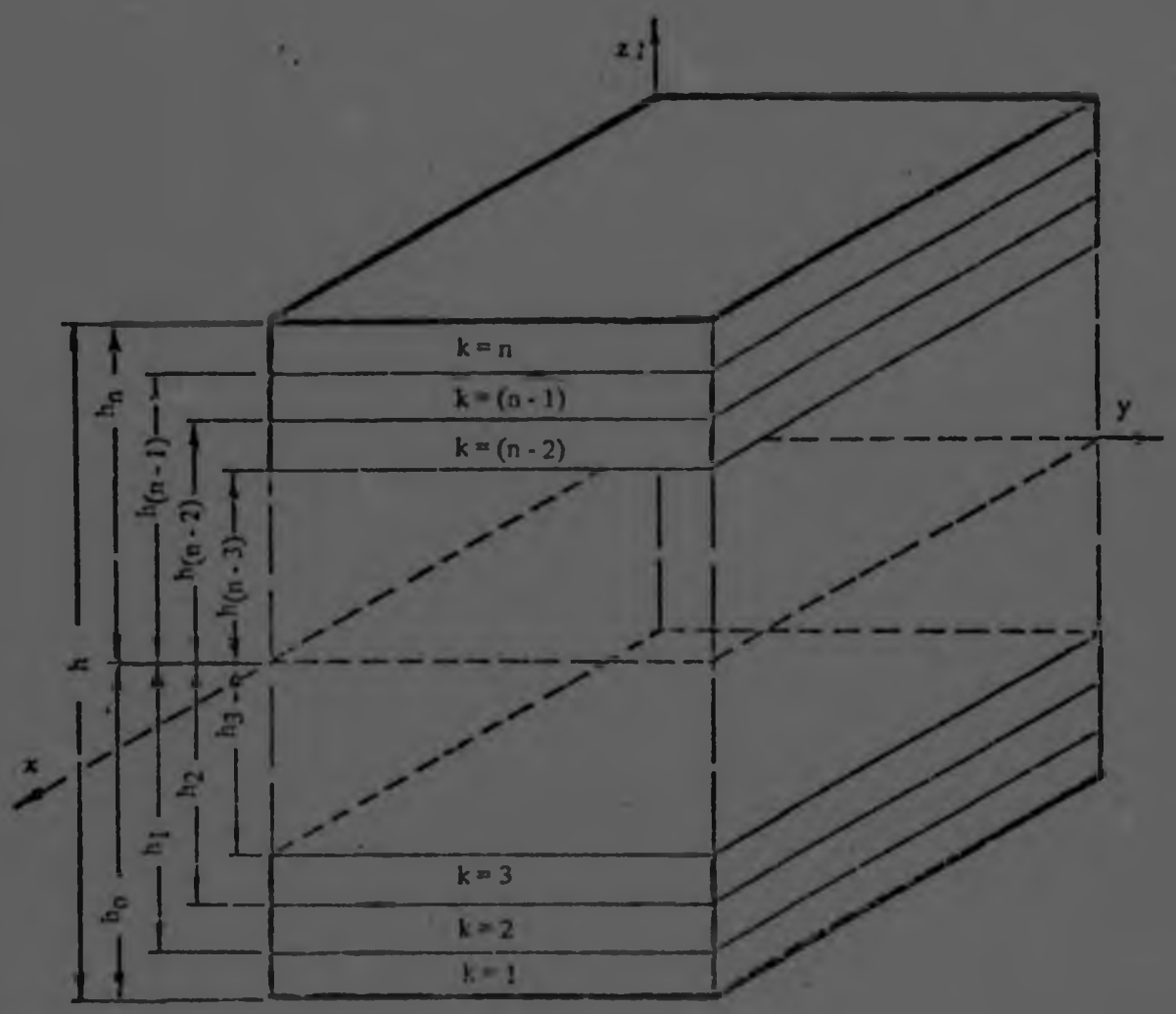

The material properties enter the analysis through formulations of the element constitutive equations. It is required to relate the net forces on the element, as shown in the figure below, to the element deformation.

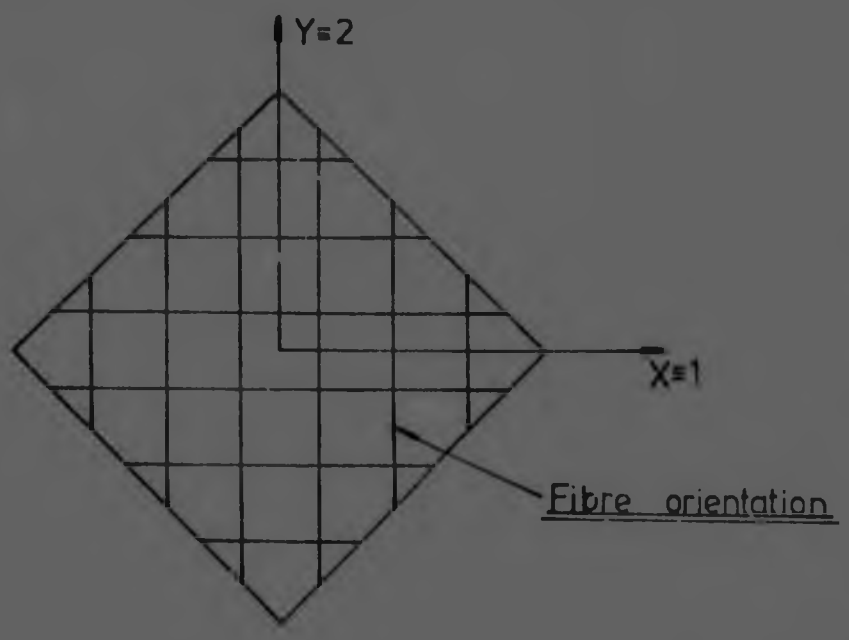

When the monolayers which are described by the above equations are part of a plate then the stresses and forces in the plate are described as follows:

$$N_x = \int_{-h/2}^{h/2} \sigma_x dz$$

$$N_y = \int_{-h/2}^{h/2} \sigma_y dz$$

$$N_{xy} = \int_{-h/2}^{h/2} \sigma_{xy} dz$$

$$M_x = \int_{-h/2}^{h/2} \sigma_x z dz$$

$$M_y = \int_{-h/2}^{h/2} \sigma_y z dz$$

$$M_{xy} = \int_{-h/2}^{h/2} \sigma_{xy} z dz$$

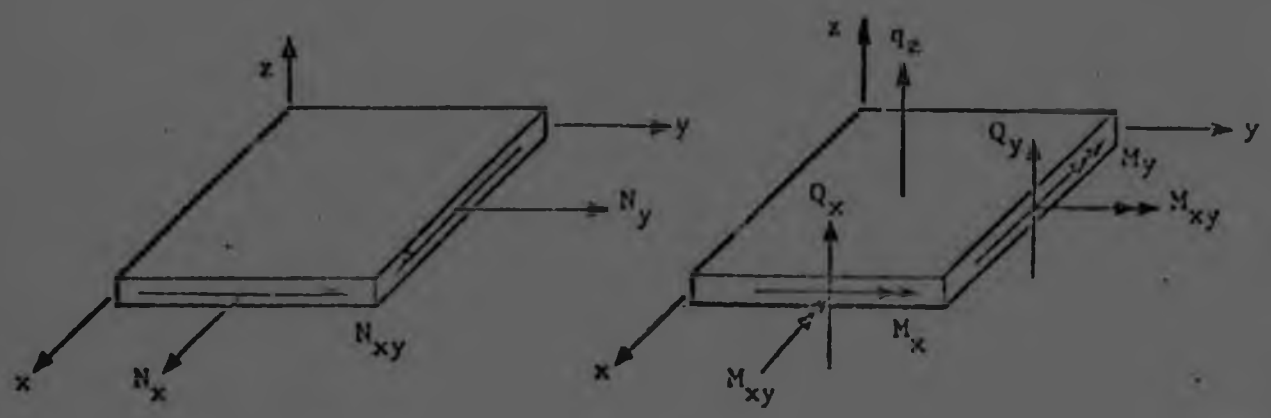

The results of the completed integrations of the equations above are as follows:

$$\left[\begin{array}{c} N_x \\ N_y \\ N_{xy} \\ \hline M_x \\ M_y \\ M_{xy} \end{array}\right] = \left[\begin{array}{ccc:ccc} A_{11} & A_{12} & A_{16} & B_{11} & B_{12} & B_{16} \\ A_{12} & A_{22} & A_{26} & B_{12} & B_{22} & B_{26} \\ A_{16} & A_{26} & A_{66} & B_{16} & B_{26} & B_{66} \\ \hline B_{11} & B_{12} & B_{16} & D_{11} & D_{12} & D_{16} \\ B_{12} & B_{22} & B_{26} & D_{12} & D_{22} & D_{26} \\ B_{16} & B_{26} & B_{66} & D_{16} & D_{26} & D_{66} \end{array}\right] \left[\begin{array}{c} \varepsilon_x \\ \varepsilon_y \\ \varepsilon_{xy} \\ \hline k_x \\ k_y \\ k_{xy} \end{array}\right]$$

where the following applies

$$A_{ij} = \sum_{k=1}^{n} (Q_{ij})_k |h_k - h_{(k-1)}|$$

$$B_{ij} = \tfrac{1}{2} \sum_{k=1}^{n} (q_{ij})_k |h_k^2 - h_{(k-1)}{}^2|$$

$$D_{ij} = \tfrac{1}{3} \sum_{k=1}^{n} (Q_{ij})_k |h_k^3 - h_{(k-1)}{}^3|$$

The equation above can be written as follows:

$$\left[\begin{array}{c} N \\ \\ M \end{array}\right] = \left[\begin{array}{c:c} A & B \\ \hline B & D \end{array}\right] \left[\begin{array}{c} \varepsilon \\ \\ k \end{array}\right]$$

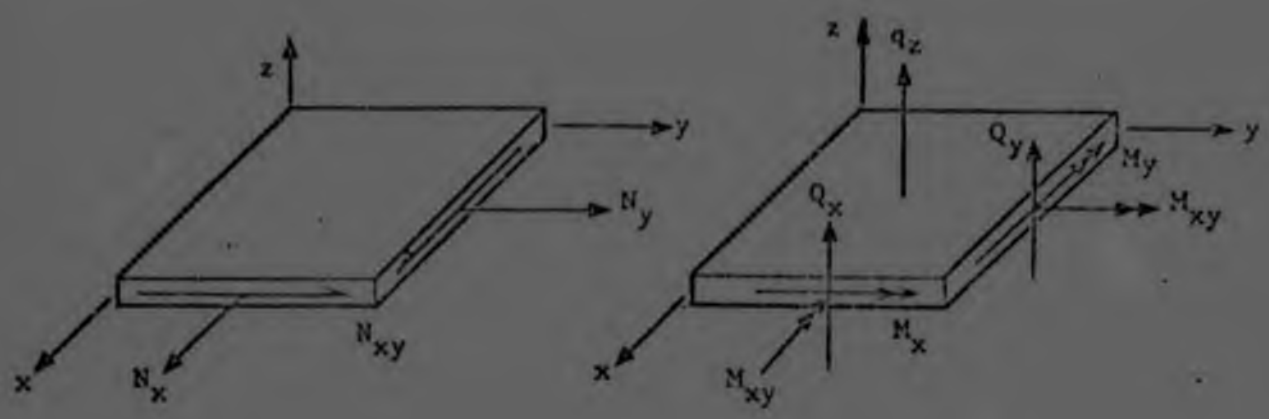

The results of the completed integrations of the equations above are as follows:

$$\begin{bmatrix} N_x \\ N_y \\ N_{xy} \\ \hline M_x \\ M_y \\ M_{xy} \end{bmatrix} = \left[\begin{array}{ccc:ccc} A_{11} & A_{12} & A_{16} & B_{11} & B_{12} & B_{16} \\ A_{12} & A_{22} & A_{26} & B_{12} & B_{22} & B_{26} \\ A_{16} & A_{26} & A_{66} & B_{16} & B_{26} & B_{66} \\ \hdashline B_{11} & B_{12} & B_{16} & D_{11} & D_{12} & D_{16} \\ B_{12} & B_{22} & B_{26} & D_{12} & D_{22} & D_{26} \\ B_{16} & B_{26} & B_{66} & D_{16} & D_{26} & D_{66} \end{array}\right] \begin{bmatrix} \varepsilon_x \\ \varepsilon_y \\ \varepsilon_{xy} \\ \hline k_x \\ k_y \\ k_{xy} \end{bmatrix}$$

where the following applies

$$A_{ij} = \sum_{k=1}^{n} (Q_{ij})_k |h_k - h_{(k-1)}|$$

$$B_{ij} = \frac{1}{2} \sum_{k=1}^{n} (q_{ij})_k |h_k^2 - h_{(k-1)}^2|$$

$$D_{ij} = \frac{1}{3} \sum_{k=1}^{n} (Q_{ij})_k |h_k^3 - h_{(k-1)}^3|$$

The equation above can be written as follows:

$$\begin{bmatrix} N \\ \\ M \end{bmatrix} = \left[\begin{array}{c:c} A & B \\ \hdashline B & D \end{array}\right] \begin{bmatrix} \varepsilon \\ \\ k \end{bmatrix}$$

The complexity of the equations given here decreases for laminates with higher degrees of symmetry. A laminate which is symmetrical about the (x,y) midplane would be described by $Q_{ij}(z) = Q_{ij}(-z)$.

Then

$$B_{ij} = 0$$

This means that the laminate constitutive equations are uncoupled and thus

$$\begin{bmatrix} N \\ M \end{bmatrix} = \begin{bmatrix} A & \\ & D \end{bmatrix} \begin{bmatrix} \varepsilon \\ k \end{bmatrix}$$

All laminates may be reduced to the uncoupled form by utilizing mid-surface symmetry for the monolayer orientations. Often, it is a necessary restriction, since single stage cured plates can not be made to remain flat. Membrane shrinkage following the laminate cure is coupled with curvature change. That is why unbalanced laminates are normally warped.

The concept of average stresses and strains may be applied to the calculations of monolayer stresses in multilayer laminates.

Thus

$$\begin{bmatrix} N_x \\ N_y \\ N_{xy} \end{bmatrix} = \begin{bmatrix} A_{11} & A_{12} & A_{16} \\ & A_{22} & A_{26} \\ & & A_{66} \end{bmatrix} \begin{bmatrix} \varepsilon_x \\ \varepsilon_y \\ \varepsilon_{xy} \end{bmatrix}$$

Dividing both sides by h and defining

of the middle plane of the plate are ignored. Therefore it is sufficient for us to calculate the strain energy by bending and twisting only as this will be applicable, for reasons of the above assumption, to all loading cases. Thus, the total strain energy U of the rectangular plate a x b is, from Ref 11,

$$U = \frac{D}{2} \int_0^a \int_0^b \{ (\frac{\partial^2 w}{\partial x^2} + \frac{\partial^2 w}{\partial y^2})^2 - 2(1 - \nu) | \frac{\partial^2 w}{\partial x^2} \frac{\partial^2 w}{\partial y^2} - (\frac{\partial^2 w}{\partial x \partial y}) | \} dx\, dy \qquad (1)$$

The potential energy of in-plane loads is, for the general case of compressive loads acting on both sides of the plate as well as shear loads,

$$V = -\tfrac{1}{2} \int_b^a \int_o^b | N_x (\frac{\partial w}{\partial x})^2 + N_y (\frac{\partial w}{\partial y})^2 + 2N_{xy} \frac{\partial w}{\partial x} \frac{\partial w}{\partial y} | dw\, dy \qquad (2)$$

The energy formulation of the Rayleigh-Ritz method, in mathematical terms states:

$$\frac{\partial (U + V)}{\partial A_{mm}} = 0 \qquad (3)$$

where A_{mn} are the unknown coefficients of the deflection $w(x,y)$ of the plate in the buckled state.

Defining a mathematical function which both satisfies the boundary conditions for clamped edges,

$$\frac{\partial w}{\partial x} = w = 0 \qquad \text{at } x = 0,a$$

$$\frac{\partial w}{\partial y} = w = 0 \qquad \text{at } y = 0,b$$

and adequately simulates the buckled shape of the plate, and substituting in the equations above, yields the buckling stress of the panel.

$$\begin{bmatrix} \bar{\sigma}_x \\ \bar{\sigma}_y \\ \bar{\sigma}_{xy} \end{bmatrix} = \frac{1}{h} \begin{bmatrix} N_x \\ N_y \\ N_{xy} \end{bmatrix}$$

$$\frac{A_{ij}}{h} = a_{ij} (i,j = 1,2,6)$$

We obtain:

$$\begin{bmatrix} \bar{\sigma}_x \\ \bar{\sigma}_y \\ \bar{\sigma}_{xy} \end{bmatrix} = \begin{bmatrix} a_{11} & a_{12} & a_{16} \\ & a_{22} & a_{26} \\ & & a_{66} \end{bmatrix} \begin{bmatrix} \varepsilon_x \\ \varepsilon_y \\ \varepsilon_{xy} \end{bmatrix}$$

Once the laminate constitutive equations have been established we can proceed with calculating the buckling load.

Two approximations will be made,both being results of the energy Rayleigh-Ritz method of analysis.

1. The plate will be considered homogeneous and the assumption will be made that the fiber orientation is such as to make the composite isotropic.

   This means that the total sum of the strain energy produced by bending and twisting plus the potential energy of the in-plane shear load acting on the plate has a stationary value in the neutral equilibrium of its buckled state. This is equivalent to stating that the shear load,

   $N_{xy} = N_{xy,cr}$

   It must be emphasised here that in thin plate analysis we are concerned with deflections normal to the unloaded surface of the plate. These, as in the case of slender beams, are assumed to be primarily due to bending action so that the effects of shear strain and shortening or stretching

Solutions for this problem have been obtained in the form

$$\tau_{cr} = K \frac{\pi^2 E}{12(1 - \nu^2)} \left(\frac{t}{b}\right)^2$$

where the coefficients K are dependent on the edge supports and are graphically given in Ref 10.

The expression above can be redefined

$$\tau_{cr} = K \pi^2 \frac{D}{tb^2}$$

where $D = \frac{Et^3}{12(1 - \nu^2)}$, the flexural rigidity of the plate.

Since equation 1 was defined for isotropic materials the results above are applicable to anisotropic materials only if the assumption is made that the composite behaves isotropically.

2. The plate is considered anisotropic. The governing differential equation for such a plate when the laminate and fiber axes do not coincide is, according to Ref (5),

$$D_{11} \frac{\partial w}{\partial xy} + 4D_{16} \frac{\partial^4 w}{\partial x^3 \partial y} + 2(D_{12} + 2D_{66}) \frac{\partial^4 w}{\partial x^2 \partial y^2} + 4D_{26} \frac{\partial^4 w}{\partial x \partial y^3} +$$

$$D_{22} \frac{\partial^4 w}{\partial y^4} + 2N_{xy} \frac{\partial^2 w}{\partial x \partial y} = 0$$

No close form solutions are obtained for the above equation for the case of all four edges clamped. Thus the solution by the well-known static method is not only tedious but very lengthy. Therefore, the Rayleigh-Ritz method is again used. Solutions have been obtained by Ashton and Love (Ref (13)) and the method described is as follows.

The potential energy due to bending of a thin rectangular plate is given by,

$$= \frac{1}{2} \iint_A D_{11} \left(\frac{\partial^2 w}{\partial x^2}\right)^2 + 2D_{12} \frac{\partial^2 w}{\partial x^2} \frac{\partial^2 w}{\partial y^2} + D_{22} \left(\frac{\partial^2 w}{\partial y^2}\right)^2 +$$

$$\frac{4\partial^2 w}{\partial x \partial y}\Big| D_{16} \frac{\partial^2 w}{\partial x^2} + D_{26} \frac{\partial^2 w}{\partial y^2} + D_{66} \frac{\partial^2 w}{\partial x \partial y}\Big| \, dx \, dy$$

In the formulation of the solutions below, the deflection $w(x,y)$ is of the form:

$$w(x,y) = \sum_{m=1}^{p} \sum_{n=1}^{q} a_{mn} X_m(x) Y_n(y)$$

where $X_m(x)$ and $Y_n(y)$ are functions which satisfy the boundary conditions of a rectangular plate at the edges $x = 0$, a and $y = 0$, b. The coefficients a_{mn} are parameters which are determined by minimizing the energy expressions. This is achieved by differentiating with respect to each a_{mn}. Substituting the series expression for $w(x,y)$ into the expression for V and differentiating with respect to a_{mn}, the following result is obtained

$$\frac{\partial V}{\partial a_{ik}} = \sum_{m=1}^{p} \sum_{n=1}^{q} d_{ikmn} a_{mn}$$

where

$$d_{ikmn} = D_{11} \psi_{3im} \psi_{1kn} \frac{b}{a^3} + D_{12} (\psi_{5im} \psi_{5nk} + \psi_{5mi} \psi_{5kn})$$

$$\times \frac{1}{ab} + D_{22} \psi_{1im} \psi_{3kn} \frac{a}{b^3} + 2D_{16} (\psi_{6mi} \psi_{4kn} + \psi_{6im} \psi_{4nk})$$

$$\times \frac{1}{a^2} + 2D_{26} (\psi_{4im} \psi_{6nk} + \psi_{4mi} \psi_{6kn})$$

$$\times \frac{1}{b^2} + 4D_{66} \psi_{2im} \psi_{2kn} \frac{1}{ab}.$$

The potential energy of the inplane loads is,

$$U = -\frac{1}{2}\int_0^a \int_0^b (N_x W^2_{,x} + N_y W^2_{,y} + 2N_{xy} W_{,x} W_{,y})dxdy$$

Substitution of the above equation of deflection w(x,y) gives, after differentiation,

$$\frac{\partial U}{\partial a_{ik}} = \sum_{m=1}^{p} \sum_{n=1}^{q} \ell_{ikmn} a_{mn}$$

where

$$\ell_{ikmn} = N_{xy}(\psi_{,im}\psi_{,nk} + \psi_{,mi}\psi_{,kn})$$

The series expressions used for the deflection of the plate, $X_m(x)$ and $Y_n(y)$, are beam mode shape functions of a unit length clamped - clamped beam. It should be noted that the larger the number of modes of vibration used in the approximating series, the better the accuracy. However the fact that computing time also increases considerably brings in a compromising factor.

The principle of stationary value of the total potential energy is then applied to the formulation. Therefore,

$$\sum_{m=1}^{p} \sum_{n=1}^{q} d_{ikmn} a_{mn} - \sum_{m=1}^{p} \sum_{n=1}^{q} \ell_{ikmn} a_{mn} = 0$$

$$i, k, m, n = 1,\ldots p(q)$$

The problem is now reduced to the common eigenvalue problem in the form

$$[A] - \lambda[B] = 0$$

where the matrix [A] is a two-dimensional array equivalent

The potential energy of the inplane loads is,

$$U = -\frac{1}{2}\int_0^a \int_0^b (N_x W^2_{,x} + N_y W^2_{,y} + 2N_{xy} W_{,x} W_{,y})dxdy$$

Substitution of the above equation of deflection w(x,y) gives, after differentiation,

$$\frac{\partial U}{\partial a_{ik}} = \sum_{m=1}^{p} \sum_{n=1}^{q} \ell_{ikmn} a_{mn}$$

where

$$\ell_{ikmn} = N_{xy}(\psi_{4im}\psi_{4nk} + \psi_{4mi}\psi_{4kn})$$

The series expressions used for the deflection of the plate, $X_m(x)$ and $Y_n(y)$, are beam mode shape functions of a unit length clamped - clamped beam. It should be noted that the larger the number of modes of vibration used in the approximating series, the better the accuracy. However the fact that computing time also increases considerably brings in a compromising factor.

The principle of stationary value of the total potential energy is then applied to the formulation. Therefore,

$$\sum_{m=1}^{p} \sum_{n=1}^{q} d_{ikmn} a_{mn} - \sum_{m=1}^{p} \sum_{n=1}^{q} \ell_{ikmn} a_{mn} = 0$$

$$i, k, m, n = 1,\ldots p(q)$$

The problem is now reduced to the common eigenvalue problem in the form

$$[A] - \lambda[B] = 0$$

where the matrix [A] is a two-dimensional array equivalent

to the four-dimensional d_{ikmn} and the same applies to the correspondence between [B] and ℓ_{ikmn}.

The lowest value of λ which satisfies the above equation is the buckling load of the panel. The solution as described above can be rapidly obtained on a high-speed digital computer and for four modes of vibration (16 × 16 matrix) this was achieved on an IBM 370-158 is less than 0,5 seconds.

EXPERIMENTAL PROCEDURE

All the composite panels were layed by hand and the method used was as follows: two glass sheets of surface area 1 m^2 were covered on one side by mould release wax and epoxy resin was spread by means of an ordinary paint roller over one of the surfaces. The in advance cut layers of fibre were then placed according to the intended fibre orientation and required plate thickness. Finally when all the necessary epoxy and fibre had been used the top glass sheet - in this case the 2nd part of the mould - was pressed onto the composite by means of a 450 N weight. The amount of epoxy to be used was calculated before laying the panels in order to achieve a constant percentage of fibre composite. This was checked in the case of fibreglass against the measured value of percentage fibre. This check was carried out as follows: a small piece of the panel was cut, after the test was completed, and weighed. This was then put into an oven at 600 ^{o}C where all the epoxy melted away. The residue (fibre only) was weighed and by knowing the densities of both the epoxy resin and the fibre the percentage fibre by volume was calculated. The value thus obtained was found to be in error by the amount corresponding to void volume and air bubbles in the composite. This means that when laying the panels an effort should be made to 'force' all air bubbles out.

Since the experimental program, including the curing of the panels, was carried out in summer, ambient temperatures were never below 15 ^{o}C and thus a 24 hour curing time was allowed.

The composite was then removed from the mould, cut to the dimensions of the frame and drilled along the edges. It was clamped in the frame and all the bolts were torqued to 20 N-m. The frame was secured in the jaws of the machine by means of two lugs. The shear test was executed according to the method explained by Ashton and Love in Ref 1. Two strain gauges in the centre of the panel on opposite sides gave the indication of buckling. However this method is not a standard procedure and could give erroneous results (see 'Discussion'). The exact procedure adopted was: the two strain gauges were oriented in the compression direction (of the resolved shear force). Thus when the plate is tested, the two strain gauges will indicate compression until, when buckling starts due to the formation of a half-wave in the centre of the panel, one of the gauges will indicate less compression than the other. It was initially decided that the exact buckling load would be defined at the point where the slope of the load vs strain curve was infinity.

The material properties used in the theoretical calculations were obtained by simple tensile tests on coupons having the fibres oriented in the direction related to the property required. The shear modulus was obtained by the method described in Ref (15). The test was carried out on: 3 aluminium panels; 4 glass fibre, 3 carbon fibre and 4 asbestos fibre composite panels.

DESCRIPTION OF THE APPARATUS

An Amsler tensile testing machine (50 Tonnes) was used to run the shear tests (test fixture as described in Ref 1). Strain gauges of the type KFC-5-C1-23 were used on the aluminium panels and since the composites tested have a thermal conductivity relatively close to that of steel, KFC-5-C1-11 gauges were used on these panels. The readings of the gauges were obtained from a strain meter where the appropriate gauge factor was selected.

An Instron testing machine (50 tonnes) was used to test the coupons of the composite materials and the strain gauges and strain meter used were the same as described above.

LIST OF PRICES

The prices of the materials used in the research program were supplied by the Commercial Air Services (Comair), [illegible] Airport, Germiston, the Council for Scientific and Industrial Research, Pretoria, and Cape Asbestos, Johannesburg. The list obtained is as follows:

Aluminium (2024 - T3):

t = 1 mm - P = 18,5 R/m^2

t = 1,27 mm - P = 22,5 R/m^2

t = 1,60 mm - P = 30,3 R/m^2

Glass Fibre (Type 181 - E - glass)

P = 3 R/m^2

Carbon Fibre (Type 2002 - Toray)

P = R40/m^2

Asbestos Fibre (Blue Fibre - Noramite)

P = 0,18 R/m^2

OBSERVATIONS

A. Aluminium

(i) Plate thickness t = 1,6 mm
Mass of the plate w = 664 g

Shear Force (kN)	$\varepsilon_1 \times 10^{-3}$	$\varepsilon_2 \times 10^{-3}$
0	0	0
2,83	-0,130	-0,124
5.66	-0,272	-0,194
8,49	-0,455	-0,219
11,31	-0,655	-0,194
12,73	-0,780	-0,169
14,14	-0,927	-0,109

(ii) Plate thickness t = 1,27 mm
Mass of the plate w = 561 g

Shear Force (kN)	$\varepsilon_1 \times 10^{-3}$	$\varepsilon_2 \times 10^{-3}$
0	0	0
0,707	-0,030	-0,030
2,120	-0,080	-0,105
3,540	-0,133	-0,195
4,950	-0,160	-0,307
6,360	-0,125	-0,455
7,07	-0,065	-0,557

(iii) Plate thickness t = 1,00 mm
Mass of the plate w = 422 g

Shear Force (kN)	$\varepsilon_1 \times 10^{-3}$	$\varepsilon_2 \times 10^{-3}$
0	0	0
0,707	-0,040	-0,047
1,414	-0,090	-0,090
2,120	-0,170	-0,117
2,830	-0,275	-0,102
3,540	-0,410	-0,057
4,240	-0,525	-0,007
4,950	-0,630	+0,032

B. Glass fibre composite

(i) Plate thickness t = 1,6 mm
Mass of the plate w = 373 g
No of layers of fibre = 4

Shear Force (kN)	$\varepsilon_1 \times 10^{-3}$	$\varepsilon_2 \times 10^{-3}$
0	0	0
0,707	-0,115	-0,095
1,417	-0,220	-0,180
2,120	-0,330	-0,240
2,830	-0,560	-0,245
3,540	-0,810	-0,132
4,240	-1,110	+0,145
4,950	-1,400	+0,345

(ii) Plate thickness t = 1,8 mm
Mass of the plate w = 450 g
No of layers of fibre = 5

Shear Force (kN)	$\varepsilon_1 \times 10^{-3}$	$\varepsilon_2 \times 10^{-3}$
0	0	0
0,707	-0,120	-0,100
1,414	-0,220	-0,190
2,120	-0,330	-0,280
2,830	-0,445	-0,340
3,540	-0,555	-0,375
4,240	-0,735	-0,370
4,950	-0,980	-0,245

(iii) Plate thickness t = 2,2 mm
Mass of the plate w = 553 g
No of layers o fibre = 6

Shear Force (kN)	$\varepsilon_1 \times 10^{-3}$	$\varepsilon_2 \times 10^{-3}$
0	0	0
0,7(7	-0,077	-0,050
2,120	-0,247	-0,165
3,540	-0,402	-0,280
4,9?0	-0,567	-0,370
6,364	-0,772	-0,410
7,778	-1,042	-0,375
8.485	-1,262	-0,280

(iv) Plate thickness t = 2,4 mm
Mass of the plate w = 615 g
No of layers of fibre = 7

Shear Force (kN)	$\varepsilon_1 \times 10^{-3}$	$\varepsilon_2 \times 10^{-3}$
0	0	0
1,414	-0,090	-0,140
2,830	-0,190	-0,275
4,240	-0,320	-0,385
5,657	-0,465	-0,485
7,071	-0,575	-0,560
8,485	-0,715	-0,620
9,899	-0,875	-0,650
10,610	-0,990	-0,630

C. Carbon fibre composite

(i) Plate thickness t = 1,40 mm
Mass of the plate w = 308 g
No of layers of fibre = 5

Shear force (kN)	$\varepsilon_1 \times 10^{-3}$	$\varepsilon_2 \times 10^{-3}$
0	0	0
0,707	-0,085	-0,05
1,414	-0,180	-0,085
2,120	-0,290	-0,092
2,830	-0,405	-0,065
3 540	-0,585	0,015

(ii) Plate thickness t = 1,50
Mass of the plate w = 370 g
No of layers of fibre = 6

Shear Force (kN)	$\varepsilon_1 \times 10^{-3}$	$\varepsilon_2 \times 10^{-3}$
0	0	0
1,414	-0,105	-0,040
2,120	-0,175	-0,055
2,830	-0,260	-0,055
3,540	-0,370	-0,020

(iii) Plate thickness t = 1,82 mm
Mass of the plate w = 430 g
No of layers of fibre = 7

Shear Force (kN)	$\varepsilon_1 \times 10^{-3}$	$\varepsilon_2 \times 10^{-3}$
0	0	0
0,707	-0,03	-0,05
2,120	-0,08	-0,16
3,536	-0,14	-0,25
4,950	-0,170	-0,36
6,360	-0,130	-0,54

D. Asbestos fibre composite

(i) Plate thickness t = 3,232 mm
Mass of the plate w = 579 g
No.of layers of fibre = 4

Shear Force (kN)	$\varepsilon_1 \times 10^{-1}$	$\varepsilon_2 \times 10^{-3}$
0	0	0
1,414	-0,195	-0,245
2,828	-0,400	-0,525
4,243	-0,575	-0,805
5,657	-0,755	-1,125
7,071	-0,915	-1,420
8,485	-0,985	-1,820
9,900	-1,015	-2,045
11,314	Buckling	

(ii) Plate thickness t = 3,4 mm
Mass of the plate w = 621 g
No of layers of fibre = 5

Shear Force (kN)	$\varepsilon_1 \times 10^{-1}$	$\varepsilon_2 \times 10^{-3}$
0	0	0
1,414	-0,205	-0,230
2,828	-0,445	-0,405
4,243	-0,715	-0,575
5,657	-1,000	-0,670
7,071	-1,285	-0,730
7,778	-1,445	-0,725
8,485	-1,670	-0,690

(iii) Plate thickness t = 4,1 mm
Mass of the plate w = 753 g
No of layers of fibre = 6

Shear Force (kN)	$\varepsilon_1 \times 10^{-3}$	$\varepsilon_2 \times 10^{-3}$
0	0	0
2,828	-0,440	-0,340
5,657	-0,920	-0,665
8,485	-1,380	-0,985
11,314	-1,865	-1,310
14,142	-2,295	-1,630
16,971	-2,705	-1,915
17,678	F A I L U R E	

(iv) Plate thickness t = 5,3 mm
Mass of the plate w = 939,5 g
No of layers of fibre = 7

Shear Force (kN)	$\varepsilon_1 \times 10^{-3}$	$\varepsilon_2 \times 10^{-3}$
0	0	0
2,828	-0,400	-0,280
5,657	-0,760	-0,640
8,485	-1,130	-1,030
14,142	-2,095	-1,490
16,971	-2,600	-1,725
19,799	-3,150	-1,960
24,749	F A I L U R E	

GRAPHS

GRAPH 1

AL-2024-T3 (ALCLAD)

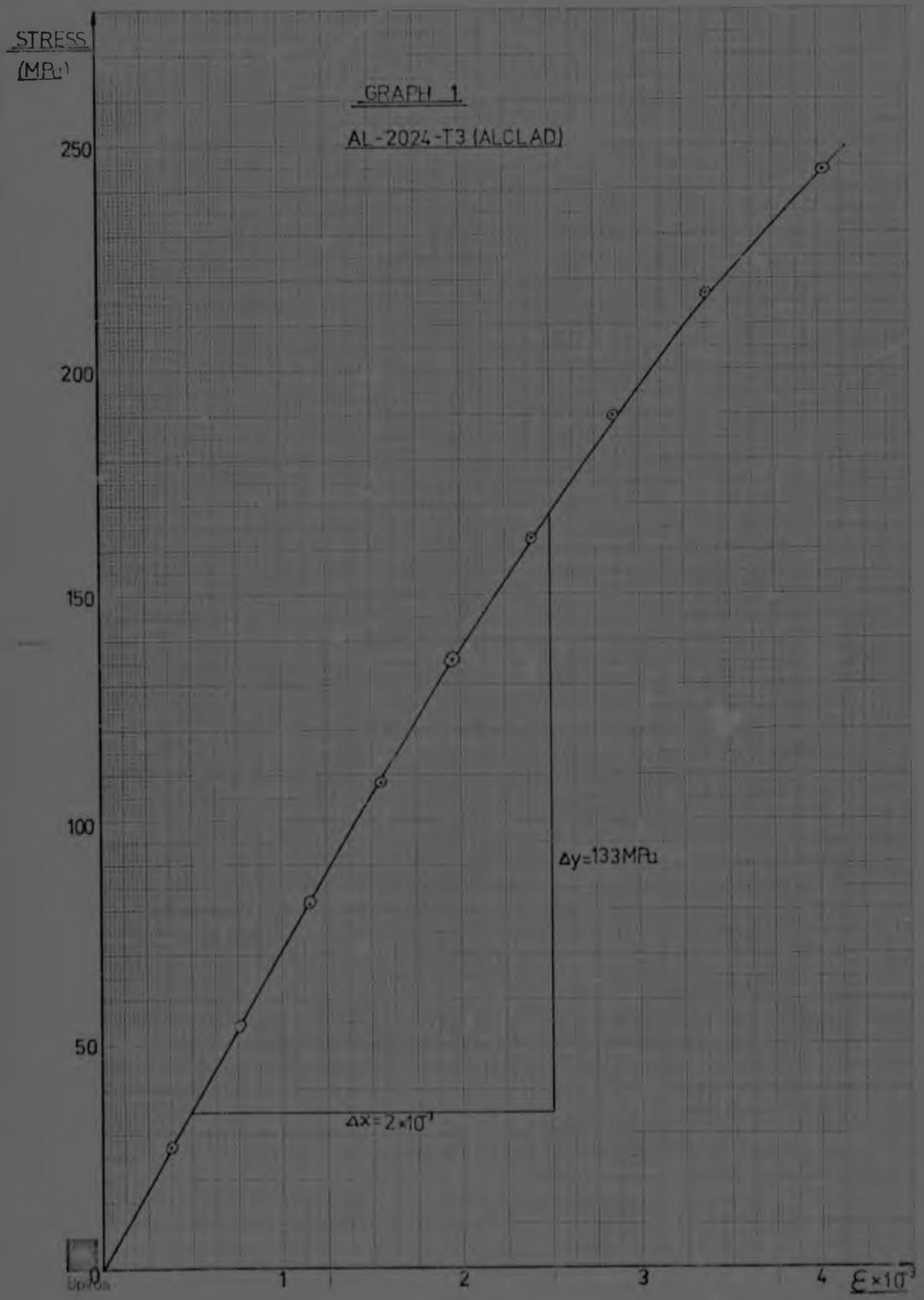

STRESS (MPa)

GRAPH 2

FIBREGLASS COMPOSITE

LONGITUDINAL RESPONSE

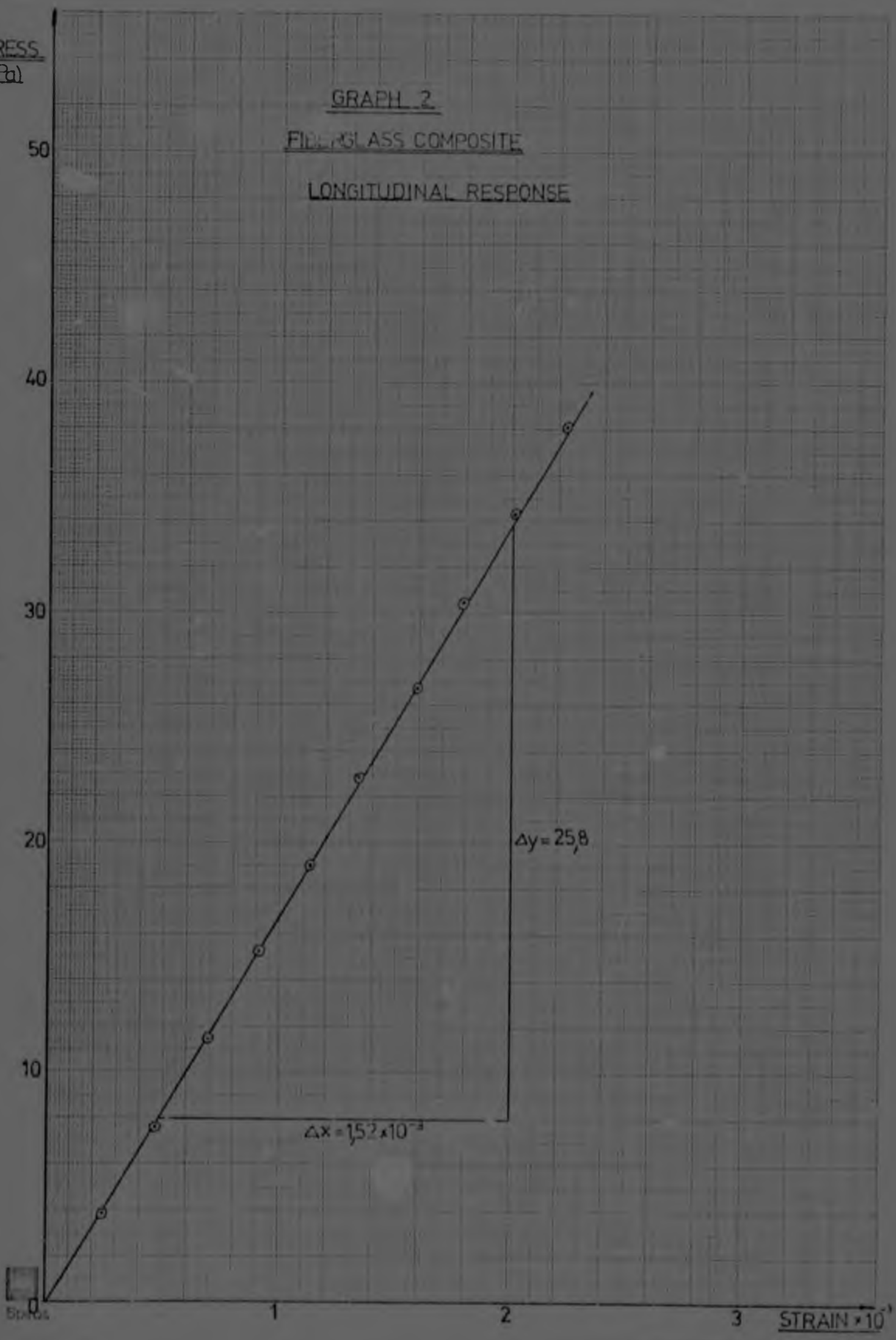

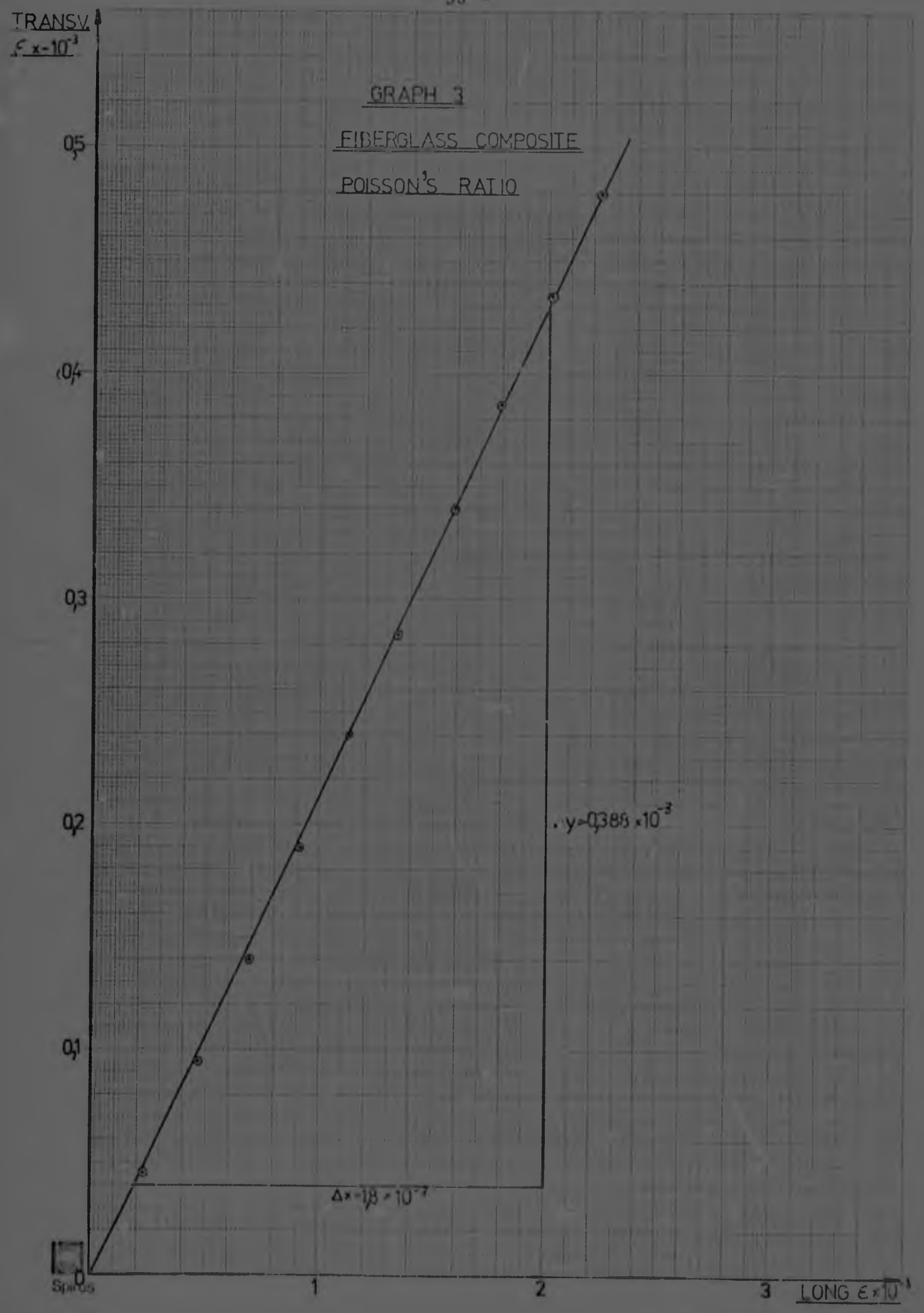
TRANSV.
$\epsilon \times 10^{-3}$
GRAPH 3
FIBERGLASS COMPOSITE
POISSON'S RATIO
0,5
0,4
0,3
0,2
0,1
0
Spross
1
2
3
LONG $\epsilon \times 10^{-3}$
$\Delta y = 0{,}386 \times 10^{-3}$
$\Delta x = 1{,}8 \times 10^{-3}$

GRAPH 4

FIBERGLASS COMPOSITE

SHEAR MODULUS

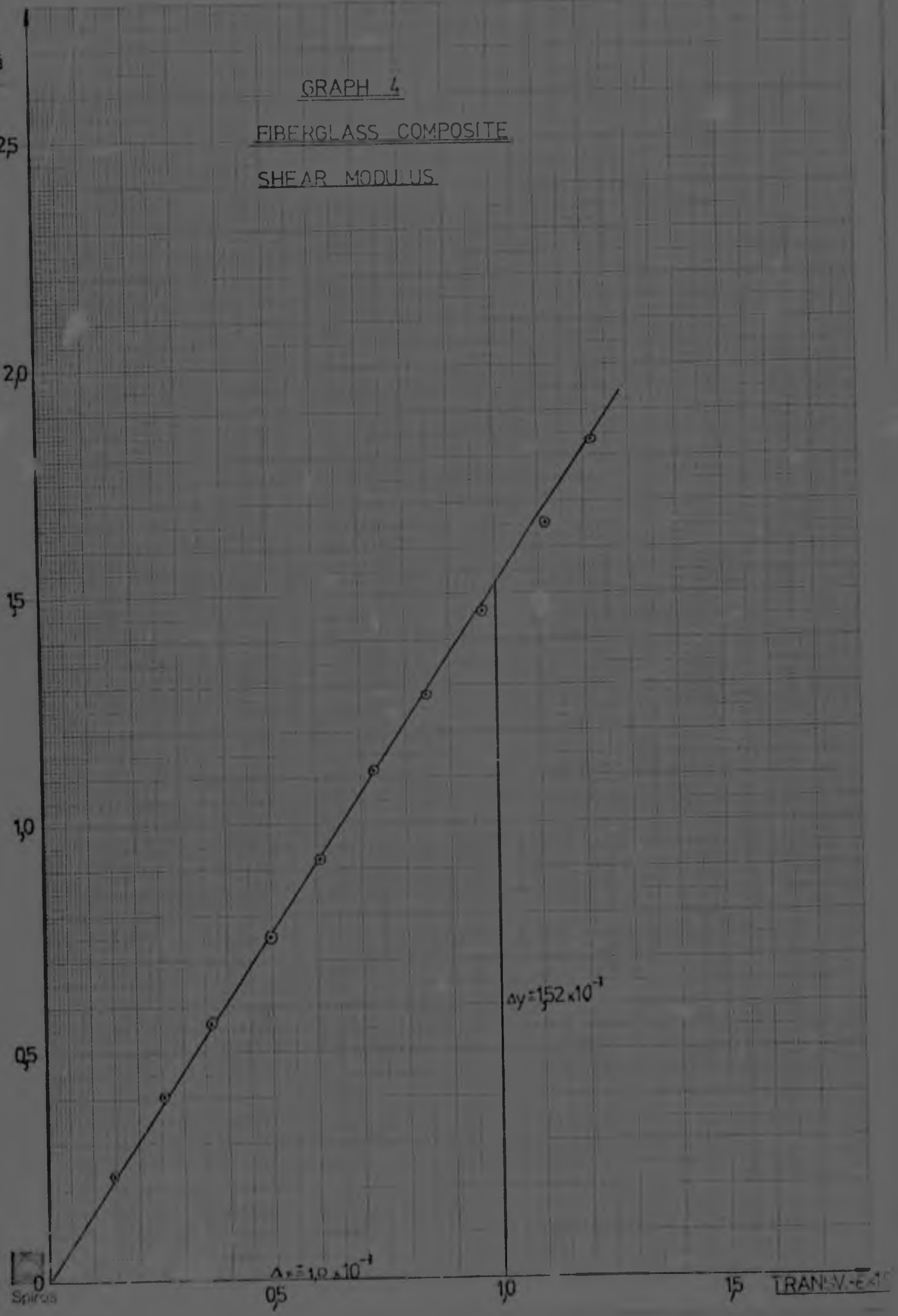

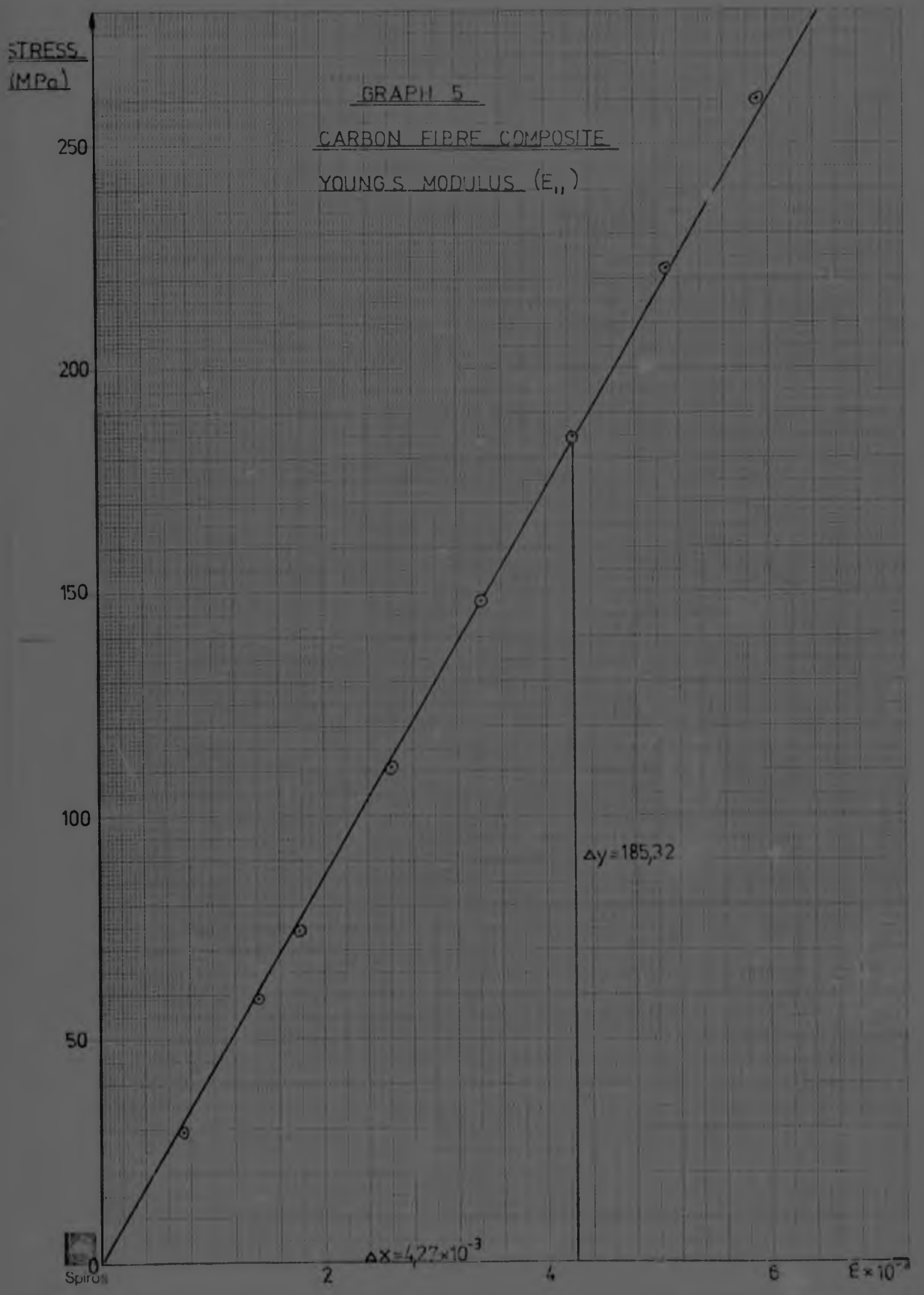
STRESS (MPa)
GRAPH 5
CARBON FIBRE COMPOSITE
YOUNG'S MODULUS ($E_{//}$)
250
200
150
100
50
0
Spiro%
2
4
6
$\varepsilon \times 10^{-3}$
$\Delta y = 185,32$
$\Delta x = 4,27 \times 10^{-3}$

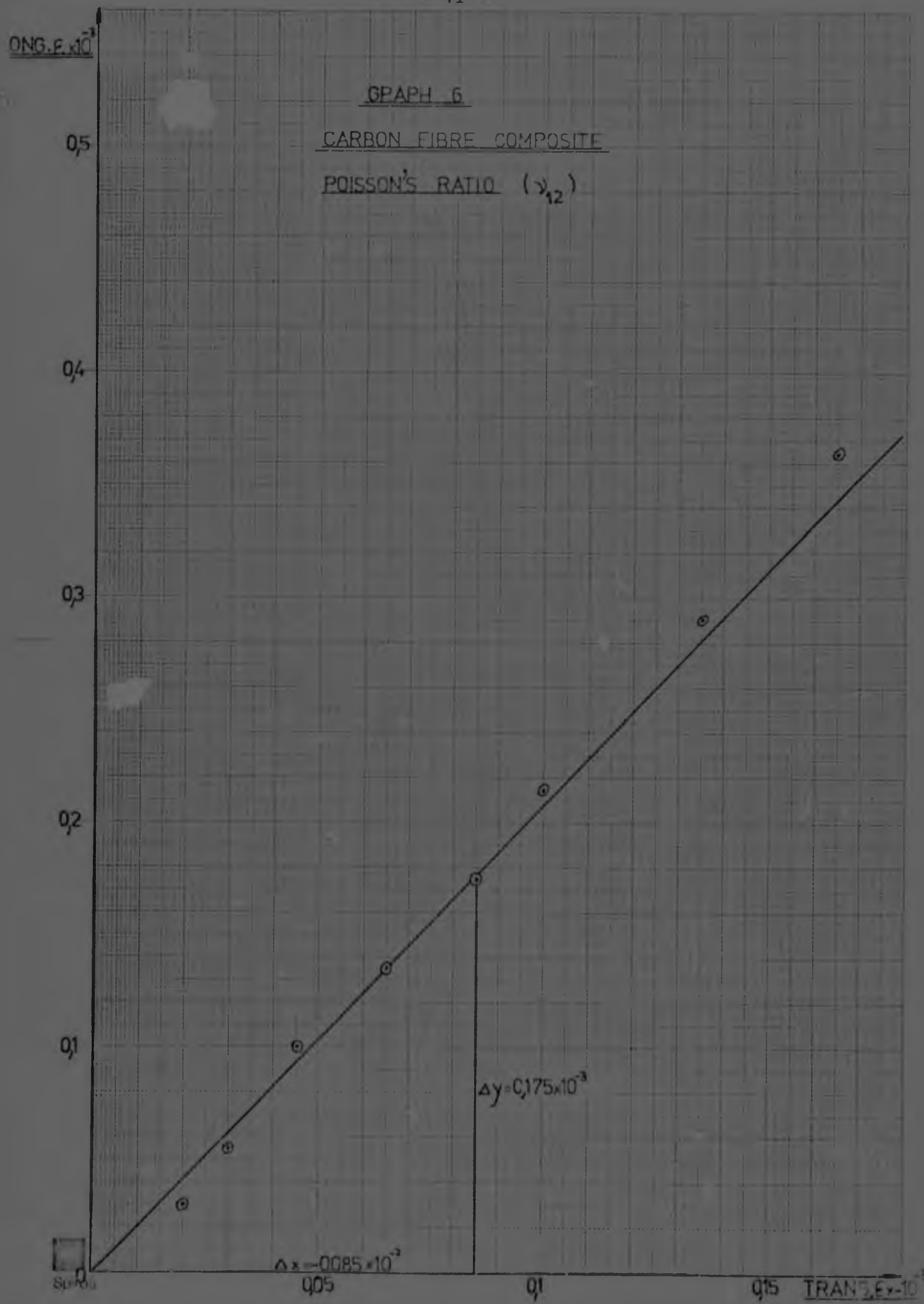

GRAPH 6

CARBON FIBRE COMPOSITE

POISSON'S RATIO (ν_{12})

GRAPH 7

CARBON FIBRE COMPOSITE

YOUNG'S MODULUS (E_{22})

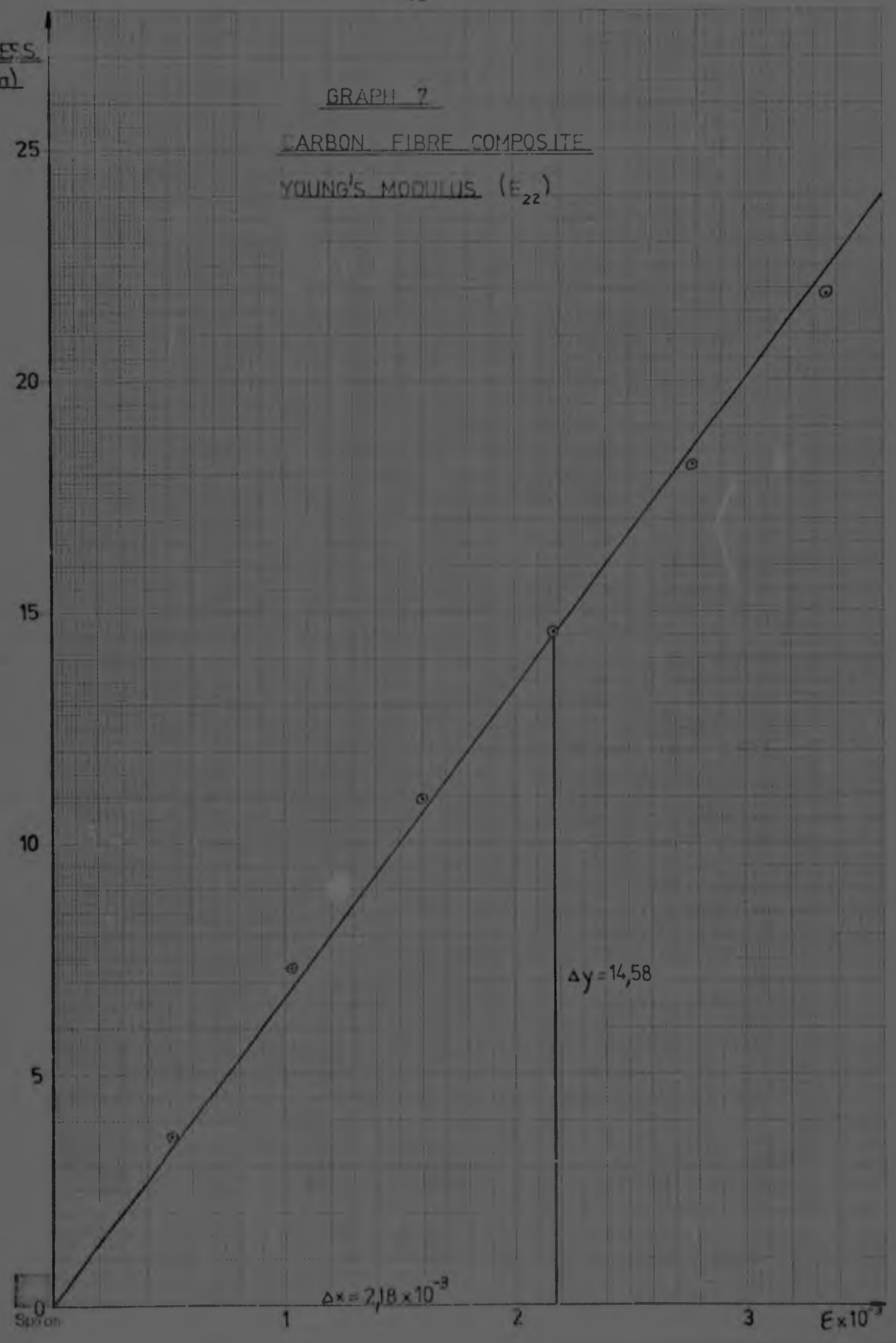

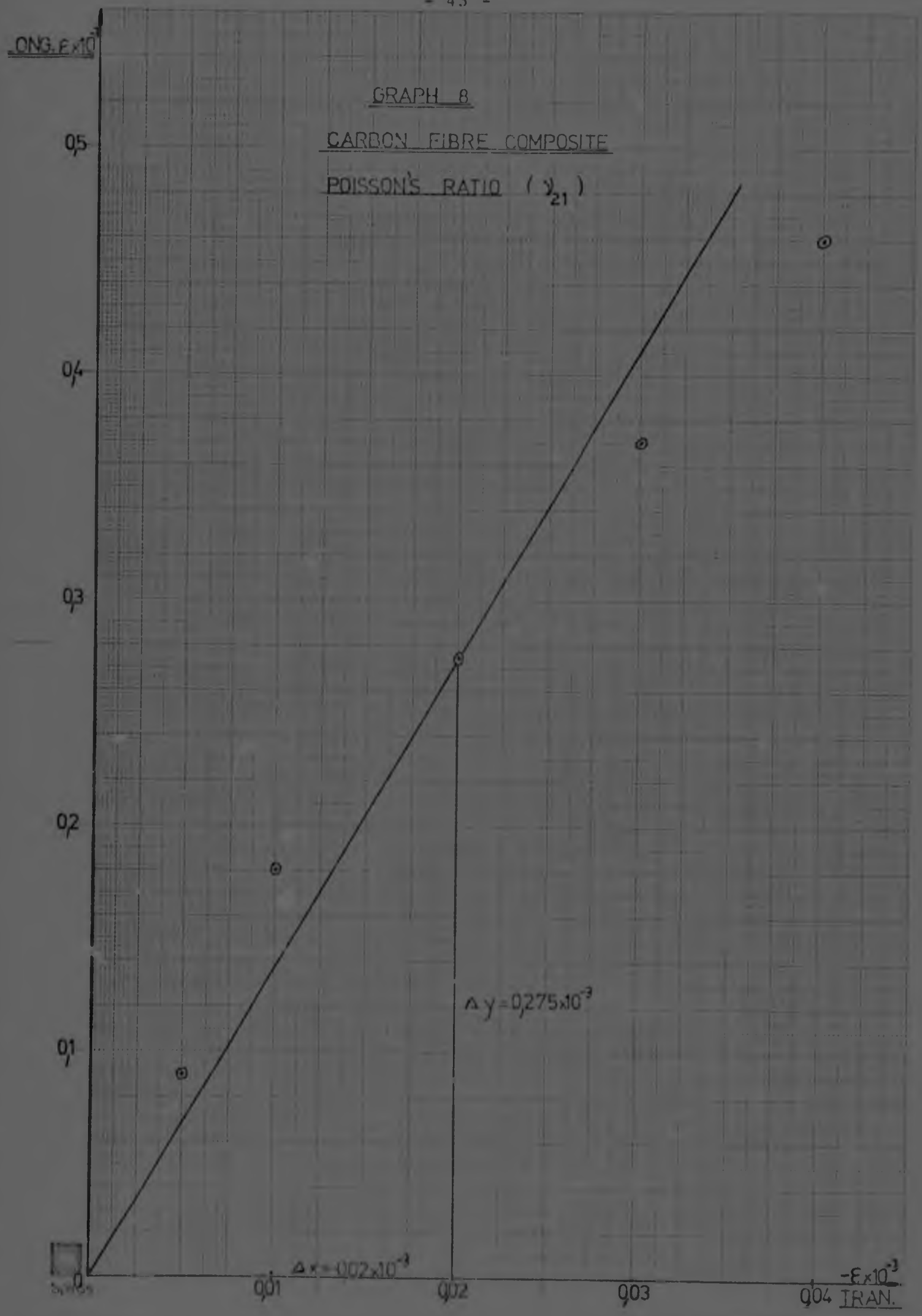
ONG. E×10³
GRAPH 8
CARBON FIBRE COMPOSITE
POISSON'S RATIO (ν21)
0,5
0,4
0,3
0,2
0,1
0
Δy = 0,275×10⁻³
Δx = 0,02×10⁻³
0,01
0,02
0,03
0,04
-E×10⁻³
IRAN.

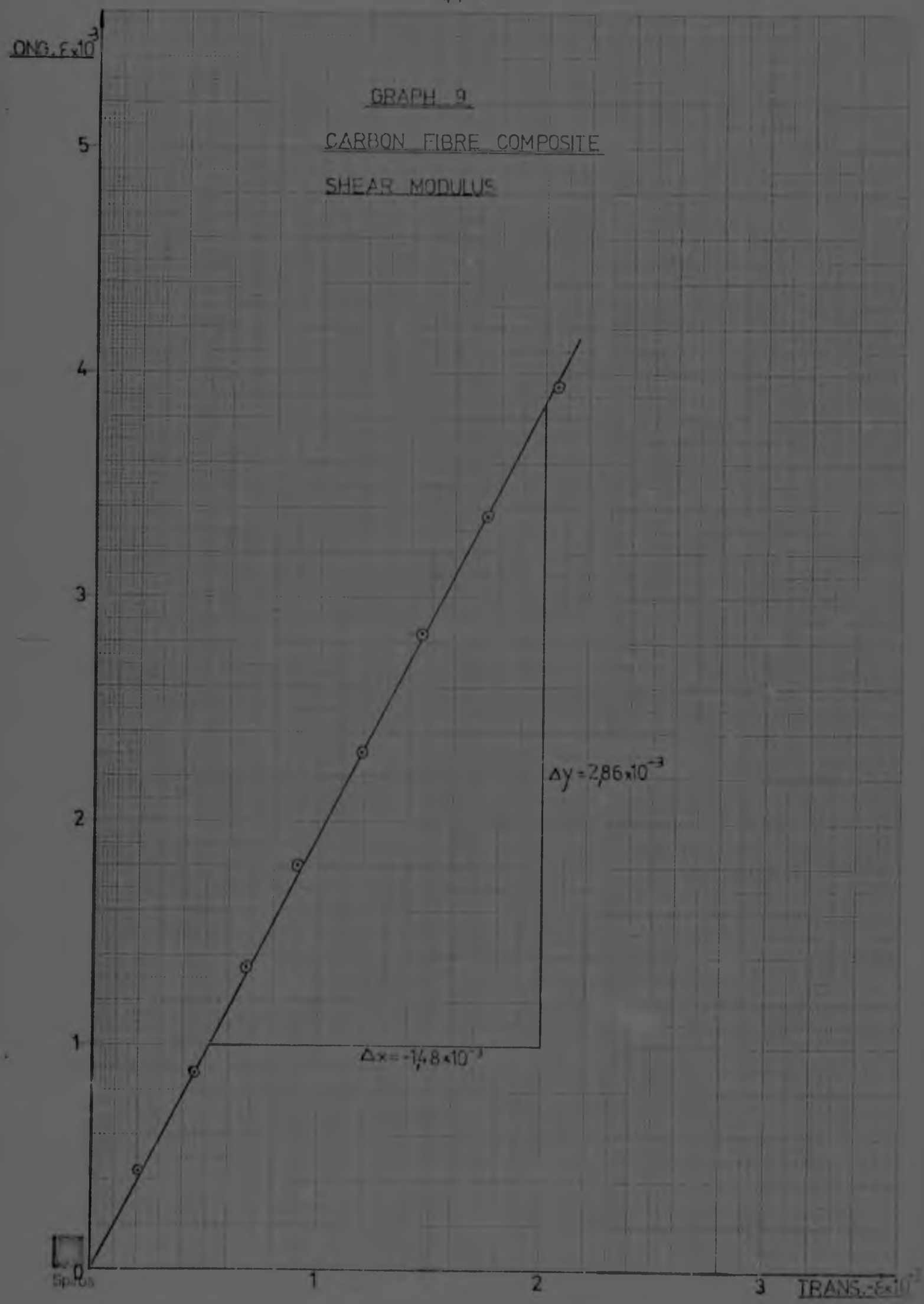
GRAPH 9
CARBON FIBRE COMPOSITE
SHEAR MODULUS
ONG. E x10^3
5
4
3
2
1
0
Δy = 2,86x10^-3
Δx = -1,48x10^-3
1
2
3
TRANS.-E x10^-3

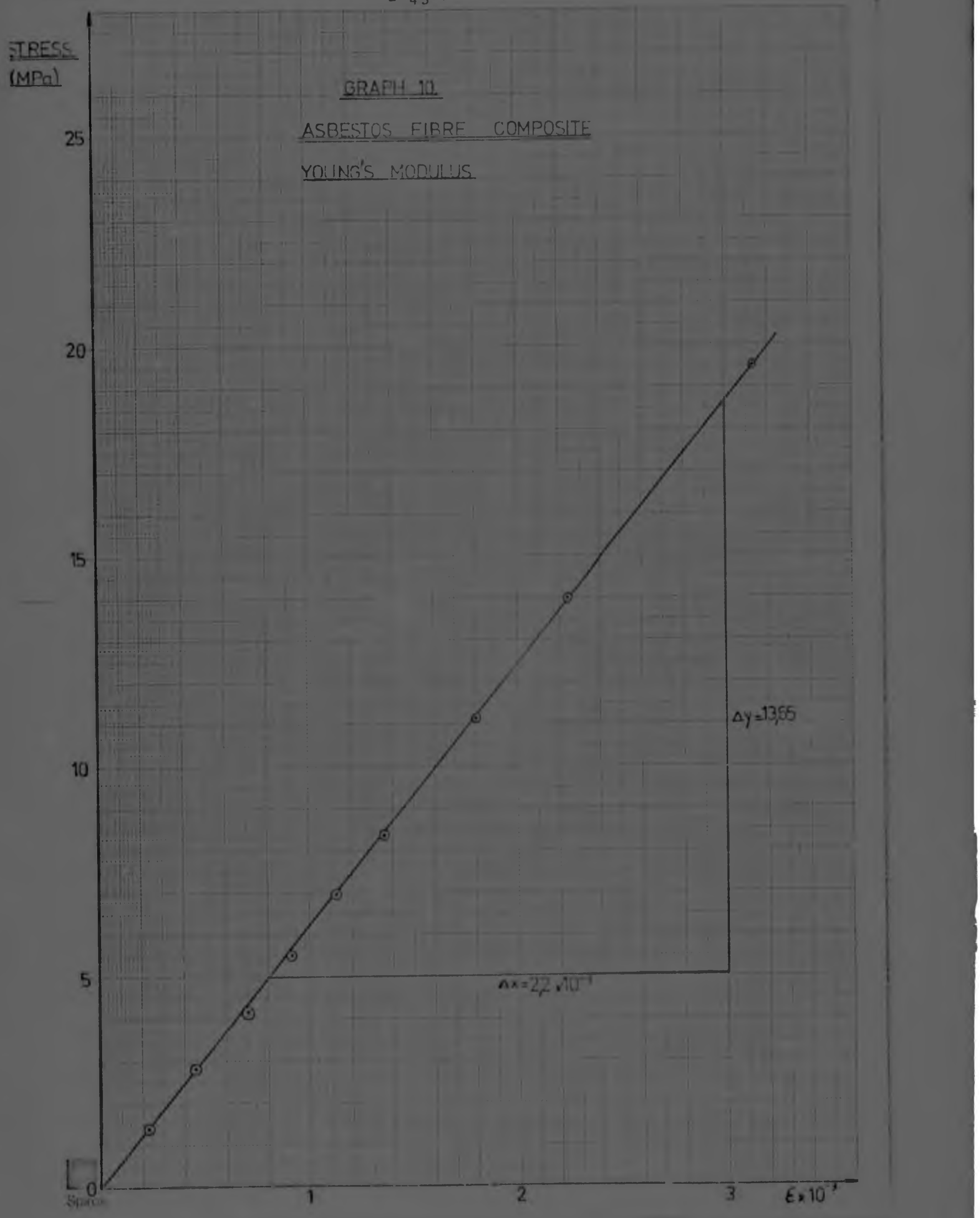
STRESS
(MPa)
GRAPH 10.
ASBESTOS FIBRE COMPOSITE
YOUNG'S MODULUS
25
20
15
10
5
0
1
2
3
Δy=13,65
Δx=2,2 x10⁻³
ε x 10⁻³

GRAPH 11

ASBESTOS FIBRE COMPOSITE

POISSON'S RATIO

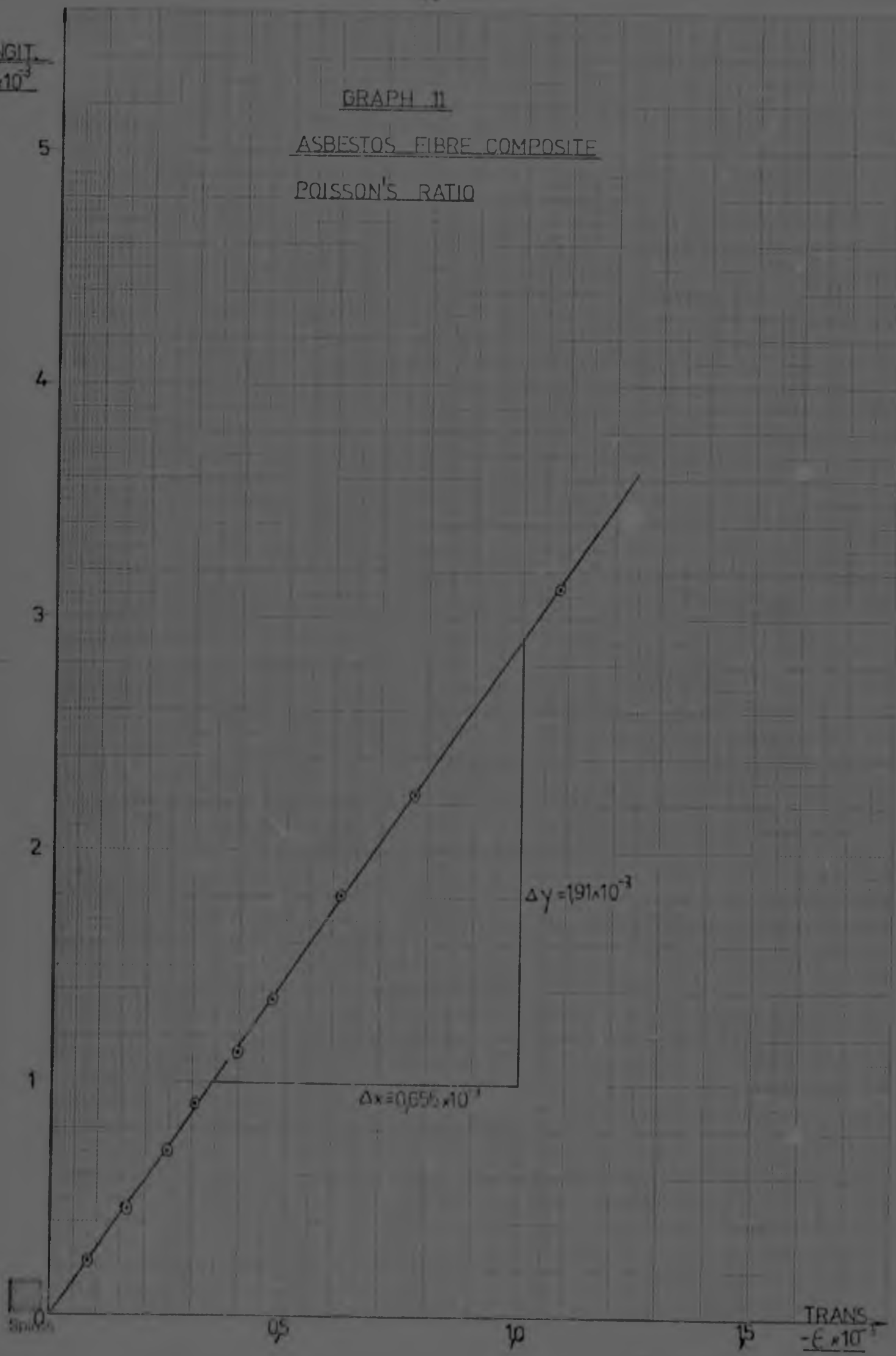

GRAPH 12

BUCKLING LOAD

ALUMINIUM t=1,6 mm

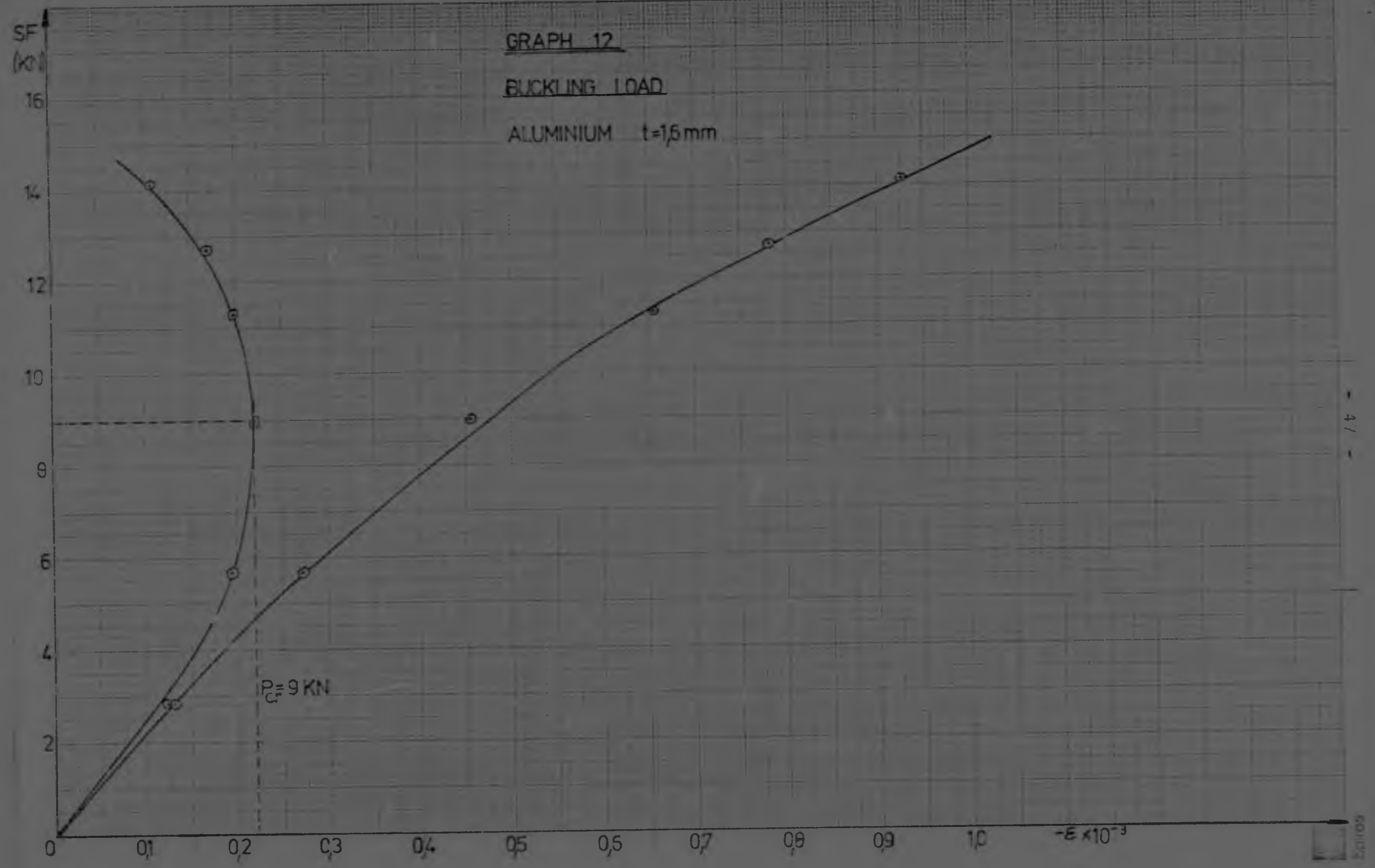

GRAPH 13

BUCKLING LOAD

ALUMINIUM t=1,27mm

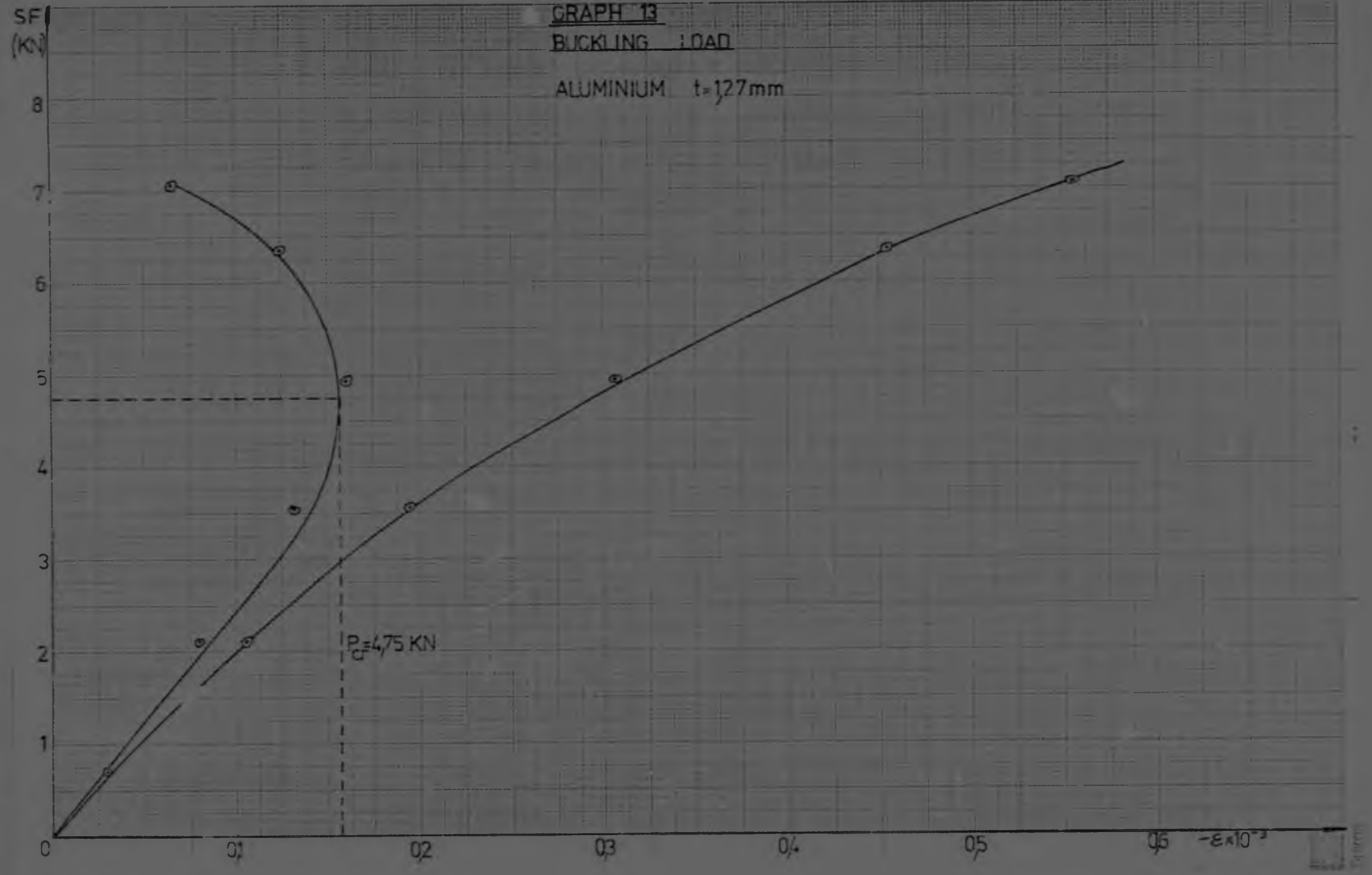

GRAPH 14

BUCKLING LOAD

ALUMINIUM t=1,00 mm

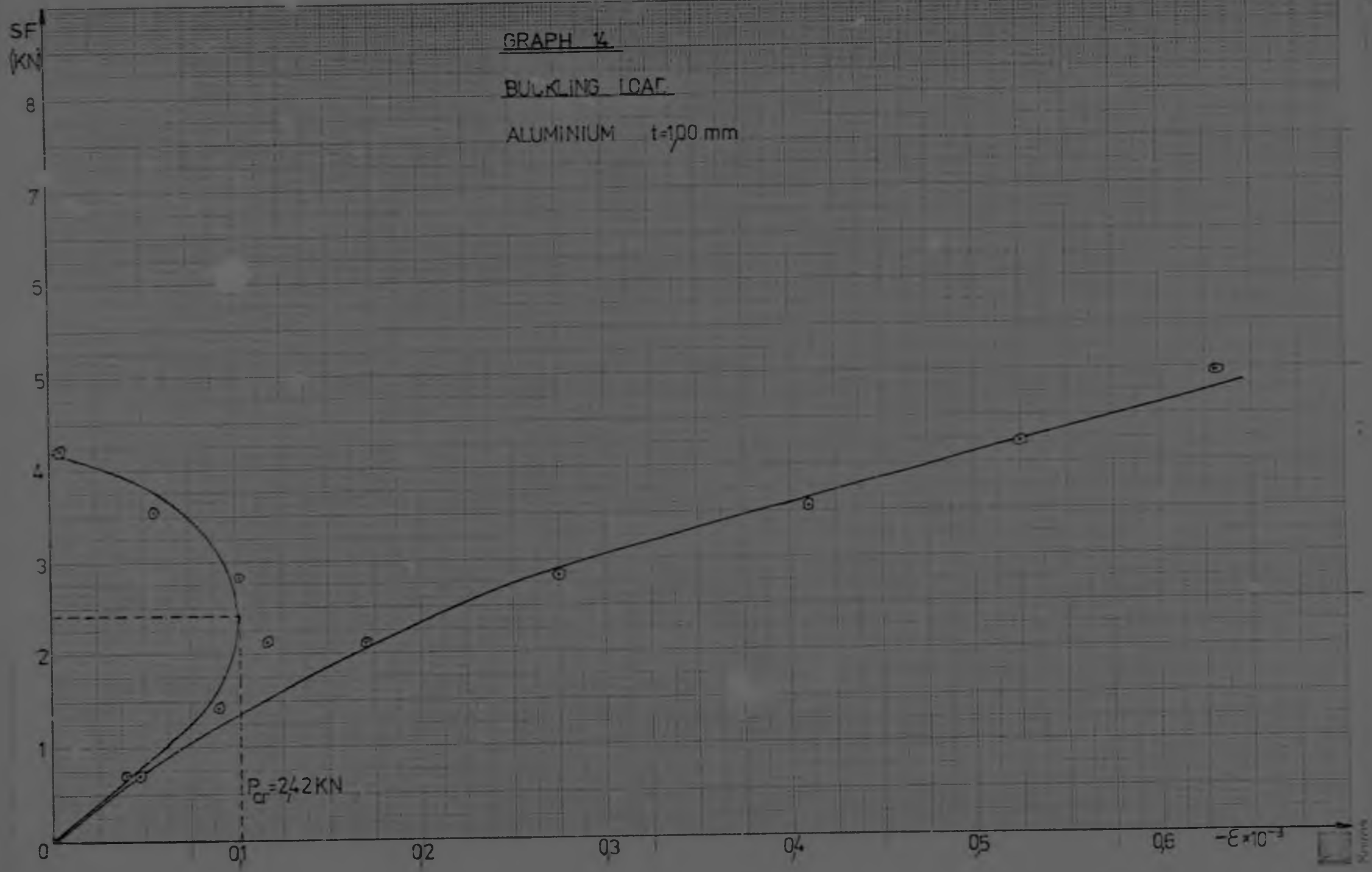

GRAPH 15

BUCKLING LOAD

GLASS FIBRE t=1,60 mm

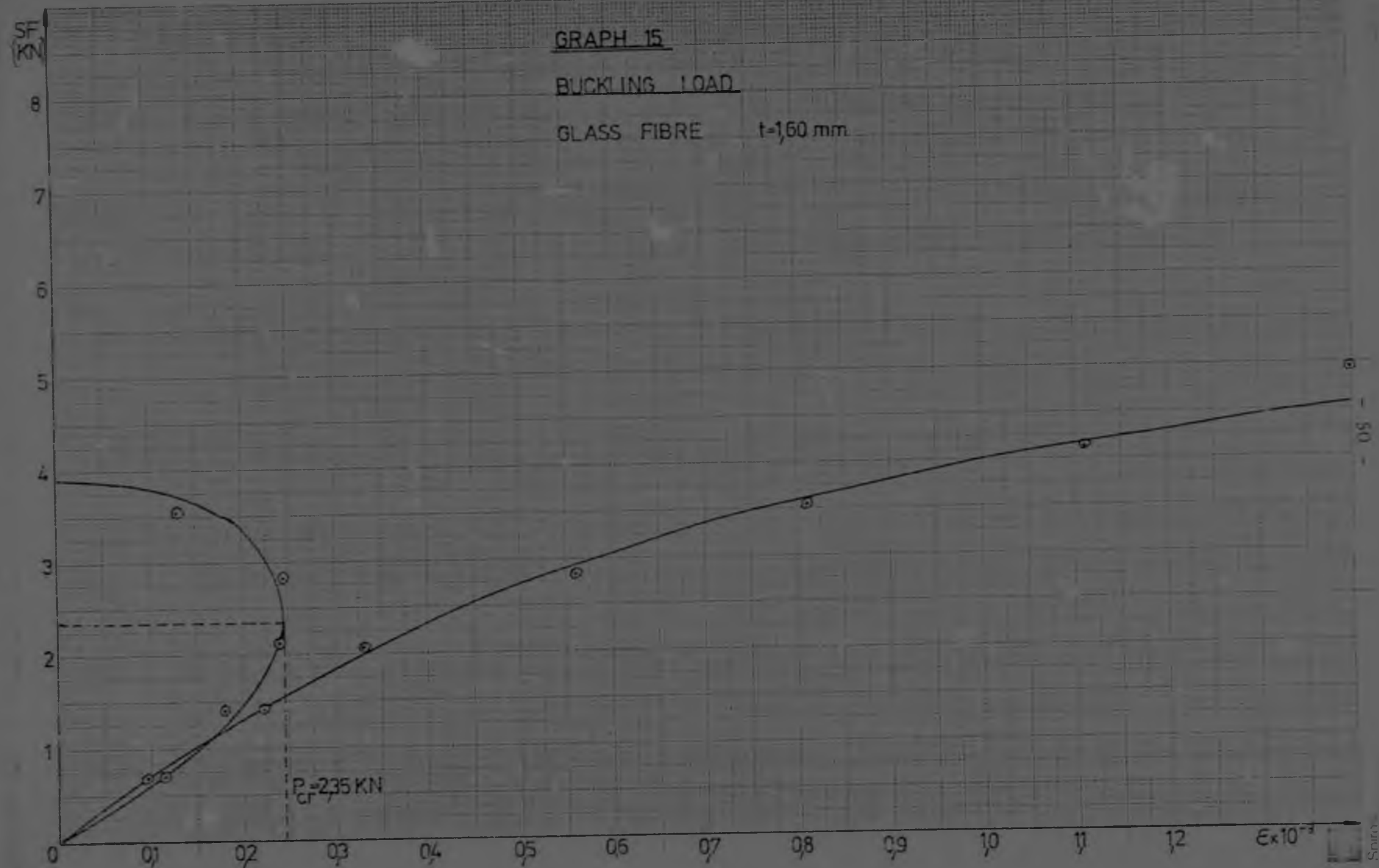

GRAPH 16

BUCKLING LOAD

GLASS FIBRE t=1,80 mm

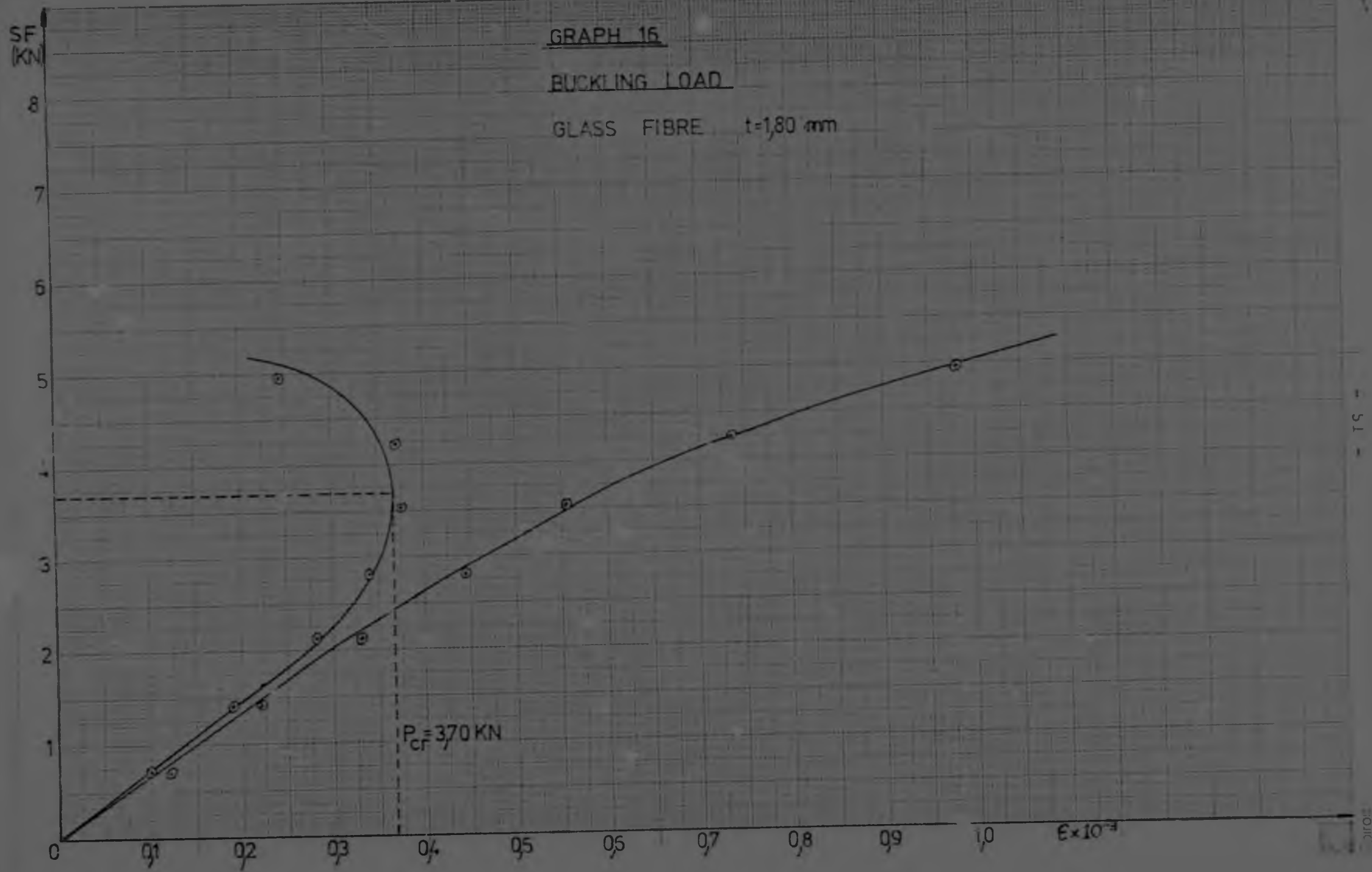

GRAPH 17

BUCKLING LOAD

GLASS FIBRE t=2,20 mm

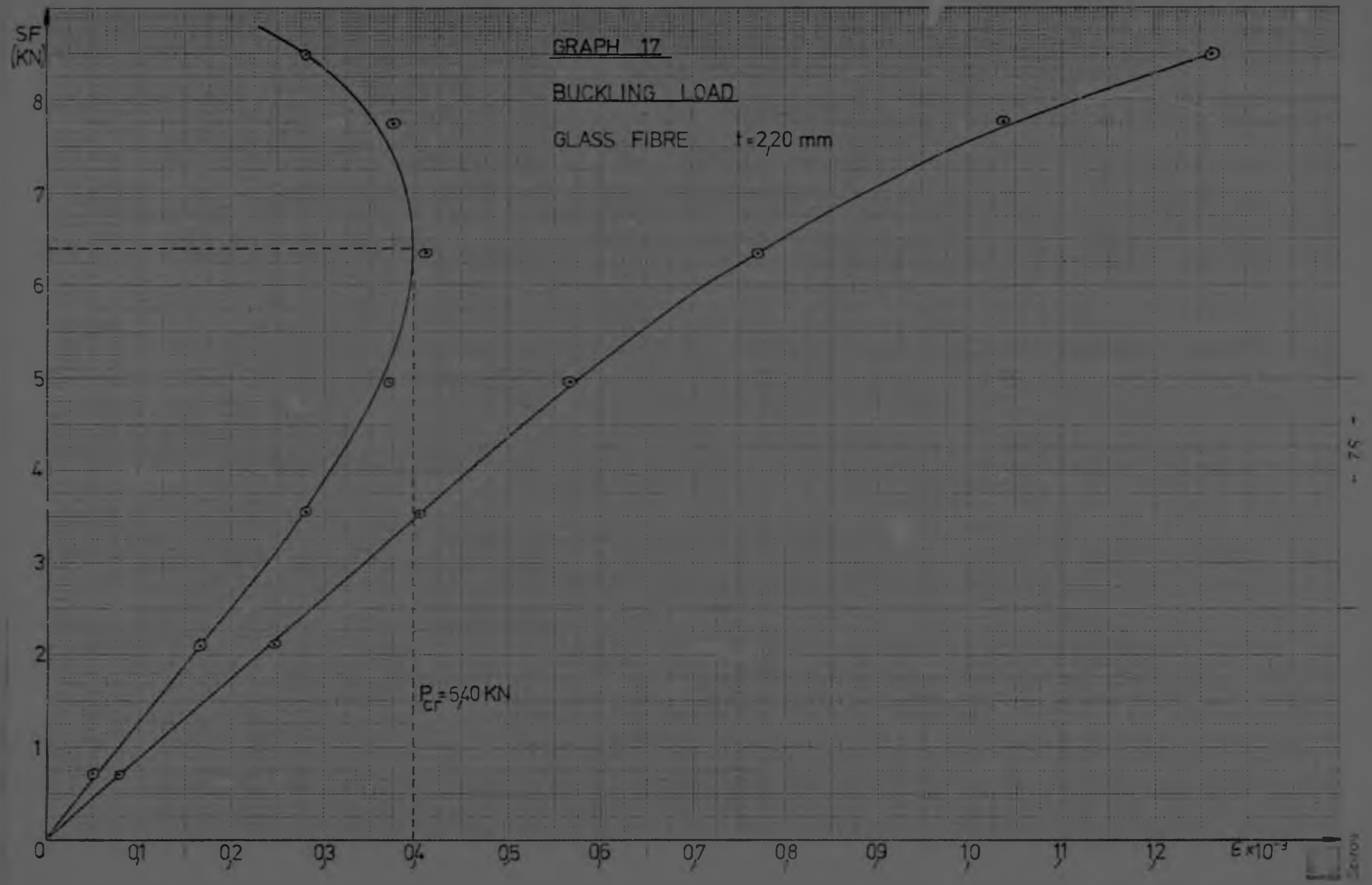

GRAPH 18

BUCKLING LOAD

GLASS FIBRE t=2,40 mm

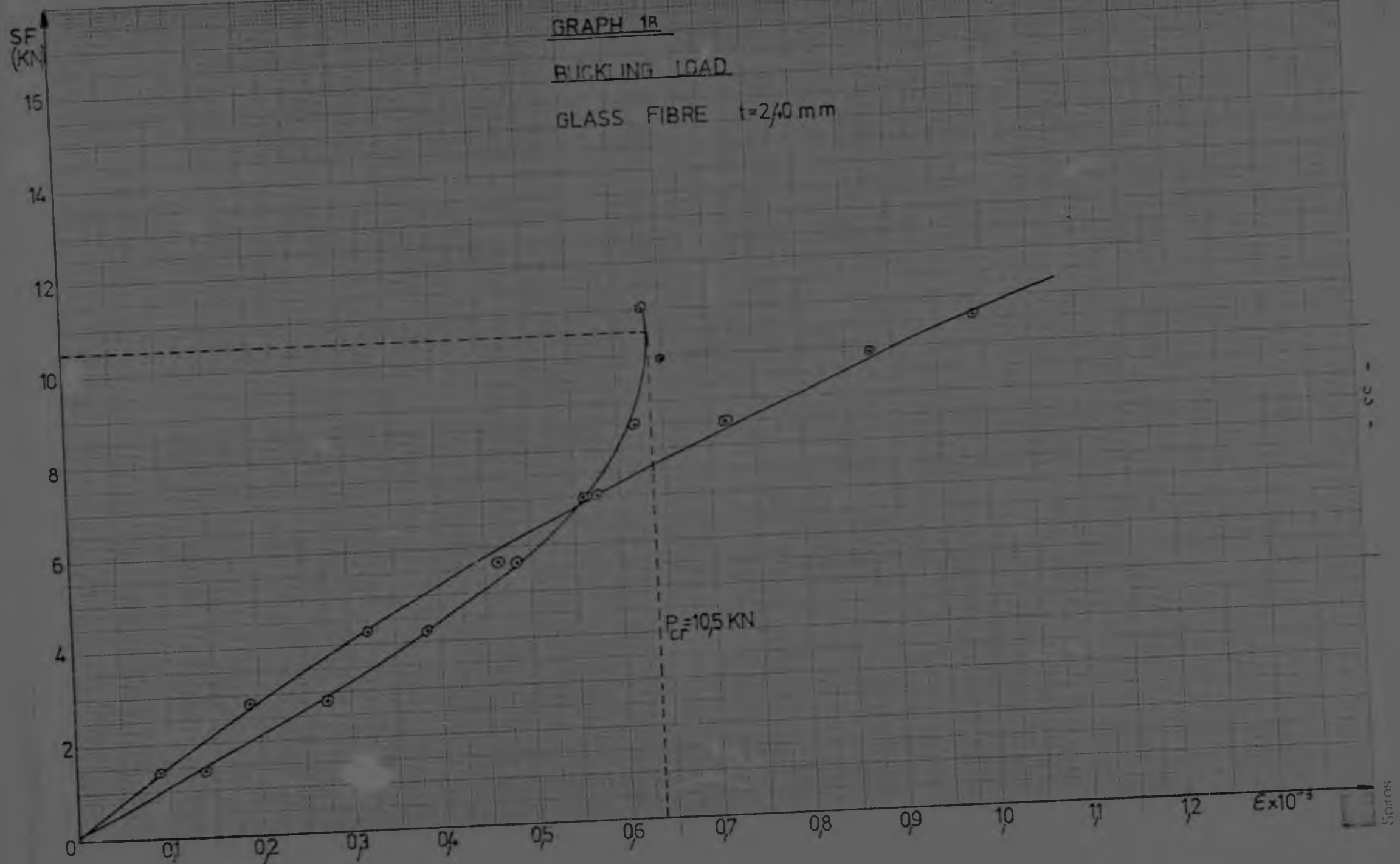

GRAPH 19

BUCKLING LOAD

CARBON FIBRE t = 1,300mm

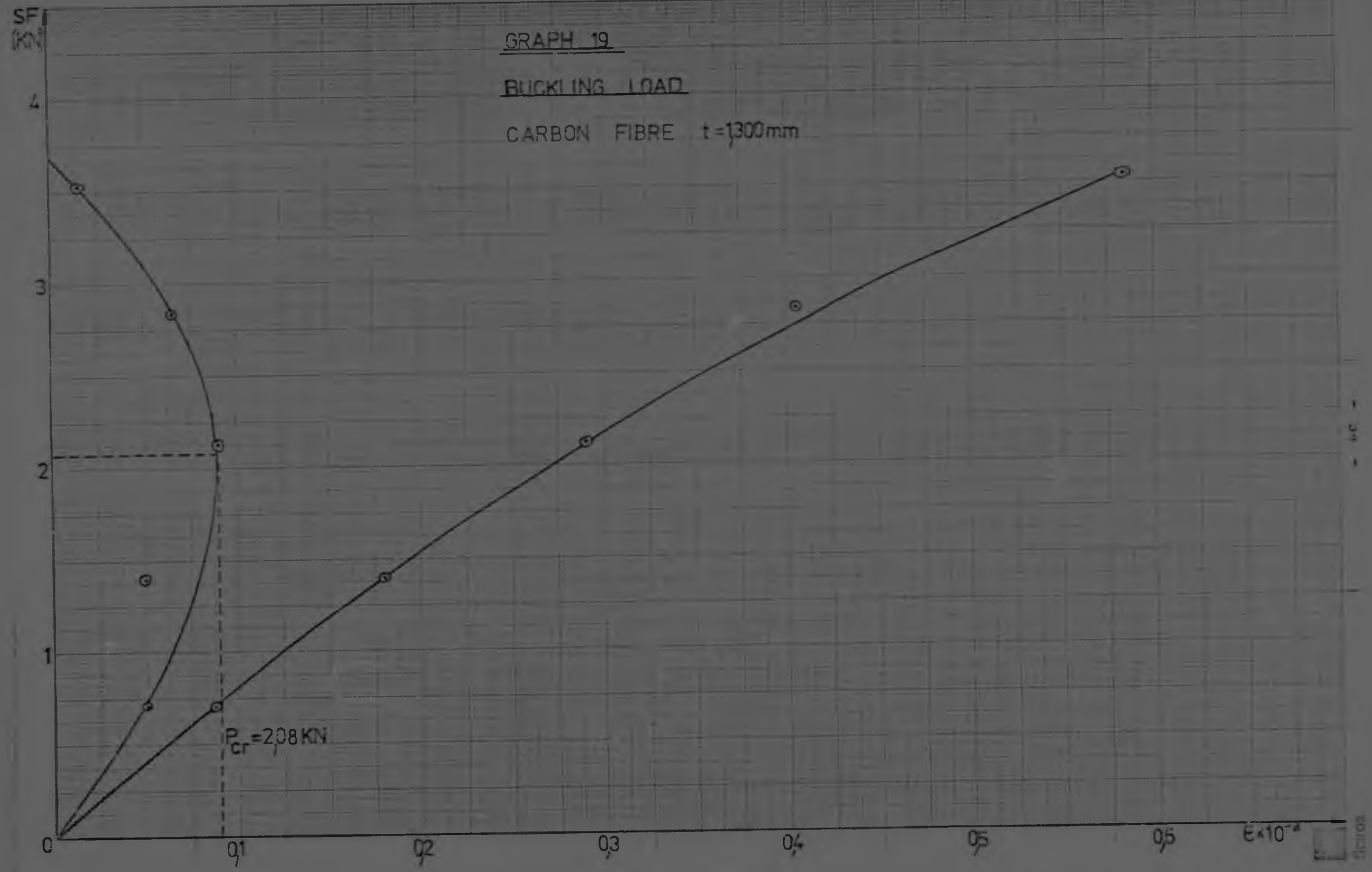

GRAPH 20

BUCKLING LOAD

CARBON FIBRE t = 1500 mm

GRAPH 21

BUCKLING LOAD

CARBON FIBRE t = 1820 mm

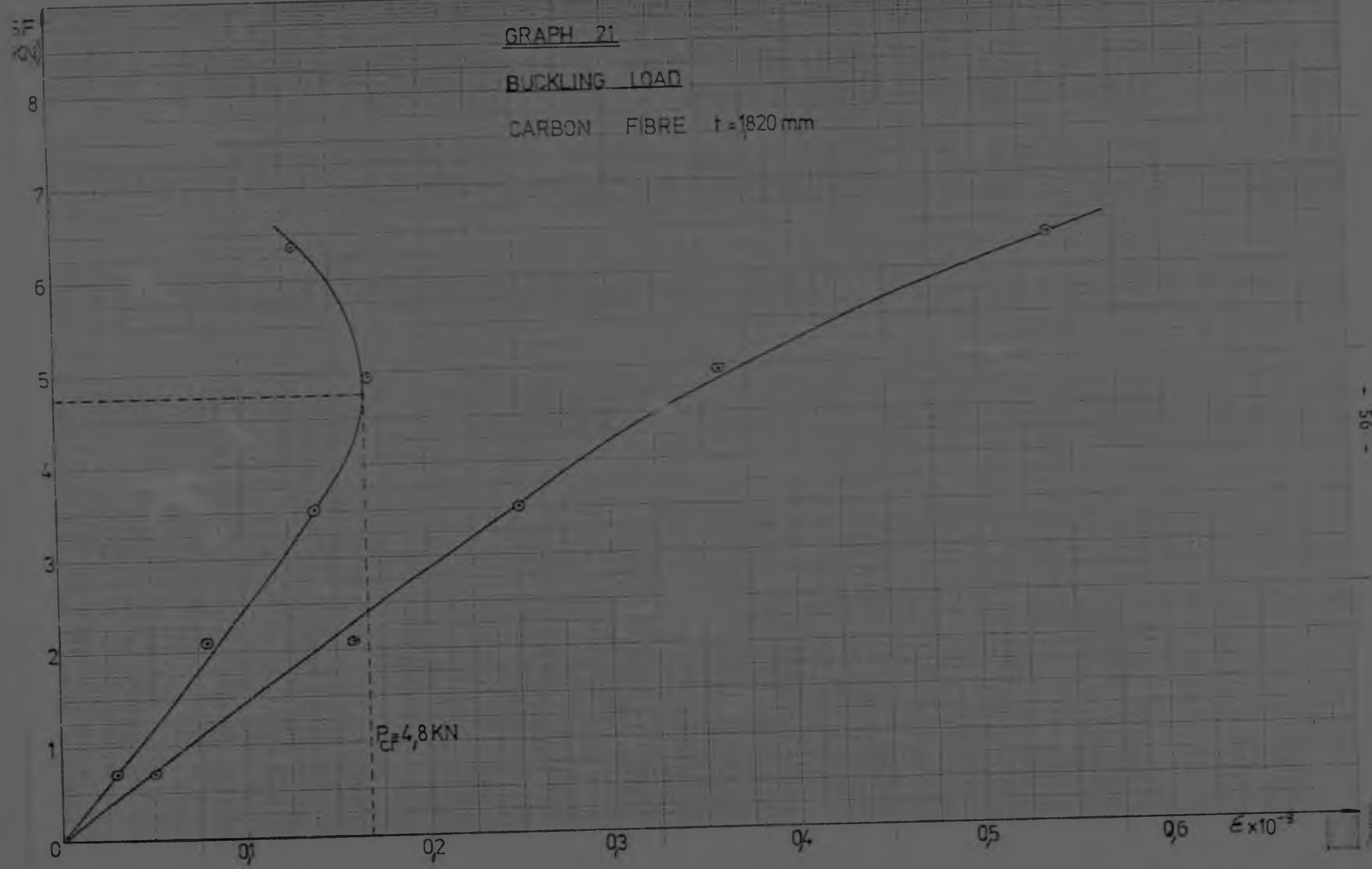

GRAPH 22

BUCKLING LOAD

ASBESTOS FIBRE t=3,23 mm

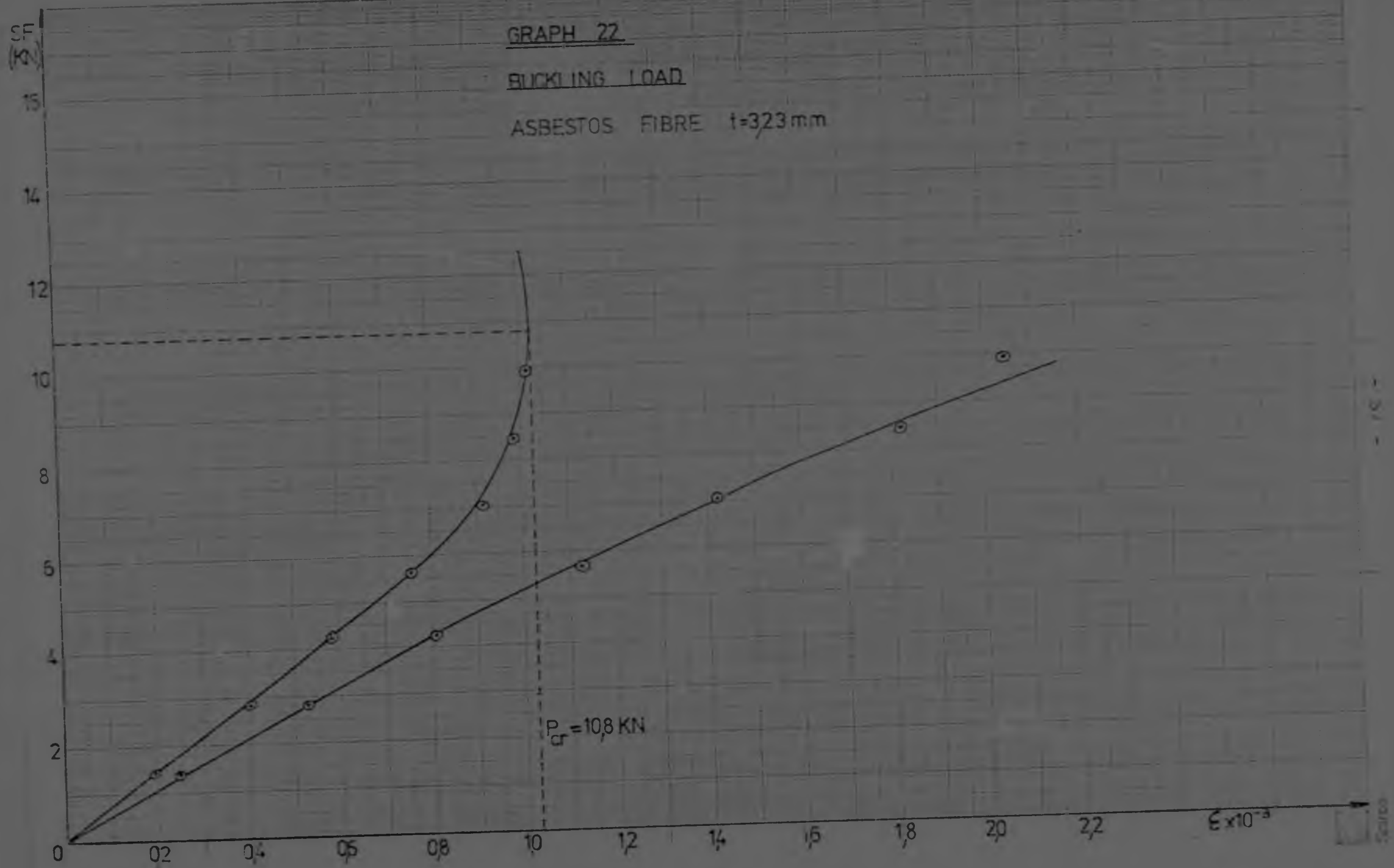

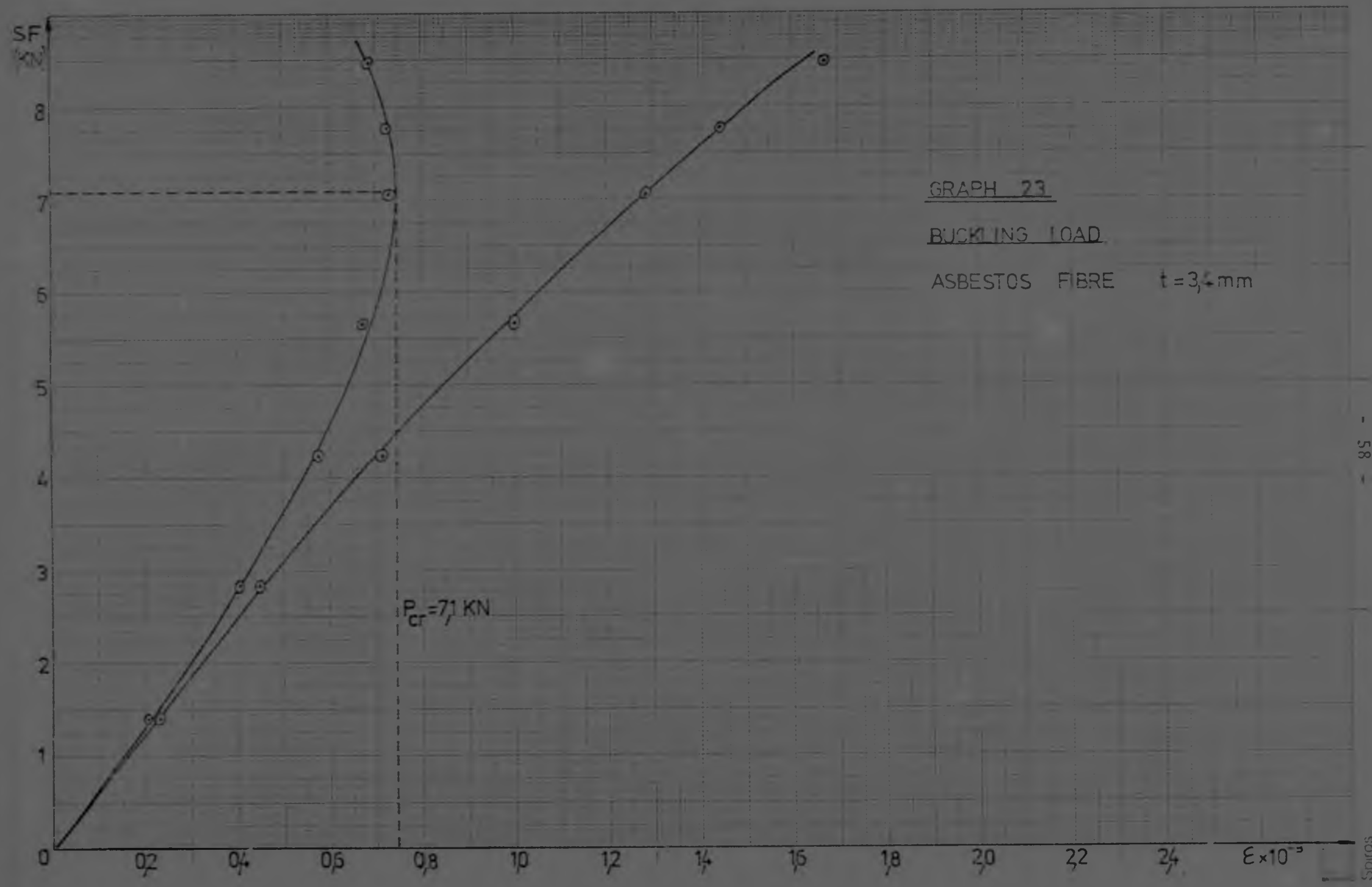

GRAPH 23

BUCKLING LOAD

ASBESTOS FIBRE t=3,4 mm

GRAPH 24

BUCKLING LOAD

ASBESTOS FIBRE t = 4,1 mm

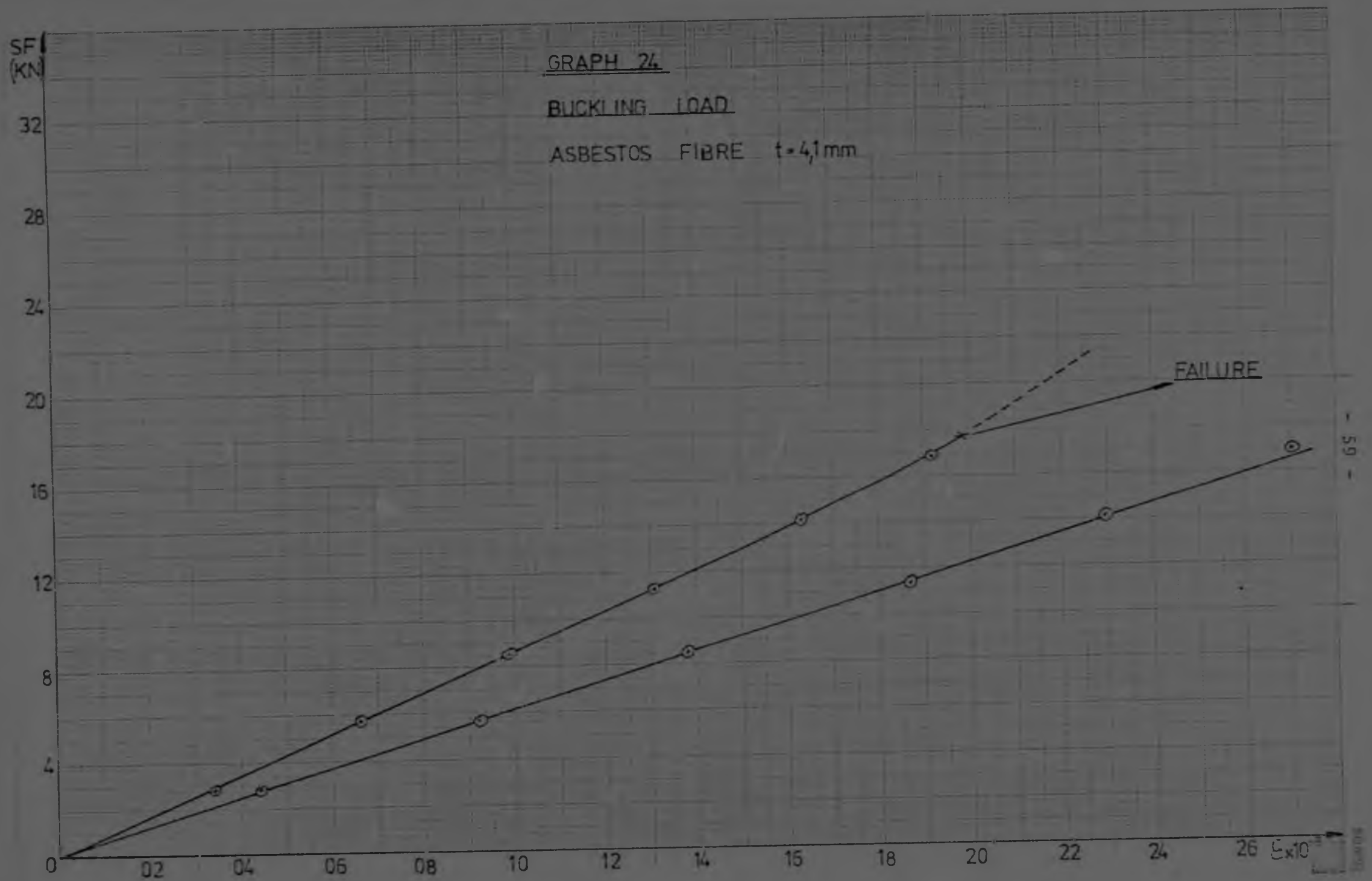

GRAPH 25.

BUCKLING LOAD

ASBESTOS FIBRE t-5,3mm

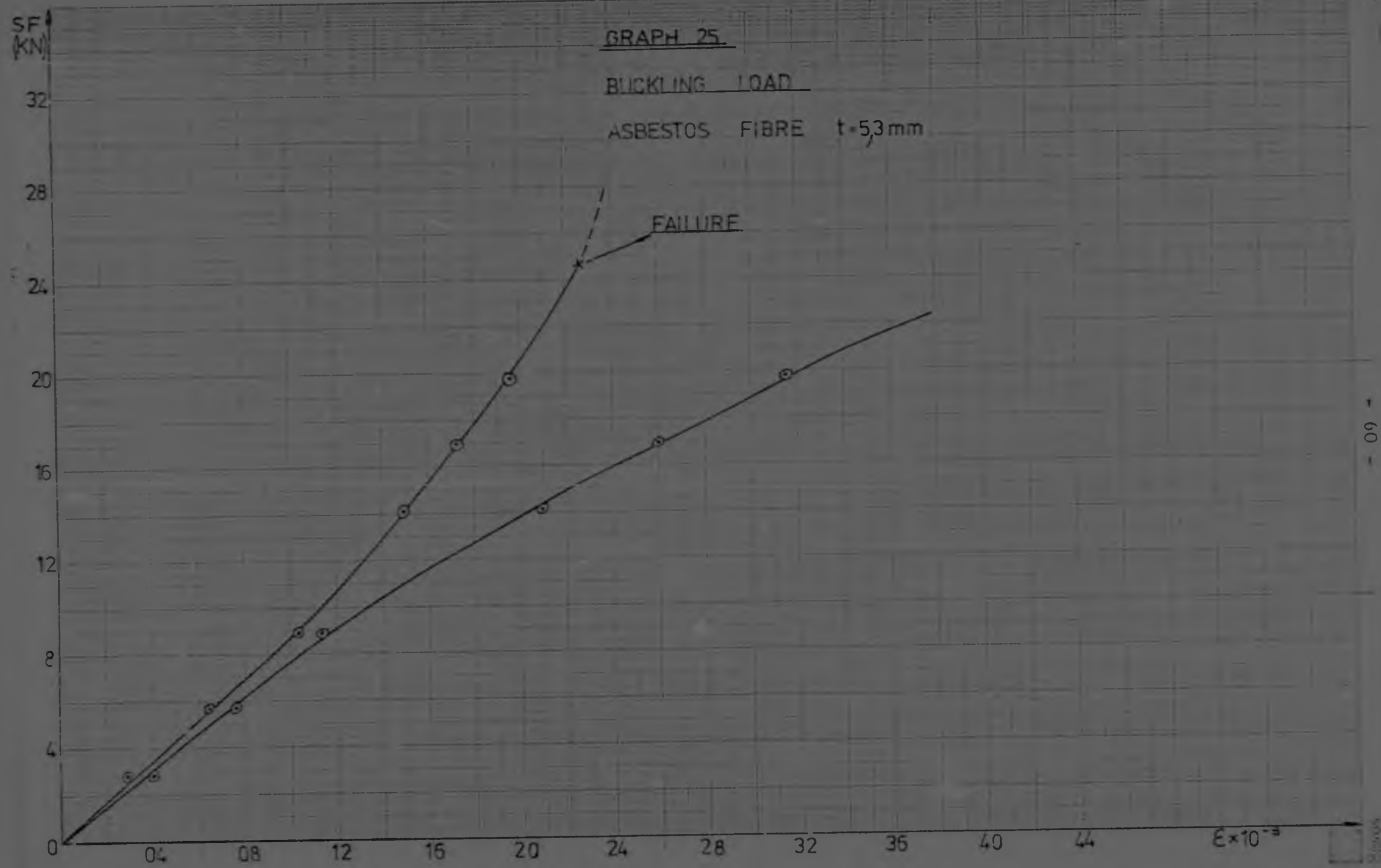

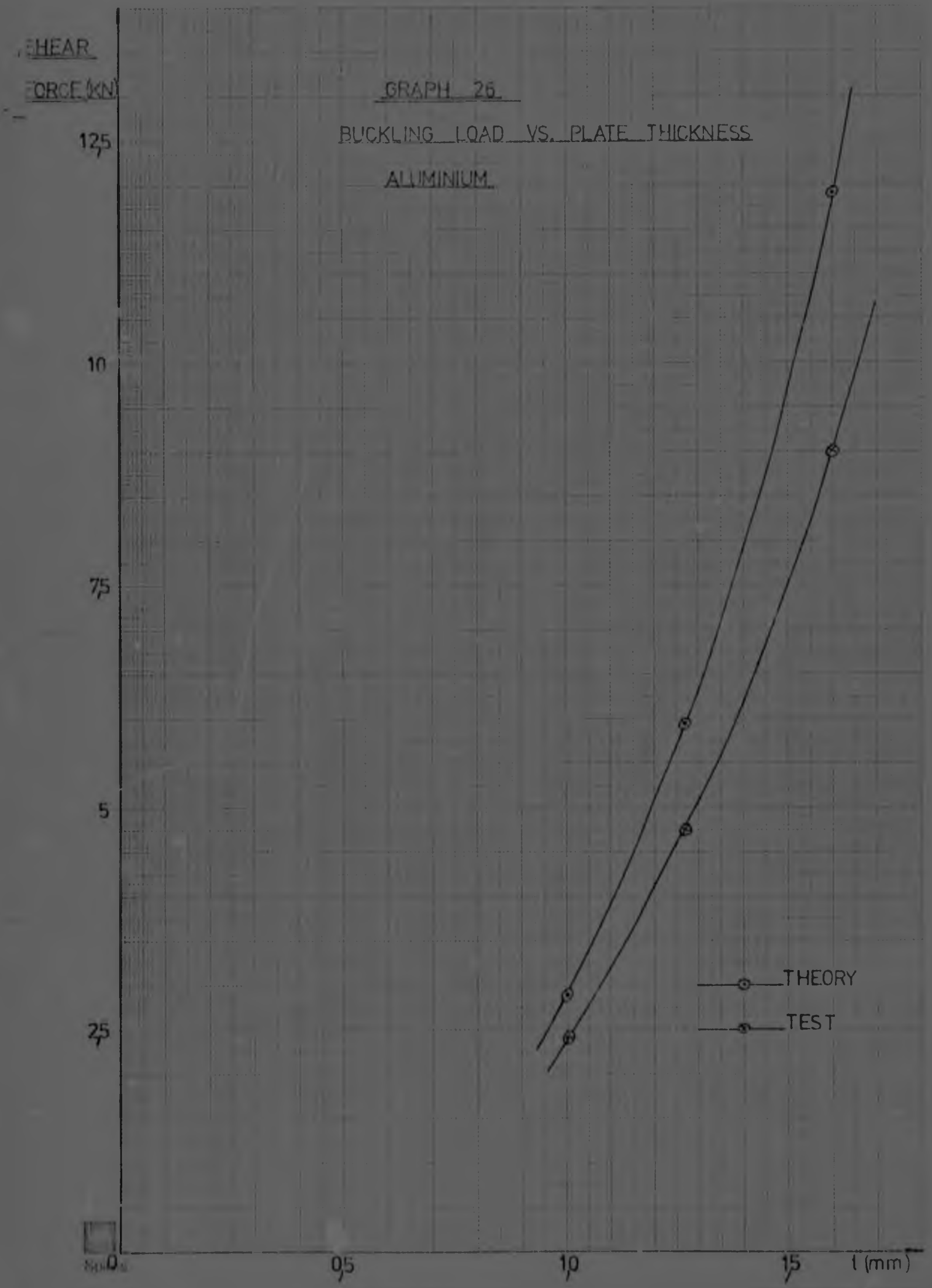
SHEAR
FORCE (KN)
GRAPH 26
BUCKLING LOAD VS. PLATE THICKNESS
ALUMINIUM
125
10
75
5
25
0
0,5
1,0
1,5
t (mm)
THEORY
TEST

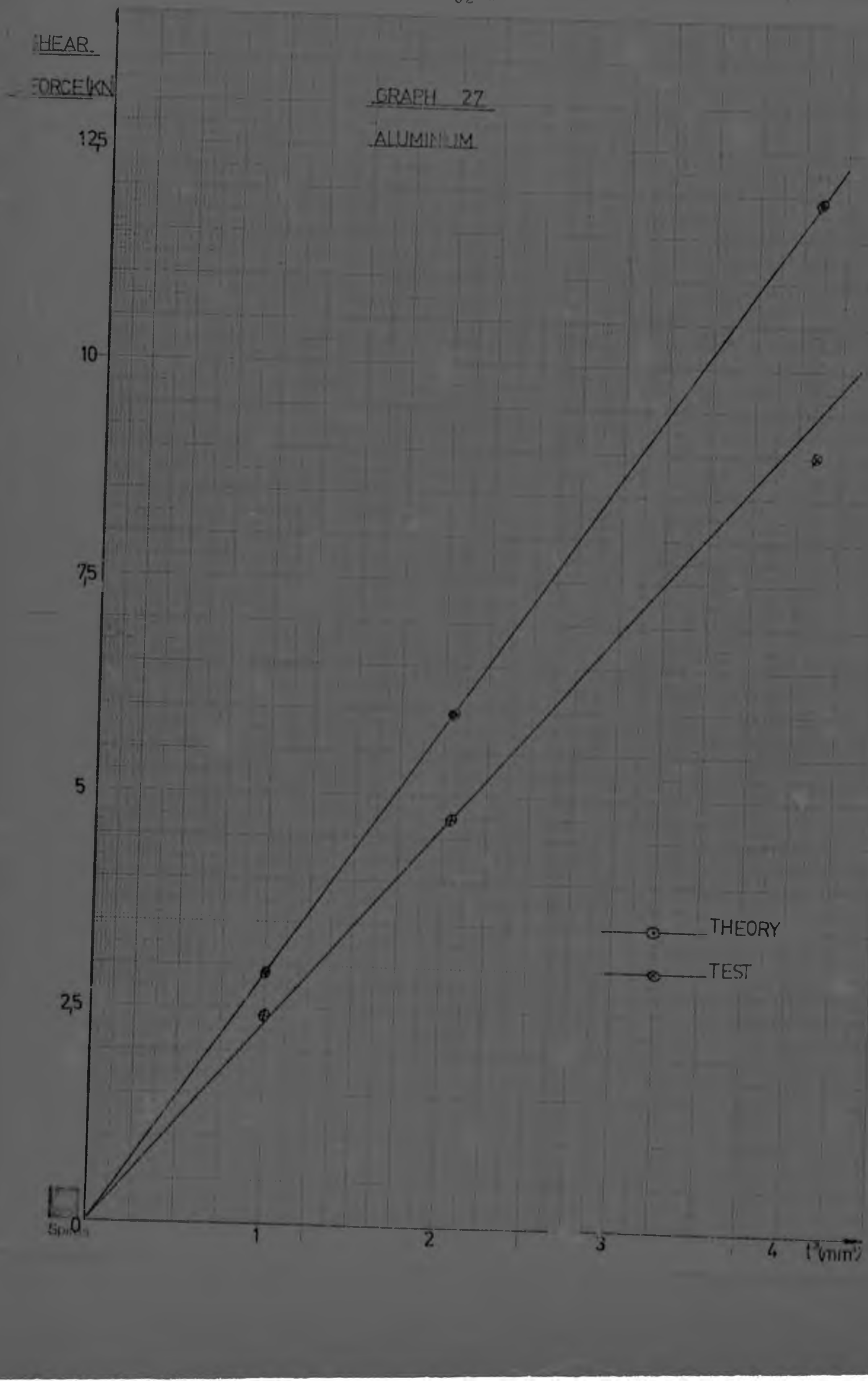
SHEAR.
FORCE (KN)
GRAPH 27
ALUMINIUM
12,5
10
7,5
5
2,5
0
1
2
3
4
P (mm)
THEORY
TEST

GRAPH 28

BUCKLING LOAD VS. PLATE THICKNESS

GLASS FIBRE

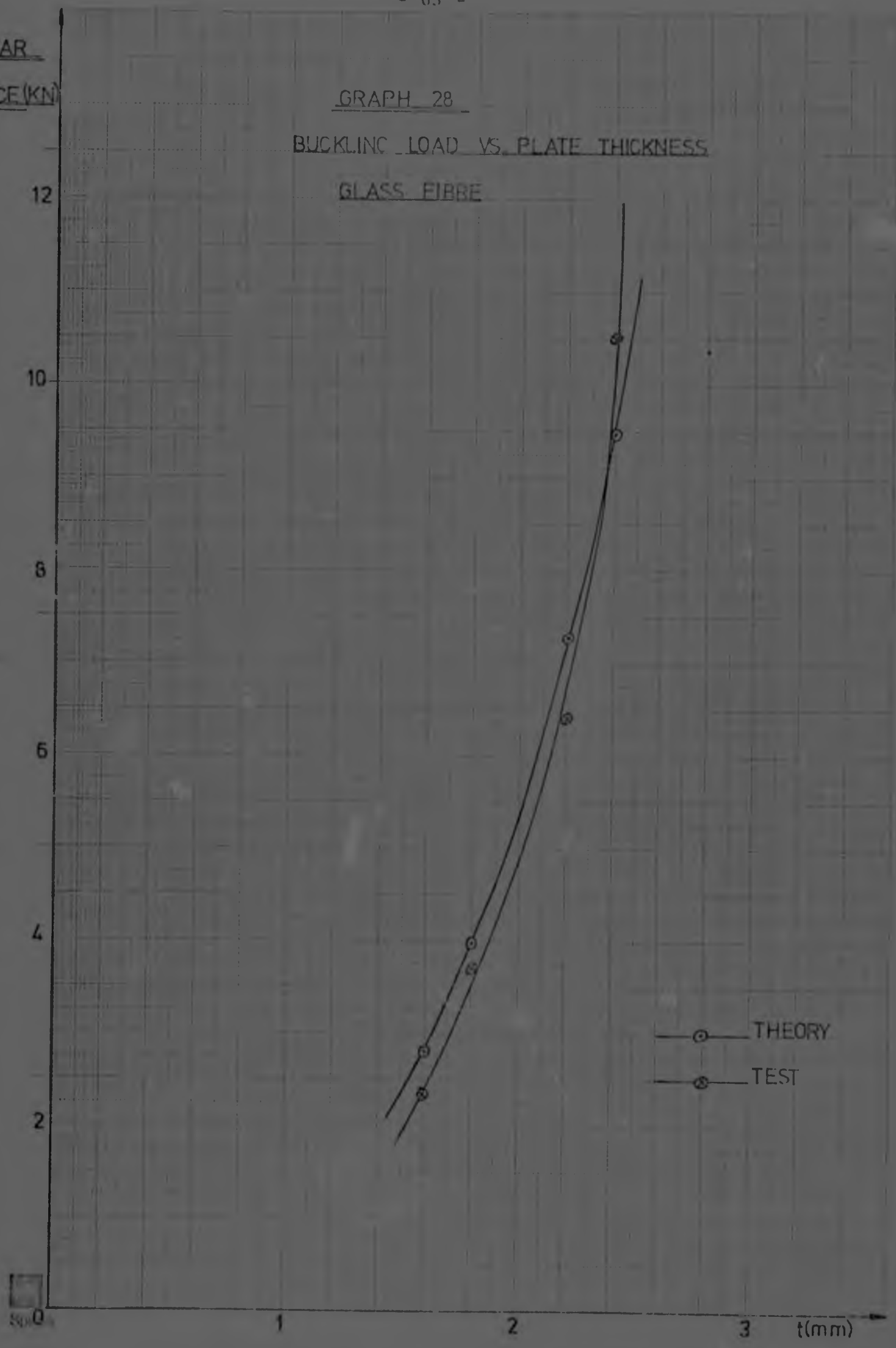

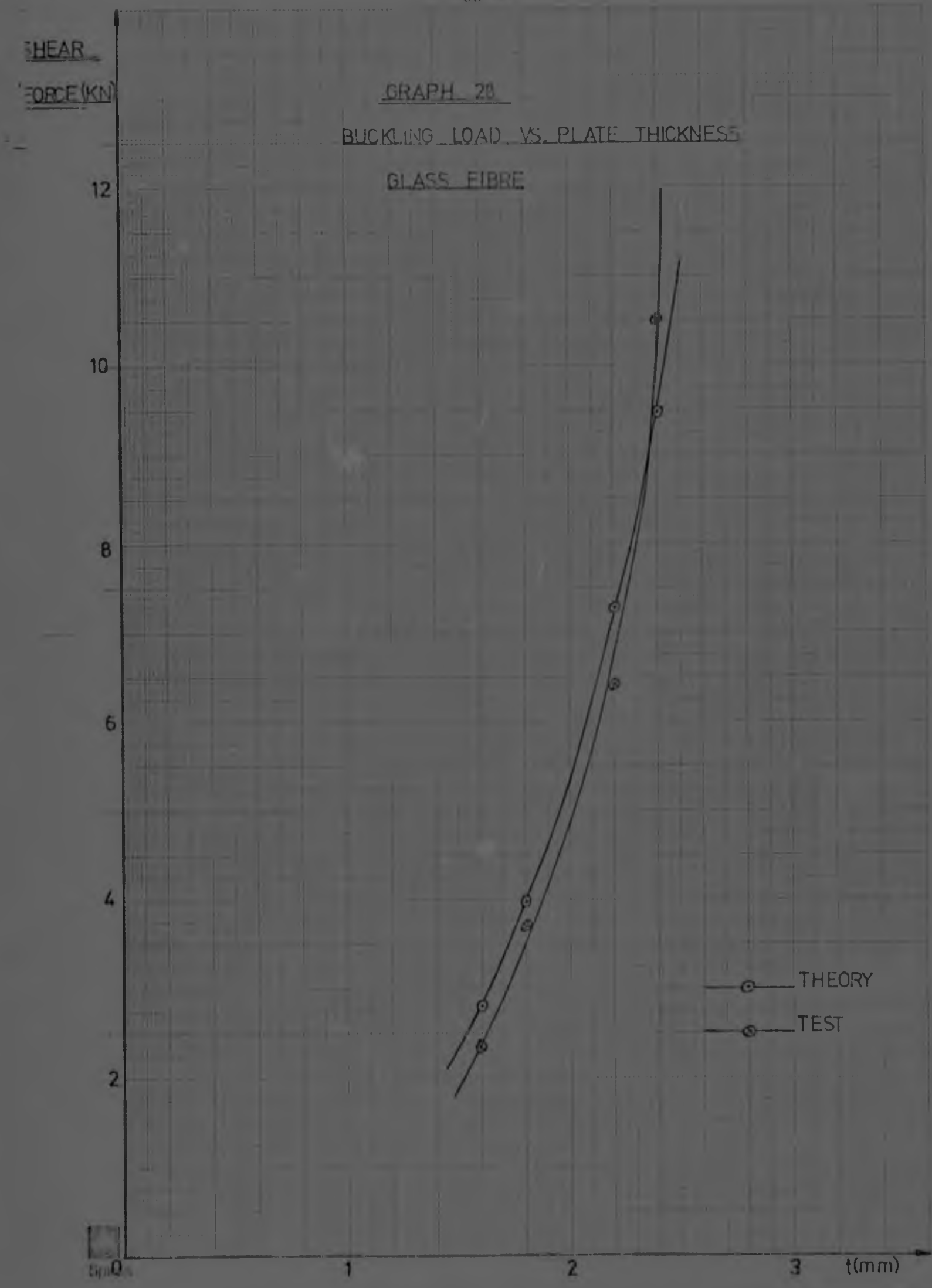
SHEAR
FORCE (KN)
GRAPH 28
BUCKLING LOAD VS. PLATE THICKNESS
GLASS FIBRE
12
10
8
6
4
2
0
1
2
3
t(mm)
THEORY
TEST

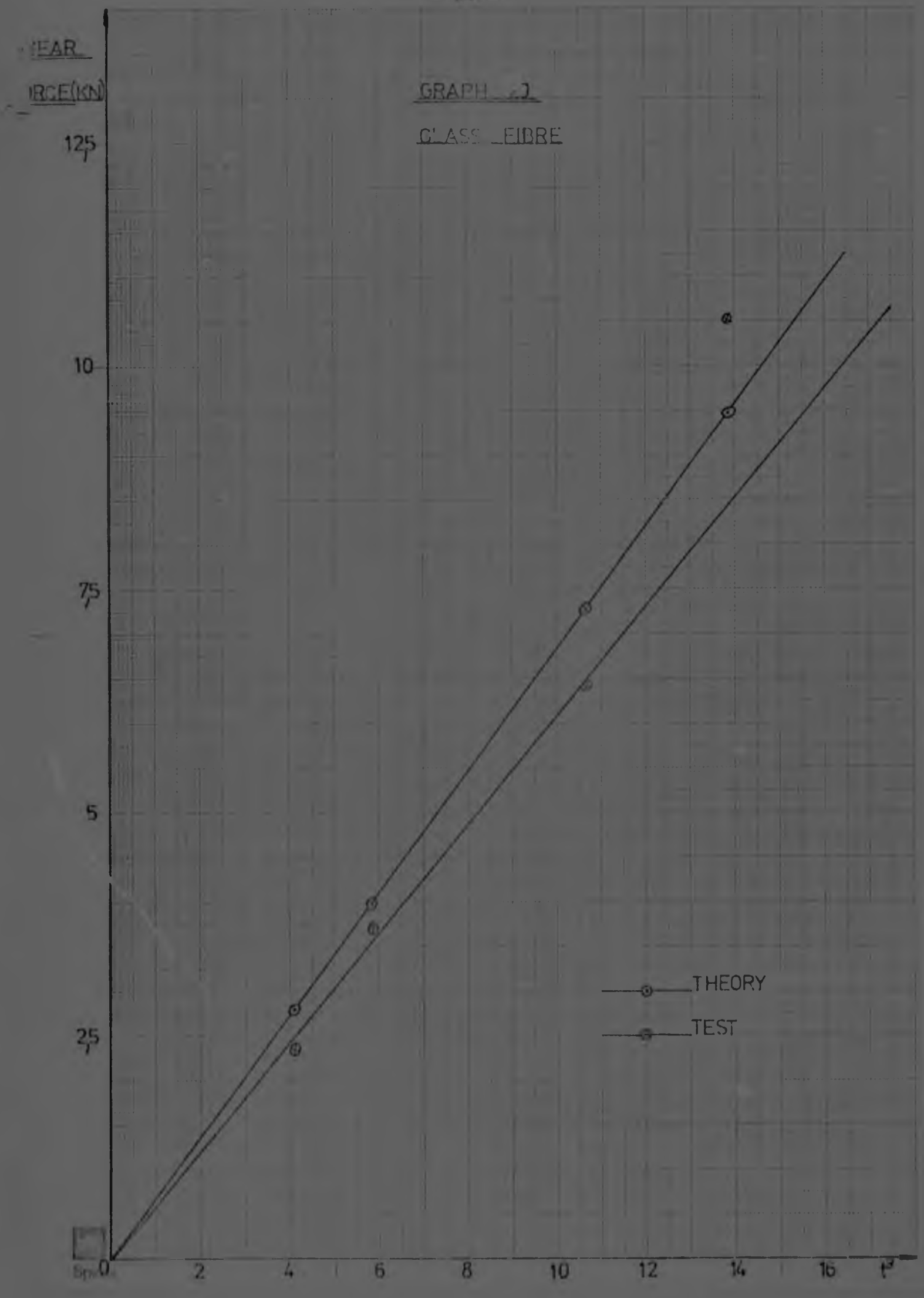
EAR
RCE(KN)
GRAPH 2
CLASS FIBRE
125
10
75
5
25
0
2
4
6
8
10
12
14
16
t²
THEORY
TEST

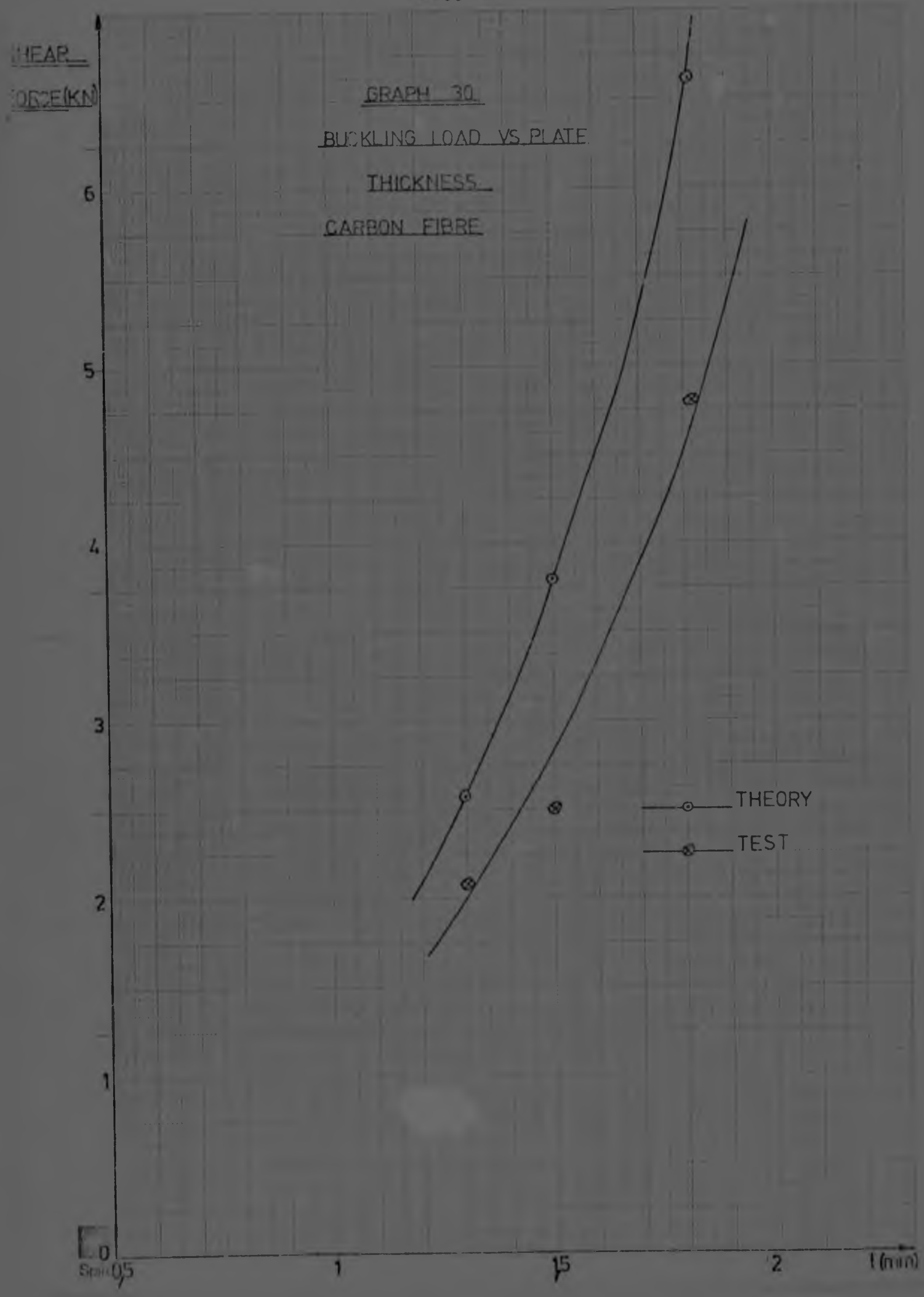
SHEAR FORCE(KN)
GRAPH 30
BUCKLING LOAD VS PLATE THICKNESS
CARBON FIBRE
6
5
4
3
2
1
0
0.5
1
1.5
2
t(mm)
THEORY
TEST

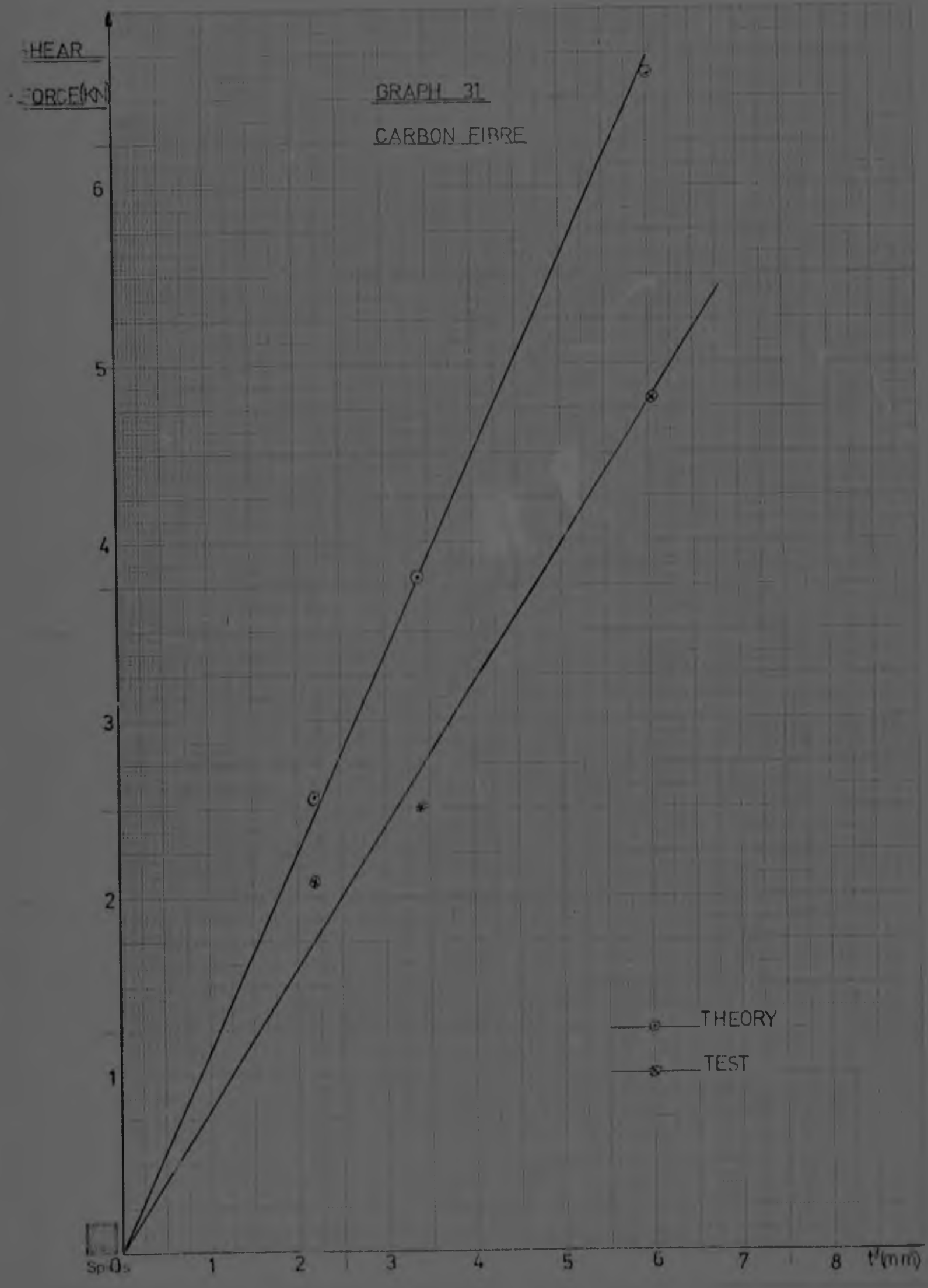
SHEAR FORCE(KN)
GRAPH 31
CARBON FIBRE
6
5
4
3
2
1
Sp.0
1
2
3
4
5
6
7
8
t'(mm)
THEORY
TEST

GRAPH 32

BUCKLING LOAD VS PLATE THICKNESS

ASBESTOS FIBRE

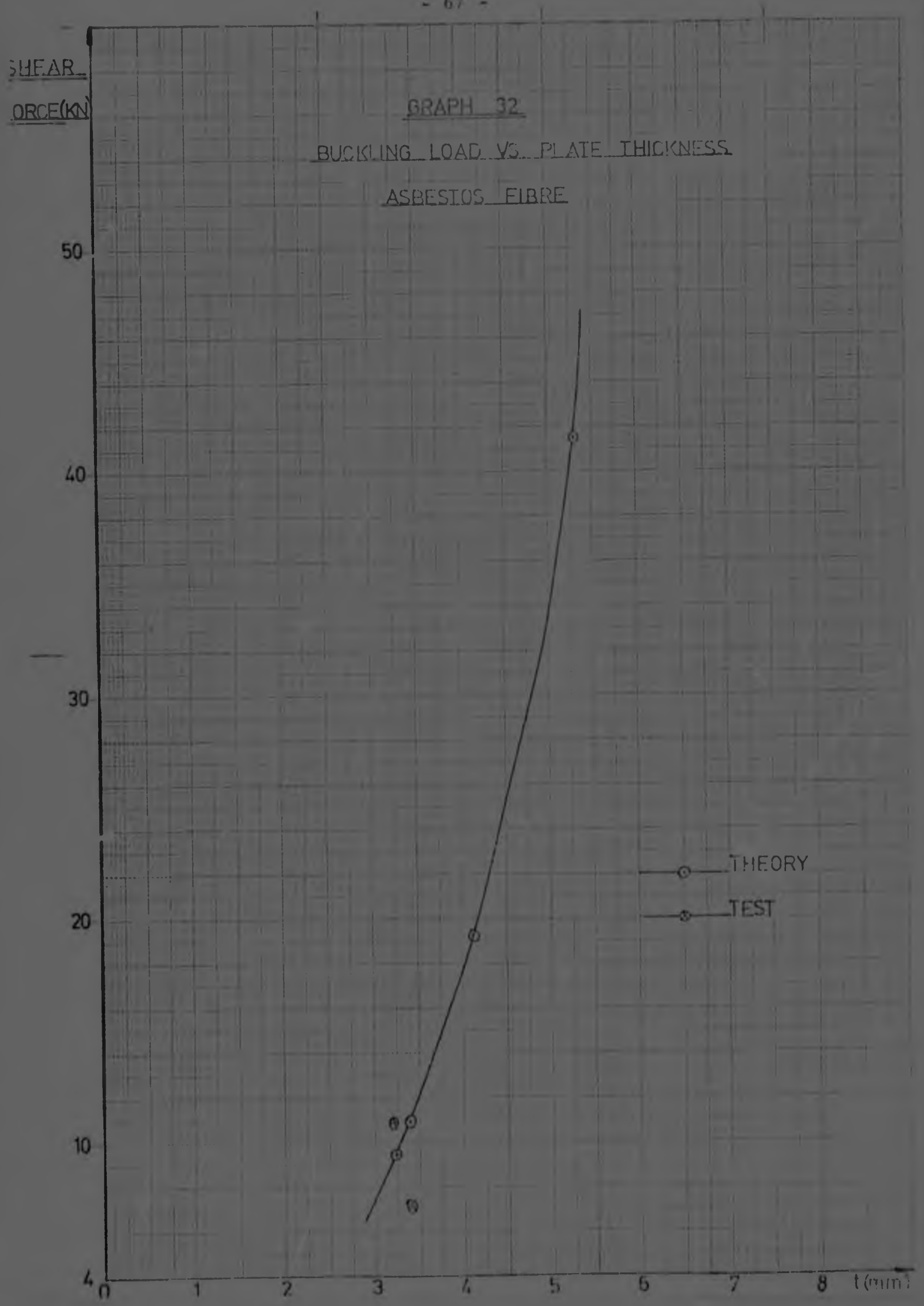

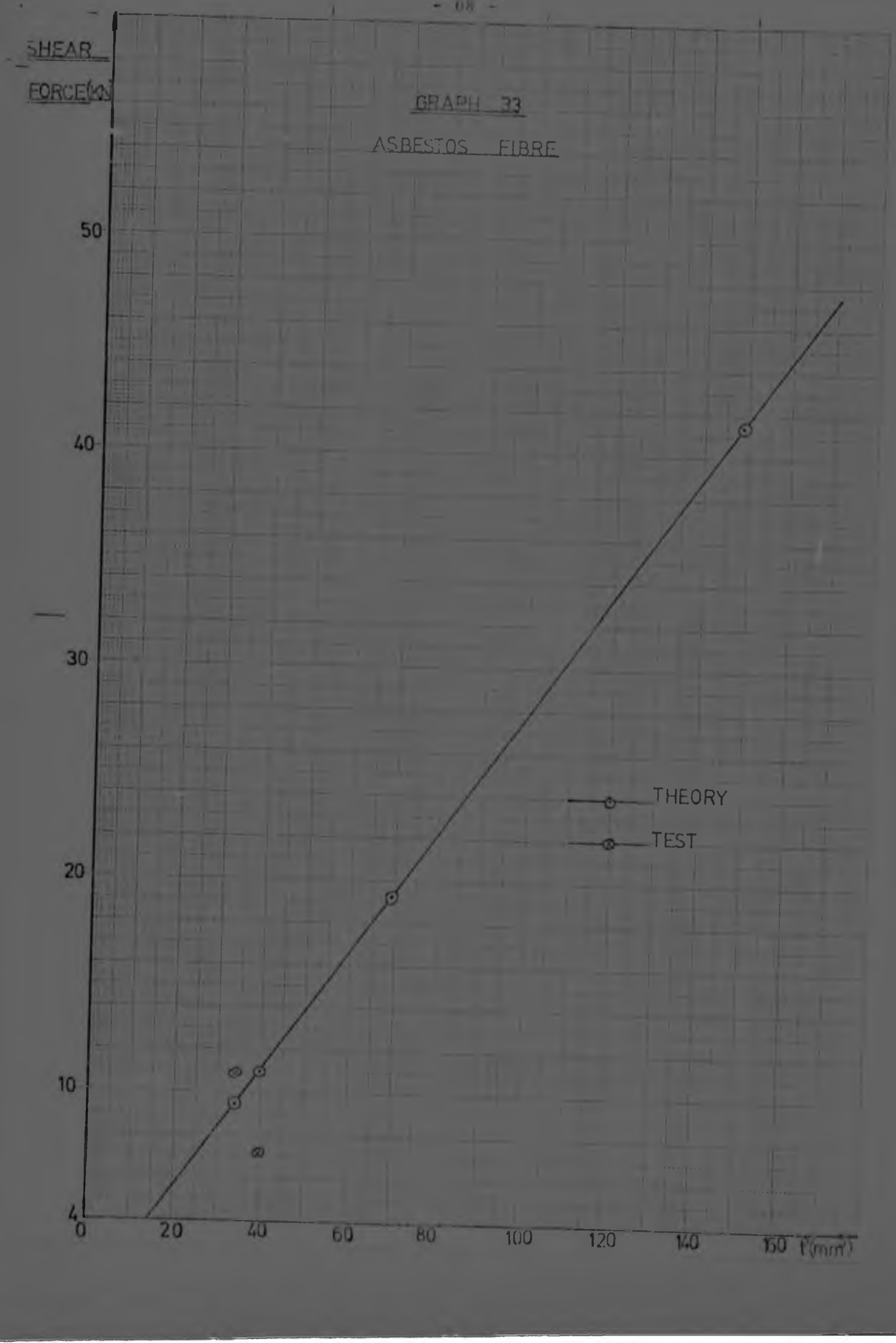
SHEAR
FORCE(KN)
GRAPH 33
ASBESTOS FIBRE
50
40
30
20
10
4
0
20
40
60
80
100
120
140
160
THEORY
TEST

GRAPH 34

BUCKLING LOAD VS. PLATE MASS

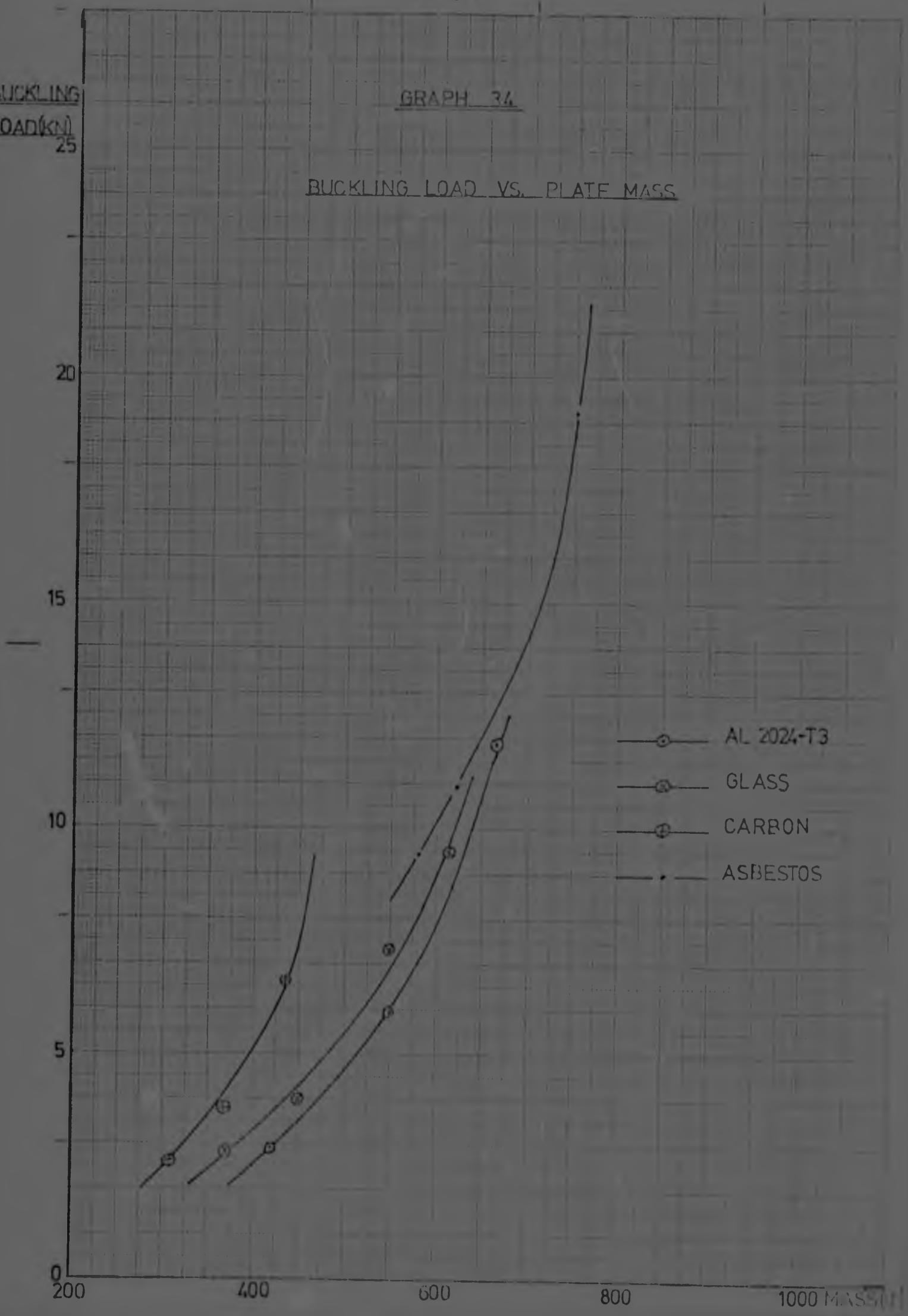

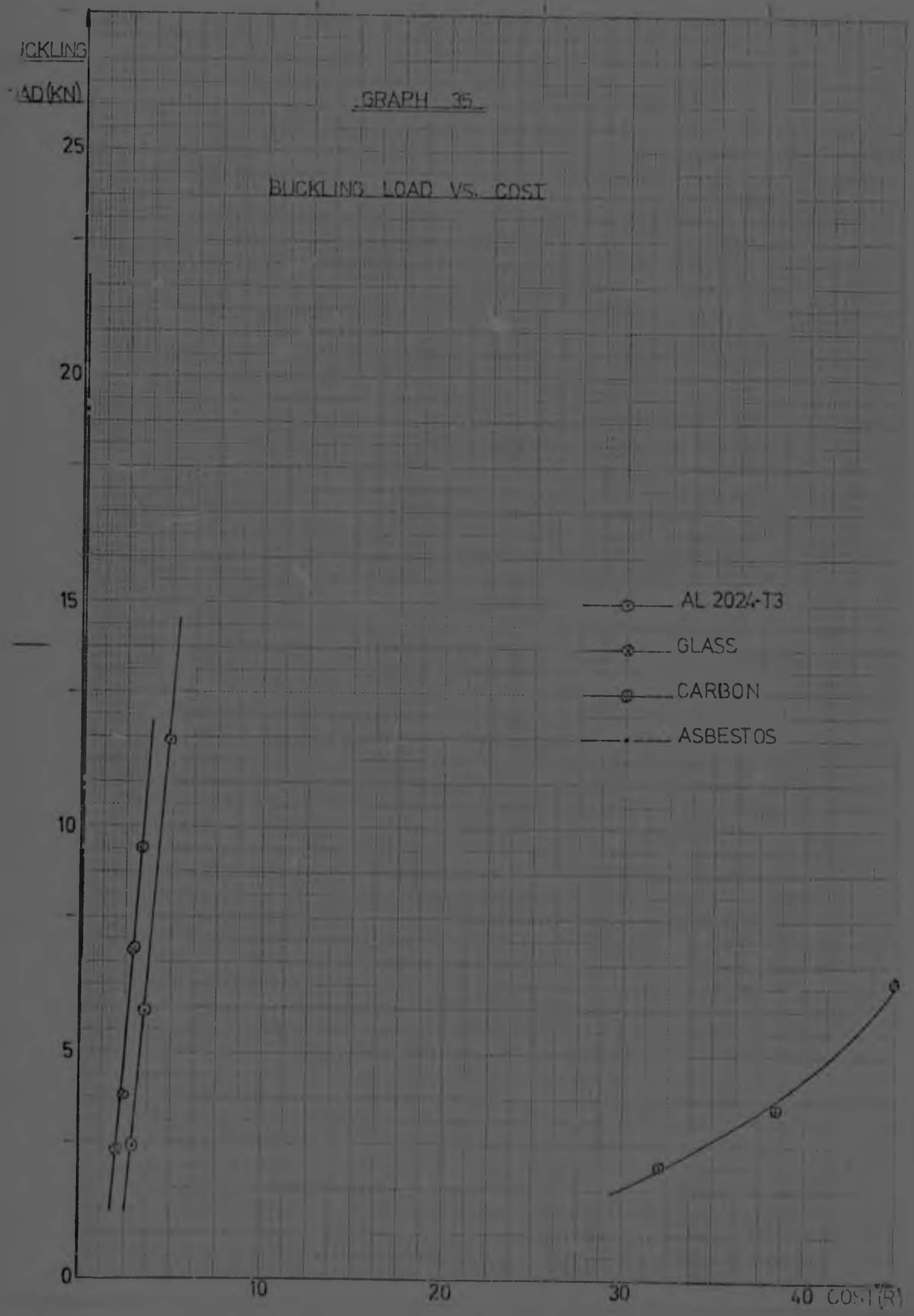
CKLING
AD(KN)
GRAPH 35.
BUCKLING LOAD VS. COST
25
20
15
10
5
0
10
20
30
40
COST(R)
AL 2024-T3
GLASS
CARBON
ASBESTOS

GRAPH 36

SHEAR BUCKLING OF CLAMPED PLATE

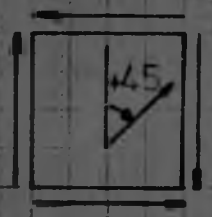

POSITIVE SHEAR DIRECTION

$N_{xy,cr} = K \frac{D_{11}}{b^2}$

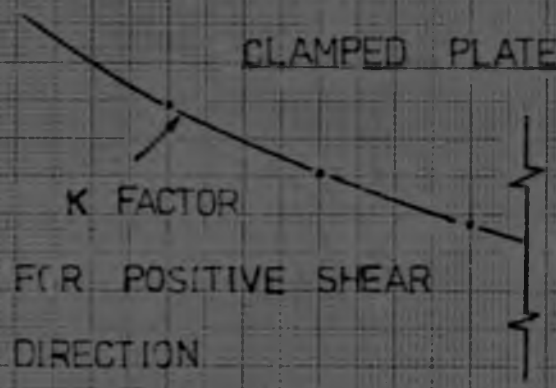

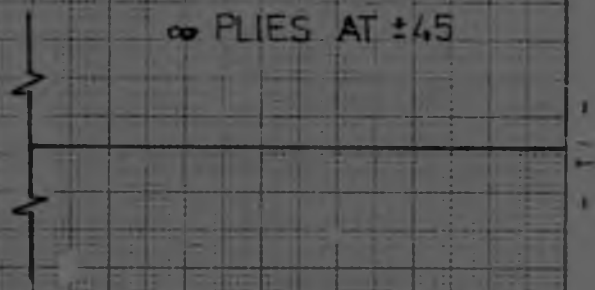

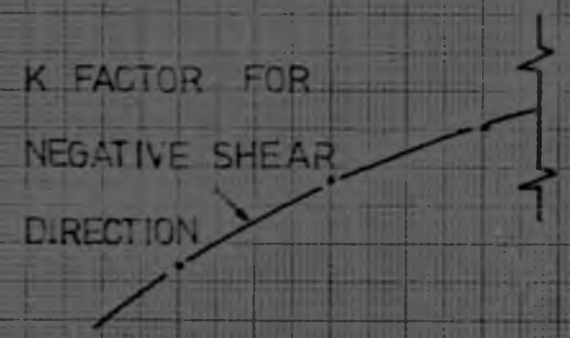

NOTE: OUTER PLIES ALWAYS AT +45

TABLE 1

Stress-strain curve for Al-2024T3 (Alclad)

Stress (MPa)	Longitudinal Strain ($\times 10^{-3}$)
0	0
27,15	0,379
54,30	0,759
81,46	1,159
108,61	1,561
135,76	1,966
162,91	2,399
190,06	2,859
217,21	3,381
244,37	4,041

TABLE 2

Longitudinal and transverse stress-strain curves for fibreglass composite

Stress (MPa)	Longitudinal Strain (10^{-3})	Transverse Strain (10^{-3})
0	0	0
3,82	0,235	-0,045
7,63	0,470	-0,095
11,45	0,695	-0,140
15,27	0,915	-0,190
19,08	1,130	-0,240
22,90	1,340	-0,285
26,72	1,585	-0,340
30,53	1,790	-0,385
34,35	2,015	-0,435
38.17	2,235	-0,480

TABLE 3

Stress-strain response of fibreglass coupon for the determination of the modulus of rigidity ($\alpha_{fibre} = \pm 45^{o}$)

Stress (MPa)	Longitudinal Strain ($\times 10^{-3}$)	Transverse Strain ($\times 10^{-3}$)	Strain at $\alpha = 45^{o}$ ($\times 10^{-3}$)
0	0	0	0
3,51	0,230	-0,145	0,07
7,02	0,405	-0,255	0,13
10,53	0,565	-0,365	0,18
14,04	0,750	-0.495	0,24
17,54	0,920	-0,605	0,29
21,05	1,105	-0,725	0,35
24,56	1,280	-0,845	0,415
28,07	1,465	-0,970	0,460
31,58	1,655	-1,115	0,525
35,09	1,835	-1,215	0,585

TABLE 4

Stress-strain response of carbon fibre coupon

i. $\alpha_f = 0^{o}$

Stress (MPa)	Longitudinal Strain ($\times 10^{-3}$)
0	0
29,65	0,725
59,30	1,435
74,13	1,770
111,19	2,630
14[illegible],26	3,440
185,32	4,270
222,39	5,095
259,45	5,895
296,52	6,670

TABLE 4 (Continued)

Stress (MPa)	Transverse Strain ($\times 10^{-3}$)
0	0
2,11	-0,02
4,22	-0,03
6,33	-0,045
8,44	-0,065
10,56	-0,085
12,67	-0,100
16,89	-0,135
21,11	-0,165

TABLE 5

2. $\alpha_f = 90^o$

Stress (MPa)	Longitudinal Strain ($\times 10^{-3}$)
0	0
3,64	0,505
7,29	1,035
10,93	1,605
14,58	2,180
18,22	2,785
21,86	3,355
25,51	3,970

Stress (MPa)	Transverse Strain ($\times 10^{-3}$)
0	0
0,76	-0,005
1,52	-0,010
2,28	-0,020
3,04	-0,030
3,81	-0,040

TABLE 6

3. $\alpha_f = 45^0$

Stress (MPa)	Longitudinal Strain ($\times 10^{-3}$)	Transverse Strain ($\times 10^{-3}$)
0	0	0
4,00	0,440	-0,215
8,01	0,875	-0,450
12,02	1,350	-0,680
16,03	1,800	-0,905
20,03	2,315	-1,185
24,04	2,840	-1,450
28,04	3,360	-1,740
32,05	3,950	-2,050

TABLE 7

Stress-strain response of Asbestos coupon

Stress (MPa)	Longitudinal Strain ($\times 10^{-3}$)	Transverse Strain ($\times 10^{-3}$)
0	0	0
1,39	0,230	-0,08
2,79	0,455	-0,165
4,18	0,700	-0,245
5,57	0,915	-0,305
6,97	1,130	-0,395
8,36	1,360	-0,475
11,15	1,805	-0,615
13,94	2,240	-0,775
19,51	3,130	-1,08
34,84	FAILURE	FAILURE

RESULTS

The following results were obtained for the buckling load of the panels tested.

A. Aluminium

			Buckling Load (kN)		
Thickness (mm)	t^3 (mm^3)	Price (R)	Theoretical	Tested	% Difference
1,00	1,00	2,96	2,90	2,42	16,6
1,27	2,048	3,60	5,95	4,75	20,2
1,60	4,096	4,85	11,90	9,00	24,4

B. Glass Fibre

			Buckling Load (kN)		
Thickness (mm)	t^3 (mm^3)	Price (R)	Theoretical	Tested	% Difference
1,60	4,096	1,92	2,80	2,35	6,1
1,80	5,832	2,40	3,99	3,70	7,3
2,20	10,648	2,88	7,29	6,40	12,2
2,40	13,824	3,36	9,46	10,50	-11,0

C. Carbon Fibre

			Buckling Load (kN)		
Thickness (mm)	t^3 (mm^3)	Price (R)	Theoretical	Tested	% Difference
1,30	2,197	32,0	2,57	2,08	19,1
1,50	3,375	38,4	3,80	2,50	34,2
1,82	6,029	44,8	6,62	4,80	27,5

D. Asbestos Fibre

			Buckling Load (kN)		
Thickness (mm)	t^3 (mm^3)	Price (R)	Theoretical	Tested	% Difference
3,232	33,761	0,12	9,40	10,80	-14,9
3,400	39,304	0,14	10,95	7,10	35,2
4,100	68,921	0,17	19,21	--	--
5,300	148,877	0,20	71,50	--	--

DISCUSSION

A theoretical method developed by J E Ashton was used in analysing the buckling behaviour of shear panels. Good agreement with the test results was demonstrated in graphs 12 to 25. The differences observed, which amount to the maximum of 35% for Asbestos fibre are due to the inaccurate test method used for the determination of the buckling load. Since this is not a standard method, two alternatives could be considered in order to improve the agreement between the theoretical calculated and the measured buckling load. Firstly one could accept that the actual buckling load is a certain percentage above the point where $dI/d\varepsilon$ is infinity. Secondly one could use a totally different method such as the Maxwell method used by Ashton in Ref (1). The disadvantage of using the first method suggested above is that the exact definition of the buckling point remains an arbitrary decision and therefore no research can be based on such comparisons. Thus only the second alternative mentioned should be used for the continuation of this research program.

From the table of results for the asbestos fibre composite, (p 76) it can be seen that no buckling load was obtained for the last two panels. This was due to the fact that the ultimate shear stress for the material was reached before the buckling load. This could only be overcome by reducing the percentage epoxy in the composite, which in turn can be achieved by using a less compact mat.

From graph 34 it can be seen that the material that has traditionally been used in aircraft primary structures is the one that compares unfavourably with advanced composite materials from the point of view of buckling load/mass ratio. As was initially expected, the more

advantageous material is carbon fibre composite which together with asbestos fibre compares favourably with glass fibre. The real advantage of asbestos fibre becomes evident from graph 35 which shows that this material is considerably cheaper than any other material tested. From this same graph it can also be noted that the carbon fibre composite is extremely expensive in comparison with the other materials and thus the previously mentioned advantage will be offset if a design has stringent cost limitations. Glass fibre composite can be seen to offer reasonable advantages over aluminium alloy in both load carrying ability and price.

Thus, if one of the above mentioned composite materials is to be used for aircraft primary structures, the only recommendations that can be made at this point is to use glass fibre composite.

This will offer improvement over aluminium alloys without introducing the cost penalty of carbon fibre or the unpredictability of asbestos fibre.

In the case of the unidirectional carbon fibre composite it is interesting to note that the panel has a preferred direction of shear. This can be seen by the fact that the lowest positive and negative eigenvalues are not equal in absolute value. The reason for this directional preference is the higher value of the moment of inertia obtained when the outer layers have the fibre oriented in the compression direction (of the resolved shear force).

Graphs 27, 29, 31 and 33 clearly show that the buckling load equation is a cubic. It is evident from all these curves that the theoretical line is always closer to a cubic relationship than the test results. This is also due to the unsatisfactory test method used in determining the exact buckling load.

CONCLUSIONS AND RECOMMENDATIONS

1. All the composite materials investigated offer certain advantages over Al-2024T3 as far as the buckling load is concerned. However these advantages, with the exception of glass fibre are partially offset either by unpredictability of the results or by the cost penalty.

2. A standard method for determining the exact buckling load must be used in future if a meaningful comparison between theoretical and practical results is to be made. The method used in this report, although valid from a purely technical point of view leaves open the decision as to the exact definition of the buckling load.

3. The method used for predicting buckling loads gives very satisfactory results but more terms should be used in future. Since, as explained by Ashton in Ref (1), the solution always converges from above to the exact value of the buckling load, the more terms included in the calculations, the better the accuracy.

4. The method of manufacture of the composite panels turned out to be very unsatisfactory in that a considerable amount of air bubbles were trapped in the composite and a non-uniform thickness panel was obtained. Variations in thickness of up to 20% were measured. It is therefore paramount that in future more sophisticated manufacturing equipment be used. The vacuum bag technique is here strongly recommended.

5. If a less compact asbestos mat could be manufactured,

great posibilities for this material would exist. The only problem encountered with the NORAMITE fibre tested was unpredictability of the results due to a too low percentage fibre composite being used. If the fibre could be made in a cloth the potential for use will in all probability increase considerably since this material gives a reasonably high modulus of elasticity. The attractiveness of this material stems from the fact that it is inexpensive as compared to aluminium alloys and carbon and glass fibres.

REFERENCES

1. ASHTON J E: LOVE T S. 'Shear stability of Laminated anisotropic plates', *Composite Materials: Testing and Design ASTM STP460*, New Orleans, 11-13 Feb, 1969.

2. BROUTMAN L J; KROCK R H. *Composite materials*, Volumes 1 to 8, Academic Press, NY, 1975.

3. DAVIS J G; ZEUDER G W. 'Compressive behaviour of plates fabricated from glass filaments and epoxy resins', *NASA* TN - D 3918 (Langley Research Centre).

4. DOW N F; ROSEN B W. 'Evaluations of filament-reinforced composites for aerospace structural applications', *NASA* - CR 207 (GEC).

5. LEKHNITSKI S G. *Anisotropic plates*, Gordon and Breach, science publishers, NY.

6. VISWANATHAN A V; TAMEKUNI M and BAKER LL. 'Elastic stability of laminated, flat and curved, long rectangular plates subjected to combined inplane loads', *NASA* CR-2330 (BOEING Commercial airplane company).

7. TSAI S W. 'Strength characteristics of composite materials', *NASA* CR-224 (Philco Corporation).

8. TSAI S W. 'Structural behaviour of composite materials', *NASA* CR-71 (Philco Corporation).

9. US Department of Defense, Military Handbook No 17A, *Plastics for aerospace vehicles*.

11. BRUHN E F, *Analysis and design of flight vehicle structures*, Tri-state offset company.

12. MEGSON T H G, *Aircraft structures for Engineering Students*, Edward Arnold, London, 1972.

12. KUHN P, PETERSON J P. LEVIN L R. 'A summary of diagonal tension', *NACA* T N - 2661.

13. ASHTON J E, WADDOUPS M E. 'Analysis of anisotropic plates', *Journal of composite materials*, 3, 148-165, 1969.

14. YOUNG D, FELGAR R P. 'Tables of characteristic functions representing the normal modes of vibration of a beam', *University of Texas Publication* No 4913, 1949.

15. Creszezuk L B. 'Shear Modulus Determination of Isotropic and Composite Materials', Composite Materials: Testing and Design, ASTM STP460, New Orleans, 11-13 Feb, 1969.

11. BRUHN E F, *Analysis and design of flight vehicle structures*, Tri-state offset company.

12. MEGSON T H G, *Aircraft structures for Engineering Students*, Edward Arnold, London, 1972.

12. KUHN P, PETERSON J P. LEVIM L H. 'A summary of diagonal tension', *NACA* T N - 2661.

13. ASHTON J E, WADDOUPS M E. 'Analysis of anisotropic plates', *Journal of composite materials*, 3, 148-165, 1969.

14. YOUNG D, FELGAR R P. 'Tables of characteristic functions representing the normal modes of vibration of a beam', *University of Texas Publication* No 4913, 1949.

15. Creszezuk L B. 'Shear Modulus Determination of Isotropic and Composite Materials', Composite Materials: Testing and Design, ASTM STP460, New Orleans, 11-13 Feb, 1969.

APPENDIX 1

Determination of material properties

1. Aluminium

Since this is an isotropic material and its properties are, today, well established, only one test was performed on Young's Modulus.

From graph 1 we find

$$E = \frac{\Delta Y}{\Delta X} = \frac{133}{2\ 10^{-}} = 66,5 \text{ GPa}$$

The difference between the value obtained and the number given in ref (10) is due to the fact that the strain reading obtained relates directly to the Aluminium cladding of the specimen.

2. Glass fibre composite (30% fibre by volume)

From graph 2

$$E_{11} = E_{22} = \frac{25,8}{1,52} = 16,97 \text{ GPa}$$

This value checks favourably with the figure obtained using volume fractions

$$E_c = V_f E_f + V_v E_e$$

$$= 0,3 \times 72,5 + 0,7 \times 3,1 = 23,92 \text{ GPa}$$

The difference between the calculated and measured values

is probably due to the void volume and air bubbles in the composite.

From graph 3

$$\nu_{12} = \nu_{21} = \frac{0,388}{1,800} = 0,216$$

From graph 4 (Table 3) and the method given in Ref 1, p 142, we find (by interpolation of stress)

$$m_L = \frac{\varepsilon_L}{\sigma_1} = \frac{1,52\times10^{-3}}{29} = 5,24\times10^{-5}$$

$$m_T = \frac{\varepsilon_T}{\sigma_2} = \frac{-1,0\times10^{-3}}{29} = -3,45\times10^{-5}$$

$$G_{LT} = \frac{1}{2(5,24\times10^{-5}+3,45\times10^{-5})} = 5,75 \text{ GPa}$$

3. Carbon fibre composite (22% fibre by volume)

From graph 5

$$E_{11} = \frac{185,3}{4,27\times10^{-3}} = 43,4 \text{ GPa}$$

The calculated value using volume fraction is

$$E_{11} = 200 \times 0,22 + 3,1 \times 0,78 = 46,4$$

From graph 6

$$\nu_{12} = \frac{0,085}{0,175} = 0,486$$

From graph 7

$$E_{22} = \frac{14,58}{2,18\times10^{-3}} = 6,69 \text{ GPa}$$

From graph 8

$$\nu_{21} = \frac{0,02}{0,275} = 0,07$$

Therefore, the relationship

$$\nu_{12}E_{22} = \nu_{21}E_{11}$$

is confirmed for the composite, ie

$$\nu_{21}E_{11} = 0,070 \times 43,4 = 3,04$$

$$\nu_{12}E_{22} = 0,486 \times 6,69 = 3,25$$

From graph 9 and interpolating the relevant values of applied stress in table 6, we get, as before,

$$m_L = \frac{2,86\times10^{-3}}{22,38} = 1,278 \times 10^{-4}/\text{MPa}$$

$$m_T = \frac{-1,48\times10^{-3}}{22,38} = 6,613 \times 10^{-5}/\text{MPa}$$

$$G_{LT} = \frac{1}{2(1,278\times10^{-4}+6,613\times10^{-5})} = 2,58 \text{ GPa}$$

4. Asbestos fibre composite (6% fibre by volume)

From graph 10

$$E = \frac{13,65}{2,2\times10^{-3}} = 6,2 \text{ GPa}$$

From graph 11

$$v = \frac{0,6 \cdot 3}{1,91} = 0,34$$

From graph II

$$v = \frac{0,655}{1,91} = 0,34$$

APPENDIX 2

Determination of the reduced stiffness matrices for glass fibre and carbon fibre panels

1. Fibreglass panels

Since the glass fibre used was a balanced weave cloth, the reduced stiffness matrix remains unchanged for each and every layer of the material.

Thus, according to the theory,

$$Q_{11} = \frac{E_{11}}{1-\nu_{12}\nu_{21}} = \frac{16\ 970}{1-0,216^2} = 17\ 800 \text{ MPa}$$

$$Q_{22} = \frac{E_{22}}{1-\nu_{12}\nu_{21}} = \frac{16\ 970}{1-0,216^2} = 17\ 800 \text{ MPa}$$

$$Q_{12} = \frac{\nu_{12}E_{22}}{1-\nu_{12}\nu_{21}} \quad 17\ 800 \times 0,216 = 3\ 845 \text{ MPa}$$

$$Q_{66} = G_{12} = 5\ 750 \text{ MPa}$$

Therefore the numerical form of the matrix will be

$$Q_{ij} = \begin{bmatrix} 17\ 800 & 3\ 845 & 0 \\ 3\ 845 & 17\ 800 & 0 \\ 0 & 0 & 5,750 \end{bmatrix}$$

and since our coordinate system has to be rotated through 45^{o}, we use the transformation equation earlier described. Thus, we find,

$$U_1 = \frac{1}{8}(3\times 17\ 800+3\times 17\ 800+2\ 3\times 845+4\times 5\ 750)$$

$$= 17\ 186 \text{ MPa}$$

$$U_2 = \frac{1}{2}(17\ 800-17\ 800) = 0$$

$$U_3 = \frac{1}{8}(17\ 800+17\ 800-2\times 3\ 845-4\times 5\ 750)$$

$$= 614 \text{ MPa}$$

$$U_4 = \frac{1}{8}(17\ 800+17\ 800+6\times 3\ 845-4\times 5\ 750)$$

$$= 4\ 459 \text{ MPa}$$

$$U_5 = \frac{1}{8}(17\ 800+17\ 800-2\times 3\ 845+4\times 5\ 750)$$

$$= 6\ 364 \text{ MPa}$$

$$U_6 = \frac{1}{2}(0+0) = 0$$

$$U_7 = 0$$

Therefore,

$$Q'_{11} = 17\ 186 + 614 \times \cos 4 \times 45 = 16\ 572 \text{ MPa}$$

$$Q'_{22} = 17\ 186 + 614 \times \cos 4 \times 45 = 16\ 572 \text{ MPa}$$

$$Q'_{12} = 4\ 459 - 614 \times \cos 4 \times 45 = 5\ 073 \text{ MPa}$$

$$Q'_{66} = 6\ 364 - 614 \times \cos 4 \times 45 = 6\ 978 \text{ MPa}$$

$Q'_{16} = 0$

$Q'_{26} = 0$

2. Carbon fibre panels

Since the carbon fibre used was in the form of a unidirectional (thus unbalanced) cloth, we have,

$$Q_{11} = \frac{43\ 400}{1-0,486\times0,07} = 44\ 928 \text{ MPa}$$

$$Q_{22} = \frac{6\ 690}{1-0,486\times0,07} = 6\ 926 \text{ MPa}$$

$$Q_{12} = \frac{0,486\times6\ 690}{1-0,486\times0,07} = 5\ 366 \text{ MPa}$$

$Q_{66} = 2\ 580$ MPa

where directions 1 and 2 are defined differently for alternate layers.

Thus, for layers for which the fibre is oriented in the compression direction (of the resolved shear force) the rotation between the fibre symmetry axes and the laminate reference axes is $+45^{\circ}$ whilst for the other layers it is -45°.

Therefore we find:

$$U_1 = \frac{1}{8}(3\times44\ 928+3\times6\ 926+2\times5\ 366+4\times2\ 580)$$

$$= 21\ 577 \text{ MPa}$$

$$U_2 = \frac{1}{2}(44\ 928-6\ 926) = 19\ 001\ \text{MPa}$$

$$U_3 = \frac{1}{8}(44\ 928+6\ 926-2\times3\ 366-4\times2\ 580)$$

$$= 4\ 350\ \text{MPa}$$

$$U_4 = \frac{1}{8}(44\ 928+6\ 926+6\times3\ 366-4\times2\ 580)$$

$$= 7\ 716\ \text{MPa}$$

$$U_5 = \frac{1}{8}(44\ 928+6\ 926-2\times3\ 366+4\times2\ 580)$$

$$= 6\ 930\ \text{MPa}$$

$$U_6 = U_7 = 0$$

For a $+45^{o}$ rotation we have

$$Q'_{11} = 21\ 577 + 4\ 350\cos180 = 17\ 227\ \text{MPa}$$

$$Q'_{22} = 21\ 577 + 4\ 350\cos180 = 17\ 227\ \text{MPa}$$

$$Q'_{12} = 7,716 - 4\ 350\cos180 = 12\ 066\ \text{MPa}$$

$$Q'_{66} = 6\ 930 - 4\ 350\cos180 = 11\ 280\ \text{MPa}$$

$$Q'_{16} = -\frac{19\ 001}{2}\sin90 = -9\ 500\ \text{MPa}$$

$$Q'_{26} = -\frac{19\ 001}{2}\sin90 = -9\ 500\ \text{MPa}$$

For a -45^{o} rotation of the axes all parameters will be

the same except Q'_{16} and Q'_{26} which will have opposite signs.

Thus

$$Q'_{16} = Q'_{26} = 9\ 500 \text{ MPa}$$

APPENDIX 3

Calculation of the flexural rigidity of the panels

1. Fibreglass

(i) According to the equation given in 'theory' we have, for a 4 layer fibreglass panel, t = 1,6 mm

$$[h_k^3 - h_{(k-1)}^3] = [-0,4^3 + 0,8^3 - 0^3 + 0,4^3 + 0,4^3 - 0^3 + 0,8^3 - 0,4^3]$$

$$= 1,024 \text{ mm}^3$$

Thus

$$D_{11} = \frac{1}{3} \times 16\ 572 \times 1,024 = 5\ 657 \text{ N-mm}$$

$$D_{22} = \frac{1}{3} \times 16\ 572 \times 1,024 = 5\ 657 \text{ N-mm}$$

$$D_{12} = \frac{1}{3} \times 5\ 073 \times 1,024 = 1\ 732 \text{ N-mm}$$

$$D_{66} = \frac{1}{3} \times 6\ 978 \times 1,024 = 2\ 382 \text{ N-mm}$$

$$D_{16} = 0 = D_{26}$$

(ii) Similarly for a 5 layer panel, t = 1,80 mm

$$[h_k^3 - h_{(k-1)}^3] = 1,458 \text{ mm}^3$$

$$D_{11} = 8\ 054 \text{ N-mm}$$

D_{22} = 8 054 N-mm

D_{12} = 2 466 N-mm

D_{66} = 3 391 N-mm

$D_{16} = D_{26} = 0$

(iii) For a 5 layer panel, t = 2,2 mm

$[h_k^3 - h_{(k-1)}^3] = 2{,}662$ mm^3

D_{11} = 14 705 N-mm

D_{22} = 14 705 N-mm

D_{12} = 4 501 N-mm

D_{66} = 7 443 N-mm

$D_{16} = D_{26} = 0$

(iv) For a 7 layer panel, t = 2,4 mm

$[h_k^3 - h_{(k-1)}^3] = 3{,}456$ mm^3

D_{11} = 19 091 N-mm

D_{22} = 19 091 N-mm

D_{12} = 5 844 N-mm

D_{66} = 8 038 N-mm

$D_{16} = D_{26} = 0$

2. Carbon fibre

(i) For a 5 layer panel, t = 1,30 mm

$[h_k^3 - h_{(k-1)}^3] = 0,54\ 925\ mm^3$

$D_{11} = 3\ 154$ N-mm

$D_{22} = 3\ 154$ N-mm

$D_{12} = 2\ 209$ N-mm

$D_{66} = 2\ 065$ N-mm

$$D_{16} = \frac{1}{3}[9\ 500(-0,39^3+0,65^3) - 9\ 500(-0,13+0,39^3)$$

$$+ 9\ 500(0,13^3+0,13^3) - 9\ 500(+0,39^3-0,13^3)$$

$$+ 9\ 500(0,65^3-0,39^3)] = 10/6 \text{ N-mm} = D_{26}$$

(ii) Similarly, for a 6 layer panel, t = 1,50 mm

$[h_k^3 - h_{(k-1)}^3] = 0,84\ 375$

$D_{11} = 4\ 845$ N-mm

$D_{22} = 4\ 845$ N-mm

$D_{12} = 3\ 394$ N-mm

$D_{66} = 3\ 172$ N-mm

$D_{16} = D_{26} = 1\ 286$ N-mm

(iii) For a 7 layer panel, t = 1,82 mm

$[h_k^3 - h_{(k-1)}^3] = 1,5\ 071\ mm^3$

$D_{11} = 8\ 655$ N-mm

D_{22} = 8 655 N-mm

D_{12} = 6 062 N-mm

D_{66} = 5 667 N-mm

$D_{16} = D_{26}$ = 1 286 N-mm

APPENDIX 4

Evaluation of integrals ψ.

According to refs (14) and (1) we find,

$$\psi_{111} = \int_0^1 X'(\xi)X(\xi)d\xi$$

Taking $d\xi = 0,1$,

$$\psi_{111} = [0,189\ 1^2+0,619\ 39^2+1,096^2+1,455\ 45^2+1,588\ 15^2$$
$$+1\ 455\ 45^2+1,096^2+0,619\ 39^2+0,189\ 1^2] \times 0,1$$
$$= 1,000\ 012\ 74$$

Similarly,

$\psi_{122} = 1,000\ 155\ 319$

$\psi_{133} = 1,000\ 860\ 092$

$\psi_{144} = 1,003\ 085\ 011$

Due to orthogonality of the functions the remaining integrals in ψ_{1mn} are all zero.

Ψ_{2mn}

		n			
		1	2	3	4
m	1	12,287	0	-9,869	0
	2	0	46,045	0	-17,152
	3	-9,737	0	-98,877	0
	4	0	-18,039	0	169,800

Ψ_{3mn}

		n			
		1	2	3	4
m	1	446,966	0	11,286	0
	2	0	3 819,489	0	72,296
	3	11,286	0	14 703,369	0
	4	0	72,296	0	40 245,016

Ψ_{4mn}

		n			
		1	2	3	4
m	1	0	3,346	0	0,921
	2	-5,335	0	5,537	0
	3	0	-5,489	0	7,701
	4	0,892	0	-7,362	0

Ψ_{5mn}

		n			
		1	2	3	4
m	1	-12,310	0	9,655	0
	2	0	-46,050	0	16,608
	3	9,612	0	-98,957	0
	4	0	16,428	0	-171 596

Ψ_{6mn}

		n			
		1	2	3	4
m	1	0	121,698	0	58,394
	2	-122,140	0	474,688	0
	3	0	-178,658	0	1 180,036
	4	-60,750	0	-1 192,384	0

APPENDIX 5

Mathematical deviation of the equations of the plate potential and Kinetic energies

Suffix sum convention will be used in this derivation ie,

$$a_{ij}b_j = \sum_{j=1}^{N} d_{ij}b_j$$

Therefore,

$$W(x,y) = \sum_{i=1}^{7}\sum_{j=1}^{7} a_{ij}X_i(x)X_j(x) = a_{ij}X_i(x)X_j(y)$$

Two different notations will be used for W(x,y) only, as follows,

$$W(x,y) = a_{ik}X_iX_k = a_{mn}X_mX_n$$

where it is understood that X_i and X_m are functions of x only and X_j and X_m are functions of y only.

All integrals are reduced to the interval [0,1]. Therefore, if c is arbitrary, we let $\xi = \frac{x}{c}$ so that

$$\int_0^a F(x)dx = a\int_0^1 F(\xi)d\xi \text{ and}$$

$$\frac{dF}{dx} = \frac{dF}{d\xi}\cdot\frac{d\xi}{dx} = \frac{1}{c}\frac{dF}{d\xi}$$

$$\frac{d^2F}{dx^2} = \frac{1}{c^2}\frac{d^2F}{d\xi^2}$$

hence

$$\int_0^a F(x)dx = a\int_0^1 F(\xi)d\xi$$

$$\int_0^a \frac{dF(x)}{dx}dx = \int_0^1 \frac{dF(\xi)}{d\xi}d\xi$$

$$\int_0^a \frac{d^2F(x)}{dx^2}dx = \frac{1}{a}\int_0^1 \frac{d^2F(\xi)}{d\xi^2}d\xi$$

Using a comma to denote differentiation, we can summarize these results as follows:

$$\int_0^a F(x)dx = a\int_0^1 F(\xi)d\xi$$

$$\int_0^a F,_x dx = \int_0^1 F,_\xi d\xi$$

$$\int_0^a F,_{xx}dx = \frac{1}{a}\int_0^1 F,_{\xi\xi}d\xi$$

Thus the problem reduces to

$$\frac{\partial}{\partial a_{ij}}\Big[\frac{1}{2}\int_0^a\int_0^b D_{11}W^2,_{xx} + 2D_{12}W,_{xx}W,_{yy} + D_{22}W^2,_{yy} + 4W,_{xy}(D_{16}W,_{xx}$$

$$+D_{26}W,_{yy}+D_{66}W,_{xy})dxdy - \frac{1}{2}\int_0^a\int_0^b (N_xW^2,_x+N_yW^2,_y$$

$$+2N_{xy}W,_xW,_y)dxdy\Big] = 0$$

For convenience we write

$$V = \frac{1}{2}\int_0^a\int_0^b D_{11}W,^2_{xx}dxdy + \frac{1}{2}\int_0^a\int_0^b 2D_{12}W,_{xx}W,_{yy}dxdy + \frac{1}{2}\int_0^a\int_0^b D_{22}W,^2_{yy}dxdy$$

$$+ \frac{1}{2}\int_0^a\int_0^b 4D_{16}W,_{xy}W,_{xx}dxdy + \frac{1}{2}\int_0^a\int_0^b 4D_{26}W,_{xy}W,_{yy}dxdy$$

$$+ \frac{1}{2}\int_0^a\int_0^b fD_{66}W,_{xy}W,_{xy}dxdy = A + B + C + D + E + F$$

and similarly

$$U = -[\frac{1}{2}\int_0^a\int_0^b N_xW,^2_x2dxdy + N_yW,_y2dxdy + 2N_{xy}W,_xW,_ydxdy]$$

$$= -(G+H+I)$$

In the analysis used, G = I = 0 (only shear stress was applied).

Each of the above integrals is now evaluated in turn.

Thus we have

$$A = \frac{1}{2}\int_0^a\int_0^b fD_{11}W,_{xx}W,_{xx}dxdy$$

$$= \frac{D_{11}}{2}\int_0^a\int_0^b (a_{jk}X_iX_k),_{xx}(a_{mn}X_mX_n),_{xx}dxdy$$

$$= \frac{D_{11}}{2}\int_0^a\int_0^b a_{ik}X_i,_{xx}X_ka_{mn}X_m,_{xx}X_ndxdy$$

$$= \frac{D_{11}}{2} a_{ik}{}^{a}{}_{mn} \left(\int_0^a X_{i,xx} X_{m,xx}\, dx\right)\left(\int_0^b X_k X_n\, dy\right)$$

$$= \frac{D_{11}}{2} a_{ik}{}^{a}{}_{mn} \left(\frac{a}{a^4}\right)\left(\int_0^1 X_{i,\xi\xi} X_{m,\xi\xi}\, d\xi\right) \cdot b\left(\int_0^1 X_k X_n\, d\xi\right)$$

$$= \frac{b}{2a^3} D_{11}\, a_{ik}{}^{a}{}_{mn} \psi_{3\,im}\, \psi_{1\,kn}$$

where

$$\psi_{3mn} = \int_0^1 X_{m,\xi\xi} X_{n,\xi\xi}\, d\xi$$

$$\psi_{1mn} = \int_0^1 X_m X_n\, d\xi$$

hence

$$A = \frac{b}{2a^3} D_{11}\, a_{ik}{}^{a}{}_{mn} \psi_{3\,im}\, \psi_{1\,kn}$$

$$B = \int_0^a \int_0^b D_{12} W_{,xx} W_{,yy}\, dx\, dy = \int_0^a \int_0^b D_{12}\, a_{ik} X_{i,xx} X_k\, a_{mn} X_m X_{n,yy}\, dx\, dy$$

$$= D_{12}\, a_{ik}{}^{a}{}_{mn} \left(\int_0^a X_{i,xx} X_m\, dx\right)\left(\int_0^b X_{n,yy} X_k\, dy\right)$$

$$= D_{12}\, a_{ik}{}^{a}{}_{mn} \frac{a}{a^2}\left(\int_0^1 X_{i,\xi\xi} X_m\, d\xi\right) \frac{b}{b^2}\left(\int_0^1 X_{n,\eta\eta} X_k\, d\eta\right)$$

$$= D_{12}\, a_{ik}{}^{a}{}_{mn} \frac{1}{ab} \psi_{3\,im}\, \psi_{3\,nk}$$

where

$$\psi_{5mn} = \int_0^1 X_{m,5} X_n \, dz$$

And we can now rewrite

$$B = D_{12} a_{ik} a_{mn} \frac{1}{ab} \psi_{5im} \psi_{nk}$$

$$= \frac{D_{12}}{2ab} (a_{ik} a_{mn} \psi_{5im} \psi_{nk} + a_{ik} a_{mn} \psi_{im} \psi_{5nk})$$

$$= \frac{D_{12}}{2ab} (a_{ik} a_{mn} \psi_{5im} \psi_{5nk} + a_{mn} a_{ik} \psi_{5mi} \psi_{5kn})$$

$$= \frac{D_{12}}{2ab} a_{ik} a_{mn} (\psi_{5im} \psi_{5nk} + \psi_{5mi} \psi_{5kn})$$

$$C = \frac{1}{2} \int_0^a \int_0^b D_{22} W_{,yy} W_{,yy} \, dx dy = \frac{1}{2} \int_0^a \int_0^b D_{22} a_{ik} X_i X_k, yy \, a_{mn} X_m X_n, yy \, dx dy$$

$$= \frac{1}{2} D_{22} a_{ik} a_{mn} \left(\int_0^a X_i X_m \, dx \right) \left(\int_0^a X_k, yy \, X_n, yy \, dy \right)$$

$$= \frac{1}{2} \frac{a}{b^3} D_{22} a_{ik} a_{mn} \psi_{3kn} \psi_{1im}, \text{ etc,}$$

$$C = \frac{b}{2b^4} D_{12} a_{ik} a_{mn} \psi_{3kn} \psi_{1im}$$

$$D = 2D_{16} \int_0^a \int_0^b W_{,xy} W_{,xx} \, dx dy = 2D_{16} \int_0^a \int_0^b a_{ik} X_i, x X_k, y \, a_{mn} X_m, xx X_n \, dx dy$$

$$= 2D_{16} a_{ik} a_{mn} \left[\int_0^a X_i, x X_m, xx \, dx \right] \left[\int_0^b X_k, y X_n \, dy \right]$$

$$= 2D_{16} a_{ik} a_{mn} \frac{1}{a^2} \left(\int_0^1 X_{m,\xi\xi} X_{i,\xi} d\xi\right)\left(\int_0^1 X_{k,\xi} X_n d\xi\right)$$

$$= 2D_{16} a_{ik} a_{mn} \frac{1}{a^2} \psi_{6mi} \psi_{4kn}$$

$$= \frac{D_{16}}{a^2} a_{ik} a_{mn} \left(\psi_{6mi}\psi_{4kn} + \psi_{6im}\psi_{4nk}\right)$$

where

$$\psi_{4mn} = \int_0^1 X_{m,\xi} X_n d\xi$$

$$\psi_{6mn} = \int_0^1 X_{m,\xi\xi} X_{n,\xi} d\xi$$

$$E = 2\int_0^a \int_0^b D_{26} W_{,xy} W_{,yy} dxdy = 2D_{26} \left(\int_0^a X_{i,x} X_m dx\right)\left(\int_0^b X_{k,y} X_{n,yy} dy\right) a_{ik} a_{mn}$$

$$= 2D_{26} a_{ik} a_{mn} \frac{1}{b^2} \left[\int_0^1 X_{i,\xi} X_m d\xi\right]\left[\int_0^1 X_{n,\xi\xi} X_{k,\xi} d\xi\right]$$

$$E = \frac{1}{b^2} D_{26} a_{ik} a_{mn} \left(\psi_{6im}\psi_{6nk} + \psi_{4mi}\psi_{6kn}\right)$$

$$F = 2\int_0^a \int_0^b D_{66} W_{,xy} W_{,xy} dxdy$$

$$= 2D_{66} a_{ik} a_{mn} \left[\int_0^a X_{i,x} X_{m,x} dx\right]\left[\int_0^b X_{k,y} X_{n,y} dy\right]$$

$$= \frac{2}{ab} D_{66} a_{ik} a_{mn} \left(\int_0^1 X_{i,\xi} X_{m,\xi} d\xi\right)\left(\int_0^1 X_{k,\xi} X_{n,\xi} d\xi\right)$$

$$= \frac{2}{ab} D_{66} a_{ik} a_{mn} \psi_{2im} \psi_{2kn}$$

where

$$\psi_{2mn} = \int_0^1 X_{m,\varepsilon} X_{n,\xi} d\xi$$

$$H = \frac{1}{2}\int_0^a \int_0^b 2N_{xy} W_{,x} W_{,y} dxdy = \int_0^a \int_0^b N_{xy} a_{ik} X_{i,x} X_k a_{mn} X_m X_{n,y} dxdy$$

$$= N_{xy}\left(\int_0^a X_{i,x} X_m dx\right)\left(\int_0^b X_{n,y} X_k dy\right) a_{ik} a_{mn}$$

$$= N_{xy} a_{ik} a_{mn} \psi_{4im} \psi_{4nk} = \frac{N_{xy}}{2} a_{ik} a_{mn} \left(\psi_{4im} \psi_{4nk} + \psi_{4mi} \psi_{4kn}\right)$$

Summarising the above results we have

$$A = \frac{h}{2a^3} D_{11} a_{ik} a_{mn} \psi_{3im} \psi_{1kn} = \frac{1}{2} a_{ik} a_{mn} d^A_{ikmn}$$

where

$$d^A_{ikmn} = \frac{h}{a^3} D_{11} \psi_{3im} \psi_{1kn}$$

$$B = \frac{1}{2ab} D_{12} a_{ik} a_{mn} \left(\psi_{5im} \psi_{5nk} + \psi_{5mi} \psi_{5kn}\right)$$

$$= \frac{1}{2}a_{ik}a_{mn}d^{B}_{ikmn},\quad d^{B}_{ikmn} = \frac{1}{ab}D_{12}(\psi_{5im}\psi_{5nk}+\psi_{5mi}\psi_{5kn})$$

$$C = \frac{1}{2}a_{ik}a_{mn}d^{C}_{ikmn},\quad d^{C}_{kmn} = \frac{a}{b^3}D_{22}\psi_{3kn}\psi_{1im}$$

$$D = \frac{1}{2}a_{ik}a_{mn}d^{D}_{ikmn},\quad d^{D}_{ikmn} = \frac{2}{a^2}D_{16}(\psi_{6mi}\psi_{4kn}+\psi_{6im}\psi_{4nk})$$

$$E = \frac{1}{2}a_{ik}a_{mn}d^{E}_{ikmn},\quad d^{E}_{ikmn} = \frac{2}{b^2}D_{26}(\psi_{4im}\psi_{6nk}+\psi_{4mi}\psi_{6kn})$$

$$F = \frac{1}{2}a_{ik}a_{mn}d^{F}_{ikmn},\quad d^{F}_{ikmn} = \frac{4}{ab}D_{66}\psi_{3im}\psi_{3kn}$$

$$H = \frac{1}{2}a_{ik}a_{mn}\ell_{ikmn},\quad \ell_{ikmn} = N_{xy}(\psi_{4im}\psi_{4nk}+\psi_{4mi}\psi_{4kn})$$

Thus we can write

$$U + V = A + B + C + D + E + F - H$$

$$= \frac{1}{2}(a_{ik}a_{mn}d_{ikmn} - a_{ik}a_{mn}\ell_{ikmn})$$

$$U + V = \frac{1}{2}a_{ik}(a_{mn}d_{ikmn} - a_{mn}\ell_{ikmn})$$

where

$$d_{ikmn} = d^{A}_{ikmn} + d^{B}_{ikmn} + d^{C}_{ikmn} + d^{D}_{ikmn} + d^{E}_{ikmn} + d^{F}_{ikmn}$$

Therefore the solution is

$$\frac{\partial}{\partial a_{ik}}\left[\frac{1}{2}a_{ik}(a_{mn}d_{ikmn} - a_{mn}\ell_{ikmn})\right] = 0$$

or $d_{ikmn}a_{mn} - \ell_{ikmn}a_{mn} = 0$

APPENDIX 6

Calculation of the buckling load of the isotropic panels (Aluminium and Asbestos fibre composite).

The equation for the buckling stress in shear of an isotropic plate with clamped edges is, from Ref (10),

$$\tau_{cr} = K\frac{\pi^2}{12(1-\nu^2)} \times E \times \left(\frac{t}{b}\right)^2$$

where K = 14,5.

For Aluminium we have

E = 66 500 MPa
b = 300 mm
ν = 0,3

(i) For t = 1,6 mm

τ_{cr} = 24,789 MPa
S_{cr} = 11,9 kN

(ii) For t = 1,27 mm

τ_{cr} = 15,62 MPa
S_{cr} = 5,95 kN

(iii) For t = 1,00 mm

τ_{cr} = 9,68 MPa
S_{cr} = 2,9 kN

For Asbestos fibre composite

E = 6 200 MPa
b = 300 mm
ν = 0,34

Thus for

(i) t = 3,232 mm

τ_{cr} = 9,7 MPa

S_{cr} = 9,4 kN

(ii) t = 3,4 mm

τ_{cr} = 10,74 MPa

S_{cr} = 10,95 kN

(iii) t = 4.1 mm

τ_{cr} = 15,62 MPa

S_{cr} = 19,21 kN

(iv) t = 5,3 mm

τ_{cr} = 26,10 MPa

S_{cr} = 41,50 kN

APPENDIX 7

Working and design equation for composite materials

As explained by Ashton in Ref (1) the working equation for the buckling load in shear of a composite panel is

$$N_{xy,cr} = K\frac{D_{11}}{b^2}$$

where the value of K is

K = 148,5 for glass fibre

For carbon fibre the constant K varies both with the number of layers in the laminate and with the shear direction relative to the fibre orientation.

In the case of the panels analysed, if the shear direction was reversed we would have (from the computer output)

Carbon fibre panels:

(i) t = 1,3 mm

S_{cr} = 4,461 321(300) = 1 338,4 N

(ii) t = 1,5 mm

S_{cr} = 7,463 403(300) = 2 239,0 N

(iii) t = 1,32 mm

S_{cr} = 13,939 822(300) = 4 182,0 N

Since the flexural rigidity of the panels D_{11} remains the same for a $+45^{\circ}$ or for a -45° rotation of the axes we will have the following values of the constant K,

	Positive shear direction			Negative shear direction		
	t (mm)			t (mm)		
	1,3	1,5	1,82	1,3	1,5	1,82
K	244,5	235,3	229,5	127,3	138,6	145,0

The results presented above correlate extremely well with the graph given in Ref (13).

The values in the table above are higher than the results given by Ashton since these relate to a simply supported plate (Ref graph 36).

APPENDIX 8

Computer program and results

```
IEF376I  JOB /ANXJOB  / STOP  79025.1049 CPU    0MIN 10.79SEC
```

```
W47100I CPU WEST : TOTAL I/O COUNT =    665 BLOCKS. IO/CPU RATIO IS HI . APPROX COST OF JOB R7.46
```

```
 LEVEL 2.2  (SEPT 76)                    OS/360  FORTRAN H EXTENDED          DATE 79.025/10.47.33       PAGE    1
REQUESTED OPTIONS:
OPTIONS IN EFFECT: NAME(MAIN) OPTIMIZE(1) LINECOUNT(60) SIZE(MAX) AUTODBL(NONE)
                   SOURCE EBCDIC NOLIST NODECK OBJECT NOMAP NOFORMAT NOGOSTMT NOXREF NOALC NOANSF TERM FLAG(I)

   ISN 0002            DIMENSION H1(16,16),E1(15,16),WK(100),WKAREA(500),HN(16,16)
   ISN 0003            DIMENSION GN(15,16),EN(16,16)
   ISN 0004            COMPLEX Z(15,15),X(16)
   ISN 0005            DIMENSION A(6,4,4),F(4,4,4,4),G(4,4,4,4),H(4,4,4,4),E(4,4,4,4)
   ISN 0006            DIMENSION R(4,4,4,4),S(4,4,4,4),T(4,4,4,4),U(4,4,4,4),V(4,4,4,4)
   ISN 0007            IDGT=3
                C
                C
                C      ...THE PROGRAM READS THE DIMENSIONS OF THE PLATE
                C
                C
   ISN 0008            READ(5,100)B,C
   ISN 0009       100  FORMAT(F5.2)
                C
                C
                C      ...READING IN THE FLEXURAL RIGIDITIES OF THE PLATE
                C
                C
   ISN 0010            READ(5,101)D1,D2,D3,D4,D5,D6
   ISN 0011       101  FORMAT(F8.2)
                C
                C
                C      ...READING IN THE VALUES OF THE ORTHOGONAL FUNCTIONS "PSI" FROM DATA FILE
                C
                C
   ISN 0012            DO 3 J=1,6
   ISN 0013            DO 2 L=1,4
   ISN 0014            DO 1 I=1,4
   ISN 0015            READ(5,102)A(J,L,I)
   ISN 0016       1    CONTINUE
   ISN 0017       2    CONTINUE
   ISN 0018       3    CONTINUE
   ISN 0019       102  FORMAT(F9.3)
                C
                C
                C      ...COMPUTING THE TWO MATRICES "D", AND "E"
                C
                C
   ISN 0020            DO 4 I=1,4
   ISN 0021            DO 5 K=1,4
```

```
ISN 0023                DO 7 N=1,4
ISN 0024                F(I,K,M,N)=D1*A(3,I,M)*A(1,K,N)*B/C**3
ISN 0025                R(I,K,M,N)=D2*(A(5,I,N)*A(5,N,K)+A(5,M,I)*A(5,K,N))*1/(C*B)
ISN 0026                S(I,K,M,N)=D3*A(1,I,M)*A(3,K,N)*C/B**3
ISN 0027                G(I,K,M,N)=2*D4*(A(6,M,I)*A(4,K,N)+A(6,I,M)*A(4,N,K))*1/C**2
ISN 0028                T(I,K,M,N)=2*D5*(A(4,I,M)*A(6,N,K)+A(4,M,I)*A(6,K,M))*1/B**2
ISN 0029                U(I,K,M,N)=4*D6*A(2,I,M)*A(2,K,N)*1/(C*B)
ISN 0030                V(I,K,M,N)=-(I,K,M,N)+R(I,K,M,N)+S(I,K,M,N)+G(I,K,M,N)+T(I,K,M,N)
ISN 0031                P(I,K,M,N)=V(I,K,M,N)+U(I,K,M,N)
ISN 0032                E(I,K,M,N)=A(4,I,M)*A(4,N,K)+A(4,M,I)*A(4,K,N)
ISN 0033                J=((I-1)*4)+K
ISN 0034                L=((M-1)*4)+N

LEVEL 2.2 (SEPT 76)          MAIN          OS/360 FORTRAN H EXTENDED          DATE 79.025/10.47.33          PAGE 2

ISN 0035                E(J,L)=E(I,K,M,N)
ISN 0036                CONTINUE
ISN 0037              7 CONTINUE
ISN 0038              6 CONTINUE
ISN 0039              5 CONTINUE
ISN 0040              4 CONTINUE
                        C
                        C
                        C     ...INVERTING THE MATRIX "E", MULTIPLYING THE RESULT BY
                        C     "D" AND FINDING THE EIGENVALUES OF THE FINAL MATRIX
                        C
                        C
ISN 0041                CALL LINV2F(E,16,16,EN,IDGT,WKAREA,IER)
ISN 0042                CALL VMULFF(EN,M1,16,16,16,16,16,GN,16,IER)
ISN 0043                CALL EIGRF(GN,16,16,0,W,Z,16,WK,IER)
ISN 0044                WRITE(6,150)
ISN 0045                WRITE(6,151)
ISN 0046              151 FORMAT(//T30,'FIBERGLASS PLATE THICKNESS=1.6MM')
ISN 0047              150 FORMAT(T30,'THE CRITICAL VALUES OF THE BUCKLING LOAD ARE:')
ISN 0048                WRITE(6,105)((W(I),I=1,15))
ISN 0049              105 FORMAT(////T2,8(F12.6,2X))
ISN 0050                STOP
ISN 0051                END

*OPTIONS IN EFFECT*NAME(MAIN) OPT(SIZE(1) LINECOUNT(60) SIZE(MAX) AUTODBL(NONE)

*OPTIONS IN EFFECT*SOURCE EBCDIC NOLIST NODECK OBJECT NOMAP NOFORMAT NOGOSTMT NOXREF NOALC NOANSF TERM FLAG(I)

*STATISTICS*      SOURCE STATEMENTS =       50, PROGRAM SIZE =     20768, SUBPROGRAM NAME =  MAIN

*STATISTICS*  NO  DIAGNOSTICS GENERATED

                                                                    117K BYTES OF CORE NOT USED

*******  END OF COMPILATION  *******
```

```
C     SUBROUTINE LINV2F (A,N,IA,AINV,IDGT,WKAREA,IER)                    LI2F0010
C                                                                        LI2F0020
C-LINV2F--------S/D-----LIBRARY 1--------------------------------------LI2F0030
C                                                                        LI2F0040
C    FUNCTION              - INVERSION OF A MATRIX - FULL STORAGE MODE -  LI2F0050
C                            HIGH ACCURACY SOLUTION                      LI2F0060
C    USAGE                 - CALL LINV2F (A,N,IA,AINV,IDGT,WKAREA,IER)   LI2F0070
C    PARAMETERS   A        - INPUT MATRIX OF DIMENSION N BY N CONTAINING  LI2F0080
C                            THE MATRIX TO BE INVERTED.                  LI2F0090
C                 N        - ORDER OF A. (INPUT)                         LI2F0100
C                 IA       - NUMBER OF ROWS IN THE DIMENSION STATEMENT    LI2F0110
C                            FOR A AND AINV IN THE CALLING PROGRAM.      LI2F0120
C                            (INPUT)                                     LI2F0130
C                 AINV     - OUTPUT MATRIX OF DIMENSION N BY N CONTAINING LI2F0140
C                            THE INVERSE OF A. A AND AINV MUST OCCUPY    LI2F0150
C                            SEPARATE CORE LOCATIONS.                    LI2F0160
C                 IDGT     - INPUT OPTION.                               LI2F0170
C                            IF IDGT IS GREATER THAN 0, THE ELEMENTS OF A LI2F0180
C                              ARE ASSUMED TO BE CORRECT TO IDGT DECIMAL  LI2F0190
C                              DIGITS AND THE ROUTINE PERFORMS AN ACCURACY LI2F0200
C                              TEST.                                     LI2F0210
C                            IF IDGT EQUALS 0, THE ACCURACY TEST IS        LI2F0220
C                              BYPASSED.                                 LI2F0230
C                            ON OUTPUT, IDGT CONTAINS THE APPROXIMATE      LI2F0240
C                              NUMBER OF DIGITS IN THE ANSWER WHICH      LI2F0250
C                              WERE UNCHANGED AFTER IMPROVEMENT.         LI2F0260
C                 WKAREA   - WORK AREA OF DIMENSION GREATER THAN OR EQUAL LI2F0270
C                            TO N**2+3N.                                 LI2F0280
C                 IER      - ERROR PARAMETER                             LI2F0290
C                            TERMINAL ERROR = 128+N.                     LI2F0300
C                              N = 1 INDICATES THAT THE MATRIX IS        LI2F0310
C                                ALGORITHMICALLY SINGULAR. (SEE THE CHAPTERLI2F0320
C                                L PRELUDE).                             LI2F0330
C                              N = 3 INDICATES THAT THE MATRIX IS TOO     LI2F0340
C                                ILL-CONDITIONED FOR ITERATIVE IMPROVEMENT LI2F0350
C                                TO BE EFFECTIVE.                        LI2F0360
C                            WARNING ERROR = 32+N.                       LI2F0370
C                              N = 2 INDICATES THAT THE ACCURACY TEST.   LI2F0380
C                                FAILED.                                 LI2F0390
C                                THE COMPUTED SOLUTION MAY BE IN ERROR BY LI2F0400
C                                MORE THAN CAN BE ACCOUNTED FOR BY THE   LI2F0410
C                                UNCERTAINTY OF THE DATA.                LI2F0420
C                                THIS WARNING CAN BE PRODUCED ONLY IF IDGT LI2F0430
C                                IS GREATER THAN 0 ON INPUT.             LI2F0440
C                                SEE CHAPTER L PRELUDE FOR FURTHER       LI2F0450
C                                DISCUSSION.                             LI2F0460
C    PRECISION             - SINGLE/DOUBLE                               LI2F0470
C    REQD. IMSL ROUTINES   - SINGLE/LEQT2F,LUDATF,LUELMF,LUREFF,UERTST   LI2F0480
C                            DOUBLE/LEQT2F,LUDATF,LUELMF,LUREFF,UERTST,  LI2F0490
C                              VXPADD                                    LI2F0500
C    LANGUAGE              - FORTRAN                                     LI2F0510
C--------------------------------------------------------------------------LI2F0520
```

CALL LINV2F (A,N,IA,AINV,IDGT,WKAREA,IER)

Purpose

LINV2F computes the inverse of the N by N matrix A, where A is stored in full storage mode. The difference between this routine and routine LINV1F is that LINV2F invokes iterative improvement, if necessary, in order to improve the accuracy of the solution AINV beyond that obtained in LINV1F.

Algorithm

The inverse, AINV, is computed by first setting AINV to the N by N identity matrix, then calling LEQT2F. This routine is included in the IMSL Library mainly for convenience. Many users may prefer to call LEQT2F directly.

Programming Notes

1. The vector WKAREA in the calling program should have length at least $N^2 + 3N$.

2. A and AINV must be mutually exclusive.

Accuracy

If IDGT is greater than zero, the elements of A are assumed to be correct to IDGT decimal digits. The solution will be the exact solution, without any roundoff error, to a matrix A whose elements agree with the elements of A in the first IDGT decimal digits. The program first attempts such a solution without iterative improvement. If this fails, then iterative improvement is performed. If this also fails, solution is not possible and the program exits. Upon exit, the first columns of AINV will have been replaced by the best solution that the computer can generate and IDGT is set to the approximate number of digits in the answer which were unchanged by the improvement (see IMSL routine LUREFF). The other columns of AINV are left unchanged in this case and IER is set to 131. If IDGT equals zero, iterative improvement is automatically performed.

```
C      SUBROUTINE VMULFF (A,B,L,M,N,IA,IB,C,IC,IER)                    VMFF0010
C                                                                      VMFF0020
C-VMULFF--------S/D-----LIBRARY )-------------------------------------VMFF0030
C                                                                      VMFF0040
C    FUNCTION              - MATRIX MULTIPLICATION-FULL STORAGE MODE    VMFF0050
C    USAGE                 - CALL VMULFF (A,B,L,M,N,IA,IB,C,IC,IER)     MFF0060
C    PARAMETERS    A       - FIRST MATRIX (A IS L X M)                  VMFF0070
C                  B       - SECOND MATRIX (B IS M X N)                 VMFF0080
C                  L       - MAXIMUM VALUE OF FIRST SUBSCRIPT OF A      VMFF0090
C                  M       - MAXIMUM VALUE OF SECOND SUBSCRIPT OF A AND VMFF0100
C                              FIRST SUBSCRIPT OF B                     VMFF0110
C                  N       - MAXIMUM VALUE OF SECOND SUBSCRIPT OF B     VMFF0120
C                  IA      - VALUE OF FIRST INDEX IN DIMENSION STATEMENT VMFF0130
C                              FOR A                                    VMFF0140
C                  IB      - VALUE OF FIRST INDEX IN DIMENSION STATEMENT VMFF0150
C                              FOR B                                    VMFF0160
C                  C       - RESULT MATRIX (C IS L X N)                 VMFF0170
C                  IC      - VALUE OF FIRST INDEX IN DIMENSION STATEMENT VMFF0180
C                              FOR C                                    VMFF0190
C                  IER     - ERROR PARAMETER.                           VMFF0200
C                            TERMINAL ERROR=128+N.                      VMFF0210
C                              N = 1 INDICATES A,B,OR C WAS DIMENSIONED VMFF0220
C                                INCORRECTLY                            VMFF0230
C    PRECISION             - SINGLE/DOUBLE                              VMFF0240
C    REQD. IMSL ROUTINES   - SINGLE/UERTST                              VMFF0250
C                          - DOUBLE/UERTST,VXPADD                       VMFF0260
C    LANGUAGE              - FORTRAN                                    VMFF0270
C-------------------------------------------------------------------VMFF0280
```

CALL VMULFF (A,B,L,M,N,IA,IB,C,IC,IER)

Purpose

VMULFF performs the matrix multiplication A x B where both A and B are in full storage mode.

Algorithm

The following computation is performed:

$$C_{i,j} = \sum_{K=1}^{M} A_{i,k}B_{k,j},$$

where i = 1,...,L and J = 1,...,N.

For single precision input, computation is done in double precision. For double precision input, computation is done in extended precision.

Programming Notes

The user should be sure that L is less than or equal to IA, M is less than or equal IB, L is less than or equal IC and that C does not occupy any of the same storage as A or B.

Example

DIMENSION A(4,3), B(3,4), C(5,5)

Input:

$$A = \begin{bmatrix} 14. & 15. & 12. & x & x \\ 28. & -9. & -3. & x & x \\ 14. & -27. & 12. & x & x \\ 14. & 36. & 33. & x & x \end{bmatrix}$$

$$B = \begin{bmatrix} 1. & 2. & 1. & 1. \\ 2. & -1. & -2. & 5. \\ 3. & -1. & 1. & 8. \end{bmatrix}$$

L = 4
M = 3
N = 4
IA = 4
IB = 3
IC = 5

Output:

$$C = \begin{bmatrix} 80. & 1. & -4. & 185. & x \\ 1. & 68. & 43. & -41. & x \\ -4. & 43. & 80. & -25. & x \\ 185. & -41. & -25. & 458. & x \\ x & x & x & x & x \end{bmatrix}$$

x implies "not used by subroutine VMULFF".

```
C      SUBROUTINE EIGRF  (A,N,IA,IJOB,W,Z,IZ,WK,IER)                    EIRF0010
C                                                                       EIRF0020
C-EIGRF---------S/D-----LIBRARY 1-------------------------------------EIRF0030
C                                                                       EIRF0040
C    FUNCTION              - TO CALCULATE EIGENVALUES AND (OPTIONALLY)  EIRF0050
C                            EIGENVECTORS OF A REAL GENERAL MATRIX.     EIRF0060
C                                                                       EIRF0070
C    USAGE                 - CALL EIGRF (A,N,IA,IJOB,W,Z,IZ,WK,IER)     EIRF0080
C    PARAMETERS   A        - THE INPUT REAL GENERAL MATRIX OF ORDER N    EIRF0090
C                            WHOSE EIGENVALUES AND EIGENVECTORS ARE     EIRF0100
C                            TO BE COMPUTED. INPUT A IS DESTROYED IF    EIRF0110
C                            IJOB IS EQUAL TO 0 OR 1.                   EIRF0120
C                 N        - THE ORDER OF THE MATRIX A.                 EIRF0130
C                 IA       - THE ROW DIMENSION OF THE MATRIX A IN THE   EIRF0140
C                            CALLING PROGRAM. IA MUST BE GREATER THAN OR EIRF0150
C                            EQUAL TO N.                                EIRF0160
C                 IJOB     - INPUT OPTION PARAMETER. WHEN               EIRF0170
C                            IJOB = 0, COMPUTE EIGENVALUES ONLY         EIRF0180
C                            IJOB = 1, COMPUTE EIGENVALUES AND EIGEN-   EIRF0190
C                              VECTORS.                                 EIRF0200
C                            IJOB = 2, COMPUTE EIGENVALUES, EIGENVECTORS EIRF0210
C                              AND PERFORMANCE INDEX.                   EIRF0220
C                            IJOB = 3, COMPUTE PERFORMANCE INDEX ONLY.  EIRF0230
C                            IF THE PERFORMANCE INDEX IS COMPUTED, IT IS EIRF0240
C                            RETURNED IN WK(1). THE ROUTINES HAVE       EIRF0250
C                            PERFORMED (WELL, SATISFACTORILY, POORLY) IF EIRF0260
C                            WK(1) IS (LESS THAN 1, BETWEEN 1 AND 100,  EIRF0270
C                            GREATER THAN 100).                         EIRF0280
C                 W        - THE OUTPUT COMPLEX VECTOR OF LENGTH N,     EIRF0290
C                            CONTAINING THE EIGENVALUES OF A.           EIRF0300
C                 Z        - THE OUTPUT N BY N COMPLEX MATRIX CONTAINING EIRF0310
C                            THE EIGENVECTORS OF A.                     EIRF0320
C                            THE EIGENVECTOR IN COLUMN J OF Z CORRES-   EIRF0330
C                            PONDS TO THE EIGENVALUE W(J).              EIRF0340
C                            IF IJOB = 0, Z IS NOT USED.                EIRF0350
C                 IZ       - THE ROW DIMENSION OF THE MATRIX Z IN THE   EIRF0360
C                            CALLING PROGRAM. IZ MUST BE GREATER THAN   EIRF0370
C                            OR EQUAL TO N IF IJOB IS NOT EQUAL TO ZERO. EIRF0380
C                 WK       - WORK AREA. THE LENGTH OF WK DEPENDS        EIRF0390
C                            ON THE VALUE OF IJOB. WHEN                 EIRF0400
C                            IJOB = 0, THE LENGTH OF WK IS AT LEAST N.  EIRF0410
C                            IJOB = 1, THE LENGTH OF WK IS AT LEAST 2N. EIRF0420
C                            IJOB = 2, THE LENGTH OF WK IS AT LEAST     EIRF0430
C                              (2+N)N.                                  EIRF0440
C                            IJOB = 3, THE LENGTH OF WK IS AT LEAST 1.  EIRF0450
C                 IER      - ERROR PARAMETER                            EIRF0460
C                            TERMINAL ERROR                             EIRF0470
C                              IER = 12N+J, INDICATES THAT EQRH3F FAILED EIRF0480
C                              TO CONVERGE ON EIGENVALUE J. EIGENVALUES  EIRF0490
C                              J+1,J+2,...,N HAVE BEEN COMPUTED CORRECTLY. EIRF0500
C                              EIGENVALUES 1,...,J ARE SET TO ZERO.      EIRF0510
C                              IF IJOB = 1 OR 2 EIGENVECTORS ARE SET TO  EIRF0520
C                              ZERO. THE PERFORMANCE INDEX IS SET TO 1000. EIRF0530
C                            WARNING ERROR (WITH FIX)                   EIRF0540
C                              IER = 66, INDICATES IJOB IS LESS THAN 0 OR EIRF0550
C                                IJOB IS GREATER THAN 3. IJOB SET TO 1.  EIRF0560
C                              IER = 67, INDICATES IJOB IS NOT EQUAL TO  EIRF0570
C                                ZERO, AND IZ IS LESS THAN THE ORDER OF  EIRF0580
C                                MATRIX A. IJOB IS SET TO ZERO.          EIRF0590
C    PRECISION             - SINGLE/DOUBLE                              EIRF0600
C    REQ'D IMSL ROUTINES   - ERALAF,ERBCKF,FHBCKF,EHESSF,EQRH3F,UERTST  EIRF0610
C    LANGUAGE              - FORTRAN                                    EIRF0620
C-----------------------------------------------------------------------
```

CALL EIGRF (A,N,IA,IJOB,W,Z,IZ,WK,IER)

Purpose

EIGRF computes eigenvalues and (optionally) eigenvectors of a real matrix. It can also compute a performance index.

Algorithm

EIGRF calls IMSL routine EBALAF to balance the matrix. Then, EHESSF and EQRH3F are called to compute eigenvalues and (optionally) eigenvectors. When eigenvectors are computed, EHBCKF and EB3CKF are called to backtransform the eigenvectors.

The performance index is defined as follows

$$P = \max_{1 \le j \le N} \frac{||Az^j - w_j z^j||_1}{||A||_1 \, ||z^j||_1 \, 10(N)(EPS)}$$

where the max is taken over the j eigenvalues w_j and associated eigenvectors z^j. EPS specifies the relative precision of floating point arithmetic. When P is less than 1. the performance of the routines is considered to be excellent in the sense that the residuals Az-wz are as small as can be expected. When P is between 1 and 100 the performance is good. When P is greater than 100 the performance is considered poor.

The performance index was first developed and used by the EISPACK project at Argonne National Laboratory.

See references: Wilkinson, J. H., The Algebraic Eigenvalue Problem, Oxford, Clarendon Press, 1965.

Smith, B. T., Boyle, J. M., Garbow, B. S., Ikebe, Y., Klema, V. C., and Moler, C. B., Matrix Eigensystem Routines, Springer-Verlag, 1974.

Programming Notes

1. A is preserved when IJOB=2 or 3. In all other cases A is destroyed.

2. The eigenvalues are unordered except that complex conjugate pairs of eigenvalues appear consecutively with the eigenvalue having the positive imaginary part first.

3. The eigenvectors are not normalized.

4. When IJOB=3 (i.e., to compute a performance index only) the eigenvalues, W, and eigenvectors, Z, are assumed to be input.

Example

```
DIMENSION A(4,4),W(4),Z(4,4),WK(24)

COMPLEX Z,W,ZN

IA   =  4
IZ   =  4
N    =  4
IJOB =  2
```

$$A = \begin{bmatrix} 4.0 & -5.0 & 0.0 & 3.0 \\ 0.0 & 4.0 & -3.0 & -5.0 \\ 5.0 & -3.0 & 4.0 & 0.0 \\ 3.0 & 0.0 & 5.0 & 4.0 \end{bmatrix}$$

```
      CALL EIGRF (A,N,EA,I[illegible]H,Z,IZ,WK,IER)
C                                                  NORMALIZE EIGE[illegible]ECTORS
      DO 5 J=1,N
         ZN = Z(1,J)
         DO 5 I=1,N
            Z(I,J) = Z(I,J)/ZN
    5 CONTINUE
```

Output:

IER = 0

W = (12.0, 1.0+5.0i, 1.0-5.0i, 2.0) (eigenvalues)

$$Z = \begin{bmatrix} 1.0 \\ -1.0 \\ 1.0 \\ 1.0 \end{bmatrix}, \begin{bmatrix} 1.0 \\ 0.0 \\ 0.0 \\ -1.0 \end{bmatrix} + i \begin{bmatrix} 0.0 \\ -1.0 \\ -1.0 \\ 0.0 \end{bmatrix}, \begin{bmatrix} 1.0 \\ 0.0 \\ 0.0 \\ -1.0 \end{bmatrix} + i \begin{bmatrix} 0.0 \\ 1.0 \\ 1.0 \\ 0.0 \end{bmatrix}, \begin{bmatrix} 1.0 \\ 1.0 \\ -1.0 \\ 1.0 \end{bmatrix} \quad \text{(eigenvectors)}$$

WK(1) < 1.0 (performance index)

```
 *ONTRAN V EXTENDED COMPILER ENTERED
 *STATISTICS*     SOURCE STATEMENTS =     50, PROGRAM SIZE =    20760, SUBPROGRAM NAME = MAIN
 *STATISTICS*  NO  DIAGNOSTICS GENERATED
 ****** END OF COMPILATION ******                          117K BYTES OF CORE NOT USED


 F64-LEVEL LINKAGE EDITOR OPTIONS SPECIFIED    NONE
           DEFAULT OPTION(S) USED -  SIZE=(196608,65536)
 ****MAIN      DOES NOT EXIST BUT HAS BEEN ADDED TO DATA SET
 AUTHORIZATION CODE IS      0.
```

THE CRITICAL VALUES OF THE BUCKLING LOAD ARE:

FIBERGLASS PLATE THICKNESS= .50IN

-55.684345	0.0	55.684906	0.0	-82.880951	0.0	82.88124.	0.0
-9.348364	0.0	9.348937	0.0	-10.998810	0.0	10.998386	0.0
-23.883713	0.0	23.883774	0.0	-33.949020	0.0	33.949356	0.0
-31.060959	0.0	31.061142	0.0	-26.716248	0.0	26.716263	0.0

```
 F64-LEVEL LINKAGE EDITOR OPTIONS SPECIFIED    NONE
          DEFAULT OPTION(S) USED -  SIZE=(196608,65536)
***MAIN      DOES NOT EXIST BUT HAS BEEN ADDED TO DATA SET
AUTHORIZATION CODE IS          0.
```


THE CRITICAL VALUES OF THE BUCKLING LOAD ARE:

FIBERGLASS PLATE THICKNESS=1.800MM

-79.278763	0.0	79.278571	0.0	-117.998856	0.0	117.999435	0.0
-13.304116	0.0	13.304200	0.0	15.658950	0.0	-15.659035	0.0
-34.003342	0.0	34.003403	0.0	-48.333694	0.0	48.334122	0.0
-44.221725	0.0	44.221954	0.0	-38.035919	0.0	38.035980	0.0

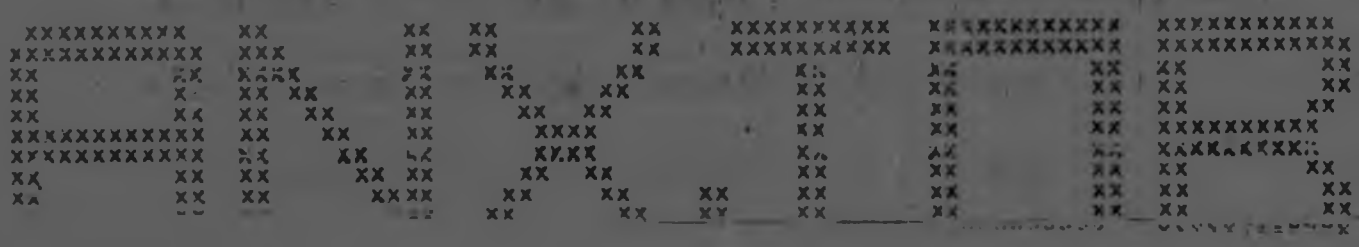

```
 F64-LEVEL LINKAGE EDITOR OPTIONS SPECIFIED    NONE
          DEFAULT OPTION(S) USED -  SIZE=(196608,65536)
***MAIN      DOES NOT EXIST BUT HAS BEEN ADDED TO DATA SET
AUTHORIZATION CODE IS          0.
```


THE CRITICAL VALUES OF THE BUCKLING LOAD ARE:

FIBERGLASS PLATE THICKNESS=1.800MM

-79.278763	0.0	79.278871	0.0	-117.998856	0.0	117.999435	0.0
-13.304116	0.0	13.304200	0.0	15.658950	0.0	-15.659035	0.0
-34.003342	0.0	34.003403	0.0	-48.333694	0.0	48.334122	0.0
-44.221725	0.0	44.221954	0.0	-38.035919	0.0	38.035980	0.0

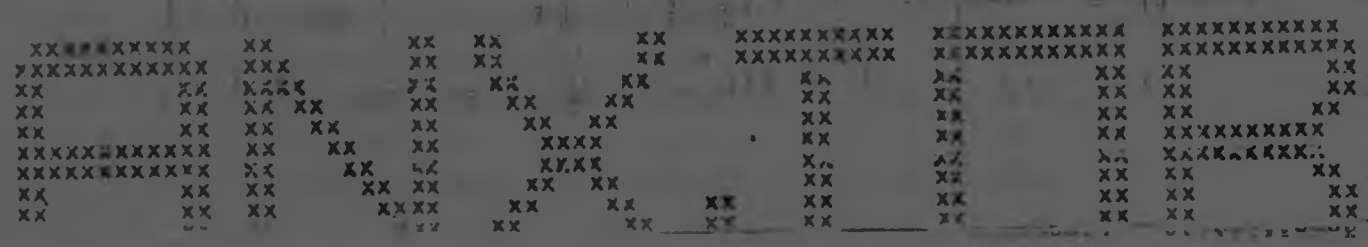

```
*STATISTICS*  NO  DIAGNOSTICS GENERATED
                                                        117K BYTES OF CORE NOT USED
****** END OF COMPILATION ******
FORTRAN H EXTENDED COMPILER ENTERED
*STATISTICS*      SOURCE STATEMENTS =      50, PROGRAM SIZE =    20768, SUBPROGRAM NAME =  MAIN
*STATISTICS*  NO  DIAGNOSTICS GENERATED
                                                        117K BYTES OF CORE NOT USED
****** END OF COMPILATION ******

F04-LEVEL LINKAGE EDITOR OPTIONS SPECIFIED   NONE
          DEFAULT OPTION(S) USED -  SIZE=(196608,65536)
0000MAIN      DOES NOT EXIST BUT HAS BEEN ADDED TO DATA SET
AUTHORIZATION CODE IS          0.

IHD2008I IBCOM - PROGRAM INTERRUPT (P) - UNDERFLOW  OLD PSW IS FF4500004297F2A2 . REGISTER CONTAINED 7FCA6D50
TRACEBACK  ROUTINE  CALLED FROM ISN   REG. 14   REG. 15   REG. 0   REG. 1
           EQRH3F                     629759CE  0097E518  00000001  0097531C
           EIGRF                      4297509A  00975120  00000011  00970138
           MAIN                       00011BC0  C0970000  00000178  009AF748
ENTRY POINT=  C0970000
STANDARD FIXUP TAKEN . EXECUTION CONTINUING
                    THE CRITICAL VALUES OF THE BUCKLING LOAD ARE:

                    FIBERGLASS PLATE THICKNESS=2.200MM

-144.747177   0.0     144.746567   0.0     -215.438400   0.0     215.439911   0.0
-24.290093    0.0     24.290093    0.0     -62.085098    0.0     62.085251    0.0
-28.590973    0.0     28.590942    0.0     -88.247849    0.0     88.247864    0.0
-69.444992    0.0     69.445602    0.0     -80.741745    0.0     80.741989    0.0
```

```
 F04-LEVEL LINKAGE EDITOR OPTIONS SPECIFIED    NONE
          DEFAULT OPTION(S) USED -  SIZE=(196608,65536)
****MAIN       DOES NOT EXIST BUT HAS BEEN ADDED TO DATA SET
AUTHORIZATION CODE IS          0.
```

THE CRITICAL VALUES OF THE BUCKLING LOAD ARE:

FIBERGLASS PLATE THICKNESS=2.400MM

-187.916193	0.0	187.915985	0.0	-279.691650	0.0	279.693604	0.0
-31.[illegible]885	0.0	[illegible]	0.0	-80.600983	0.0	80.601120	0.0
-37.117859	0.0	37.117996	0.0	-114.568849	0.0	114.569077	0.0
-90.156143	0.0	90.156601	0.0	-104.822960	0.0	104.823120	0.0

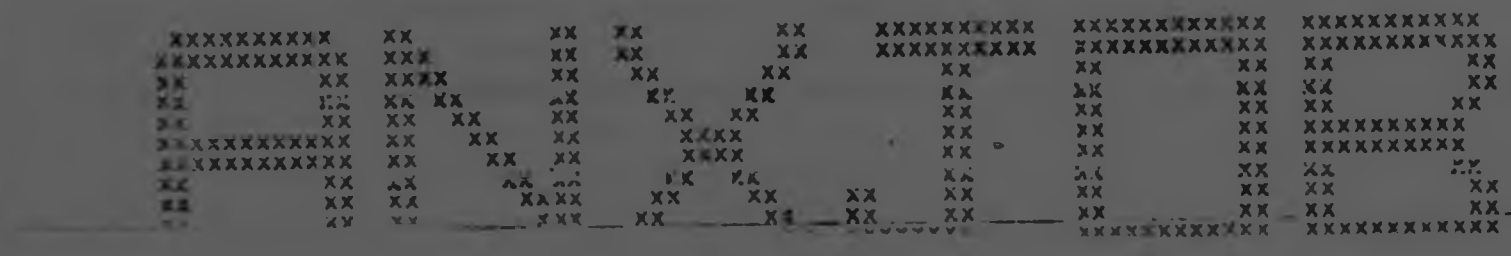

```
*STATISTICS*  NO  DIAGNOSTICS GENERATED
******* END OF COMPILATION *******                    117K BYTES OF CORE NOT USED
FORTRAN H EXTENDED COMPILER ENTERED
*STATISTICS*      SOURCE STATEMENTS =      50, PROGRAM SIZE =    20768, SUBPROGRAM NAME =  MAIN
*STATISTICS*  NO  DIAGNOSTICS GENERATED
******* END OF COMPILATION *******                    117K BYTES OF CORE NOT USED

 F64-LEVEL LINKAGE EDITOR OPTIONS SPECIFIED    NONE
           DEFAULT OPTION(S) USED -  SIZE=(196608,65536)
***MAIN      DOES NOT EXIST BUT HAS BEEN ADDED TO DATA SET
AUTHORIZATION CODE IS          0.
```

THE CRITICAL VALUE OF THE LOCAL BUCKLING LOAD IS:

CARBON FIBRE PLATE THICKNESS=1.300MM

43.208527	0.0	-31.476486	0.0	56.797653	0.0	-46.324936	0.0
8.918528	0.0	-4.461321	0.0	21.597565	0.0	-11.976189	0.0
9.920407	0.0	-5.131373	0.0	-17.694473	0.0	26.183517	0.0
-16.207123	0.0	24.773254	0.0	-13.784424	0.0	23.909256	0.0

```
64-LEVEL LINKAGE EDITOR OPTIONS SPECIFIED   NONE
        DEFAULT OPTION(S) USED -  SIZE=(196608,65536)
***MAIN      DOES NOT E..IST BUT HAS BEEN ADDED TO DATA SET
ATHORIZATION CODE IS          0.
```

THE CRITICAL VALUES OF THE BUCKLING LOAD ARE:

CARBON FIBRE PLATE THICKNESS=1.500MM

54.756927	0.0	-49.[illegible]617	0.0	-72.544220	0.0	85.801544	0.0
-17.[illegible]28	0.0	31.[illegible]	0.0	-19.687600	0.0	-7.463402	0.0
-20.129025	0.0	-26.056229	0.0	-22.312695	0.0	14.640205	0.0
79.074234	0.0	36.[illegible]6	0.0	30.746497	0.0	-8.597834	0.0

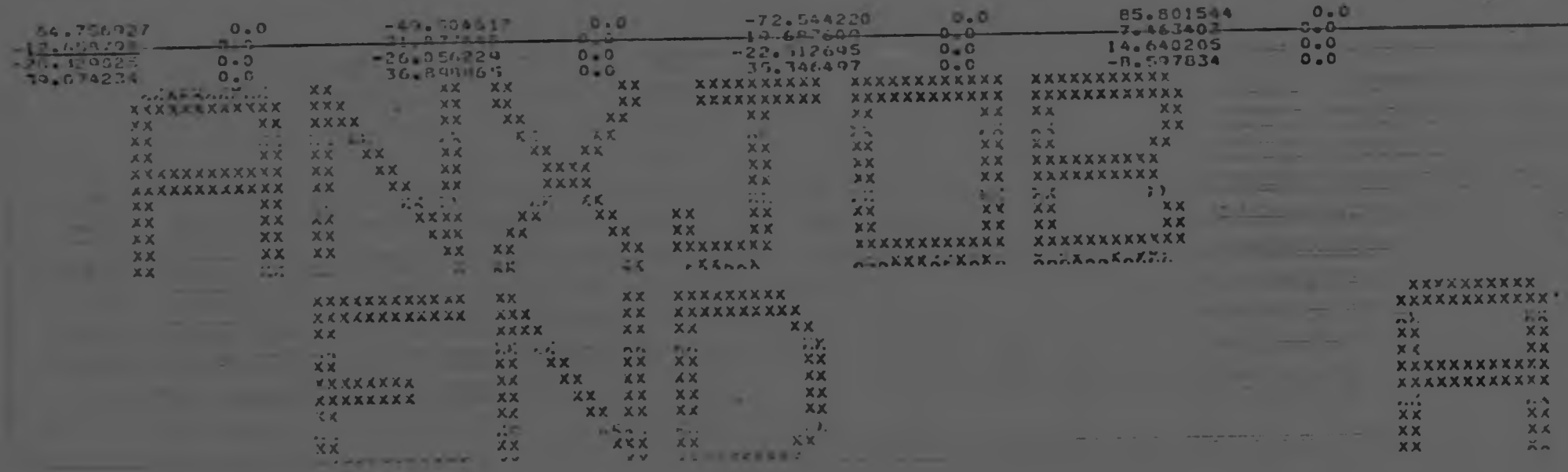

```
*STATISTICS*      SOURCE STATEMENTS =      50, PROGRAM SIZE =    20768, SUBPROGRAM NAME =  MAIN
*STATISTICS*  NO  DIAGNOSTICS GENERATED
                                                                  117K BYTES OF CORE NOT USED
******* END OF COMPILATION *******
FORTRAN H EXTENDED COMPILER ENTERED
*STATISTICS*      SOURCE STATEMENTS =      50, PROGRAM SIZE =    20768, SUBPROGRAM NAME =  MAIN
*STATISTICS*  NO  DIAGNOSTICS GENERATED
                                                                  117K BYTES OF CORE NOT USED
******* END OF COMPILATION *******

FCA-LEVEL LINKAGE EDITOR OPTIONS SPECIFIED   NONE
          DEFAULT OPTIONS USED -  SIZE=(178433,65536)
IHEMAIN     DOES NOT EXIST BUT HAS BEEN ADDED TO DATA SET
AUTOCALL CODE IS          0.
```

THE CRITICAL VALUES OF THE BUCKLING LOAD ARE:

0.2857 FIBRE PLATE THICKNESS=1.82MM

114.030363	0.0	- 0.731337	0.0	151.804016	0.0	-131.000732	0.0
22.[illegible]	0.0	-13.033822	0.0	55.634085	0.0	-36.477059	0.0
21.511300	0.0	-16.070986	0.0	-51.774445	0.0	68.635590	0.0
-47.726083	0.0	54.740051	0.0	61.738983	0.0	-41.586914	0.0